

THE MECHANISMS OF AMIDE HYDROLYSIS

THE MECHANISMS OF AMIDE HYDROLYSIS

By

John Paul Krug, B.Sc.

A Thesis

Submitted to the School of Graduate Studies

in Partial Fulfilment of the Requirements

for the Degree

Master of Science

McMaster University

MASTER OF SCIENCE (1991)

(Chemistry)

McMASTER UNIVERSITY

Hamilton, Ontario

TITLE: The Mechanisms of Amide Hydrolysis

AUTHOR: John Paul Krug, B.Sc. (Waterloo)

SUPERVISOR: Dr. R.F.W. Bader

NUMBER OF PAGES: xiv,165

ABSTRACT

This thesis presents the theoretical study of the mechanisms of gas-phase formamide hydrolysis using ab initio SCF-MO calculations. Four reaction paths were considered; (i) the reaction of formamide with OH^- (ii) the acid catalyzed hydrolysis with protonation on the nitrogen atom (iii) the acid catalyzed hydrolysis with protonation on the oxygen (iv) the uncatalyzed hydrolysis. An unconstrained optimization of all parameters was performed on the transition state and equilibrium structures. The intrinsic reaction coordinate was then followed down from the transition state to the reactants and products. All of the molecular geometries were obtained using the 4-31G basis set and all wavefunctions and energies were calculated at the 6-31G** level of theory. The theory of atoms in molecules was applied to each reaction to study the mechanisms of structural change along the reaction coordinate. Molecular graphs were calculated at

points along the reaction coordinate and these give a detailed pictorial outline of the entire reaction sequence. The Laplacian of the charge density successfully predicts the correct site of protonation and the enhanced reactivity of protonated formamide over that of neutral formamide. Both the acid catalyzed reaction with nitrogen protonation and the base enhanced hydrolysis reactions proceed without a barrier with respect to reactants and products. The acid catalyzed hydrolysis with protonation on the oxygen atom proceeds with a moderate activation barrier whereas the neutral hydrolysis involves the passage over a very high activation barrier. The two acid catalyzed reactions are competitive with the N-protonation mechanism being more favourable from a kinetic point of view while the O-protonation mechanism is thermodynamically more favourable.

ACKNOWLEDGEMENTS

I thank my supervisor, Dr. R.F.W. Bader for his guidance. I also thank Mr. J.R. Cheeseman, Mr. T.A. Keith, Mr. M.J. Krug and Dr. K.E. Laidig for their help on some of the practical aspects of this work.

TABLE OF CONTENTS

	<u>PAGE</u>
Abstract	iii
Acknowledgements	v
Table of Contents	vi
List of Figures	vii
List of Tables	x
Introduction	1
Chapter 1. A Review of Amide Bond Hydrolysis	8
Chapter 2. The Reaction of Formamide with Hydroxide ion.	18
Chapter 3. The Acid Catalyzed Hydrolysis of Formamide.	45
A. Hydrolysis with protonation on the nitrogen atom.	45
B. Hydrolysis with protonation on the oxygen atom.	75
Chapter 4. The Uncatalyzed Hydrolysis of Formamide.	107
Chapter 5. Conclusion.	143
References	163

LIST OF FIGURES

<u>FIGURE</u>		<u>PAGE</u>
II.1	The reaction scheme for the base-catalyzed hydrolysis of formamide.	19
II.2	The molecular graphs for a series of points on the reaction coordinate of the base-catalyzed hydrolysis of formamide.	22
II.3	The computed reaction profile for the base-catalyzed hydrolysis of formamide.	25
II.4	The contour maps of the charge density for a series of points along the reaction coordinate of the base-catalyzed hydrolysis of formamide.	29
II.5	The contour maps of the Laplacian of the charge density for a series of points along the reaction coordinate of the base-catalyzed hydrolysis of formamide.	39
III.A.1	The reaction scheme for the hydrolysis of N-protonated formamide.	48
III.A.2	The molecular graphs for a series of points on the reaction coordinate of the hydrolysis of N-protonated formamide.	51
III.A.3	The computed reaction profile for the hydrolysis of N-protonated formamide.	54

LIST OF FIGURES (cont'd)

<u>FIGURE</u>		<u>PAGE</u>
III.A.4	The contour maps of the charge density for a series of points along the reaction coordinate of the hydrolysis of N-protonated formamide.	59
III.A.5	The contour maps of the Laplacian of the charge density for a series of points along the reaction coordinate of the hydrolysis of N-protonated formamide.	67
III.B.1	The reaction scheme for the hydrolysis of O-protonated formamide.	77
III.B.2	The molecular graphs for a series of points on the reaction coordinate of the hydrolysis of O-protonated formamide.	80
III.B.3	The computed reaction profile for the hydrolysis of O-protonated formamide.	84
III.B.4	The contour maps of the charge density for a series of points along the reaction coordinate of the hydrolysis of O-protonated formamide.	90
III.B.5	The contour maps of the Laplacian of the charge density for a series of points along the reaction coordinate of the hydrolysis of O-protonated formamide.	98

LIST OF FIGURES (cont'd)

<u>FIGURE</u>		<u>PAGE</u>
IV.1	The reaction scheme for the uncatalyzed hydrolysis of formamide.	108
IV.2	The molecular graphs for a series of points along the reaction coordinate of the uncatalyzed hydrolysis of formamide.	111
IV.3	The computed reaction profile for the uncatalyzed hydrolysis of formamide.	115
IV.4	The contour maps of the charge density for a series of points along the reaction coordinate of the uncatalyzed hydrolysis of formamide.	122
IV.5	The contour maps of the Laplacian of the charge density for a series of points along the reaction coordinate of the uncatalyzed hydrolysis of formamide.	126
V.1	Relief maps of the Laplacian in formamide.	152

LIST OF TABLES

<u>TABLE</u>		<u>PAGE</u>
II.1	The geometrical parameters and energies for the reaction of formamide with OH^- .	24
II.2	The values of ρ and $\nabla^2\rho$ at the critical points in $\rho(r)$ for the reaction of formamide with OH^- .	33
II.3	The atomic populations for the reaction of formamide with OH^- .	35
II.4	The atomic energies for the reaction of formamide with OH^- .	36
II.5	The properties of the nonbonded (3,-3) critical point in $\nabla^2\rho$ at the nitrogen atom for the reaction of formamide with OH^- .	43
III.A.1	The geometrical parameters and energies for the hydrolysis of N-protonated formamide.	53
III.A.2	The values of ρ and $\nabla^2\rho$ at the critical points in $\rho(r)$ for the reaction of N-protonated formamide with water.	63
III.A.3	The atomic populations for the hydrolysis of N-protonated formamide.	65

LIST OF TABLES (cont'd)

<u>TABLE</u>		<u>PAGE</u>
III.A.4	The atomic energies for the hydrolysis of N-protonated formamide.	66
III.A.5	The properties of the (3,+1) critical point in $\nabla^2\rho$ at the carbon atom for the hydrolysis of N-protonated formamide.	71
III.A.6	The properties of the nonbonded (3,-3) critical point in $\nabla^2\rho$ at the oxygen atom for the hydrolysis of N-protonated formamide.	72
III.B.1	The geometrical parameters and energies for the hydrolysis of O-protonated formamide leading to the intermediate.	82
III.B.2	The geometrical parameters and energies for the decomposition of the intermediate in the hydrolysis of O-protonated formamide.	83
III.B.3	The values of ρ and $\nabla^2\rho$ at the critical points in $\rho(r)$ for the reaction of O-protonated formamide with water.	94

LIST OF TABLES (cont'd)

<u>TABLE</u>		<u>PAGE</u>
III.B.4	The atomic populations for the hydrolysis of O-protonated formamide.	96
III.B.5	The atomic energies for the hydrolysis of O-protonated formamide.	97
III.B.6	The properties of the (3,+1) critical point in $\nabla^2\rho$ at the carbon atom for the hydrolysis of O-protonated formamide.	103
III.B.7	The properties of the nonbonded (3,-3) critical point in $\nabla^2\rho$ at the oxygen atom for the hydrolysis of O-protonated formamide.	104
III.B.8	The properties of the nonbonded (3,-3) critical point in $\nabla^2\rho$ at the nitrogen atom for the hydrolysis of O-protonated formamide.	105
IV.1	The geometrical parameters and energies for the uncatalyzed hydrolysis of formamide leading to the intermediate.	113
IV.2	The geometrical parameters and energies for the decomposition of the intermediate in the uncatalyzed hydrolysis of formamide.	114

LIST OF TABLES (cont'd)

<u>TABLE</u>		<u>PAGE</u>
IV.3	The values of ρ and $\nabla^2\rho$ at the critical points in $\rho(r)$ for the uncatalyzed hydrolysis of formamide.	119
IV.4	The properties of the (3,+1) critical point in $\nabla^2\rho$ at the carbon atom for the uncatalyzed hydrolysis of formamide.	133
IV.5	The properties of the nonbonded (3,-3) critical point in $\nabla^2\rho$ at the nitrogen atom for the uncatalyzed hydrolysis of formamide.	135
IV.6	The properties of the nonbonded (3,-3) critical point in $\nabla^2\rho$ at the oxygen atom for the uncatalyzed hydrolysis of formamide.	136
IV.7	The atomic populations for the uncatalyzed hydrolysis of formamide.	138
IV.8	The atomic energies for the uncatalyzed hydrolysis of formamide.	139
V.1	The atomic populations of protonated formamide.	146
V.2	The properties of the C-N bond critical point.	148
V.3	The atomic energies of protonated formamide.	149

LIST OF TABLES (cont'd)

<u>TABLE</u>		<u>PAGE</u>
V.4	The properties of the (3,+1) critical point in $\nabla^2\rho$ at the carbon atom of formamide and protonated formamide.	156

INTRODUCTION

The catalyzed hydrolysis of an amide bond is one of the most fundamental reactions in biochemistry. Proteins and peptides are composed of amino acids linked together by amide (peptide) bonds. A study of the reaction coordinate for the hydrolysis of an amide bond will give a better understanding of the mode of activation of a peptide bond when acted on by proteases. Formamide is a suitable candidate for use as an analogy of the peptide bond in a theoretical study on amide bond hydrolysis. It has the same planar geometry as the amidic bond found in proteins and peptides and since it is small, the ab initio calculations of the molecular wavefunction can be done very accurately. For these reasons the hydrolysis of formamide has been extensively studied both theoretically and experimentally. Both approaches complement each other, the experimental results being used to reinforce or refute the proposed mechanism. The theoretical approach allows for the study of the reaction sequence as a function of the internal coordinates of the system. A theoretical investigation of a reaction provides a means for detecting the changes in electron-

ic properties with structure and may be performed on species which are unavailable or difficult to produce. In addition, ab initio calculations allow the prediction of transition state structures and this data is not in general obtainable experimentally. This allows for the comparison and evaluation of alternative reaction pathways.

The potential energy hypersurface gives the energy of the reacting molecules as a function of their shape and relative position. A qualitative determination of the relative reaction rates can be obtained by a comparison of the barrier heights. The local minima and saddle points on the potential energy hypersurface correspond to the various intermediates and transition state structures formed during the reaction. All geometric changes that lead from the reactants to the products may be regarded as reaction coordinates. For a given set of reaction coordinates the minimum energy path is obtained by progressing along the reaction coordinate at appropriate increments while minimizing the energy with respect to all other coordinates. The minimum energy path corresponds to an idealized, infinitely slow (adiabatic) rearrangement of the nuclei in

which no vibration or rotation occurs. The minimum energy path concept is very useful because it allows distinct reaction mechanisms to be associated with distinct minimum energy paths. The precise definition of the reaction coordinate given by Fukui (Fukui, 1981) places the reaction coordinate concept on a physical basis. This definition is referred to as the intrinsic reaction coordinate approach (IRC) for defining the reaction path. By progressing along this coordinate a reaction path is obtained which connects reactant and product minima to the saddle point and is orthogonal to any equipotential contours crossed.

The ability of the intrinsic reaction coordinate to unequivocally define the reaction path connecting the relevant stable points to the transition state makes it invaluable for studying the potential energy hypersurface of a reaction. It is often difficult to determine whether a calculated transition state actually connects the reactants to the products by studying the geometry of the transition state alone. It is often necessary to follow the reaction path from the transition state down to the reactants and products in order to verify that a given transition state does lie on the reaction path of interest. Following the reac-

tion path also gives detailed information about the reaction mechanism by showing the sequence of changes in geometry and energy during the course of the reaction.

There are many practical problems involved in following the intrinsic reaction coordinate of a reaction. For many reactions the potential energy surface is rather complicated with tightly curved reaction paths which are difficult to follow. An obvious solution to this problem would be to use very small step sizes, however this can make the computational time prohibitive for complex reactions. It is possible to circumvent this problem by using an algorithm in which points on the reaction path are obtained by constrained optimizations such that the reaction path is given by the arc of a circle and the gradient at each point is tangent to the path (Gonzalez and Schlegel, 1989). This algorithm allows for the use of larger step sizes thus making it possible to follow the reaction path for a complicated reaction.

The theory of atoms in molecules demonstrates that the concepts of atoms and bonds may be rigorously defined and given physical expression in terms of the topological properties of the observable distribution of charge for a molecular system and the properties of the atoms are defined by quantum mechanics. This theory is used extensively in the present investigation to study the mechanisms of structural change for the hydrolysis of formamide. Two atomic properties are reported in this thesis to monitor the progress of the hydrolysis reaction, the atomic population and atomic energy. The electron population of atom Ω , $N(\Omega)$, is obtained by integrating the electronic charge density, $\rho(\mathbf{r})$, over the basin of the atom;

$$N(\Omega) = \int_{\Omega} \rho(\mathbf{r}) d\tau. \quad (1)$$

where $\rho(\mathbf{r})$ is given by;

$$\rho(\mathbf{r}) = N \sum (\text{spins}) \left\{ \int d\tau_2 \int d\tau_3 \dots \int d\tau_N \psi^*(\mathbf{x}) \psi(\mathbf{x}) \right\}. \quad (2)$$

The energy of an atom in a molecule is given in terms of the corresponding electronic kinetic energy using the atomic statement of the virial theorem;

$$E_e(\Omega) = -T(\Omega) \quad (3)$$

where $T(\Omega)$ is given by;

$$T(\Omega) = (\hbar^2/2m) \int_{\Omega} d\mathbf{r} \{ \nabla \cdot \nabla' \Gamma^{(1)}(\mathbf{r}, \mathbf{r}') |_{\mathbf{r}=\mathbf{r}'} \} \quad (4)$$

where $\Gamma^{(1)}$ is the first-order density matrix given by;

$$\Gamma^{(1)}(\mathbf{r}, \mathbf{r}') = N \int d\tau' \psi^*(\mathbf{x}_1, \mathbf{x}_2, \dots, \mathbf{x}_N) \psi(\mathbf{x}'_1, \mathbf{x}'_2, \dots, \mathbf{x}'_N). \quad (5)$$

These kinetic energies have been corrected for the small error which arises because the approximate wavefunctions do not exactly satisfy the virial theorem. Hence the ratio of $-V/T$ does not equal precisely two as it should for an equilibrium geometry and the sum of the $T(\Omega)$ values does not equal $-E$. The departure of the ratio $-V/T = \gamma$ from two is very small so the values of $T(\Omega)$ have been scaled by the factor γ^{-1} to obtain a set of atomic energies which correctly sum to E . The Laplacian of the charge density is used to predict the relative reactivities of the reactants and the relative orientation of the nucleophilic site with the approaching nucleophile. The predicted reactivities are then verified by a comparison with the experimental results and a comparison with the computed barrier heights.

In order to make a comparison of the various reaction pathways meaningful, all calculations in this *ab initio* study were performed at the same level of

theory. All reactant, product and transition state geometries were optimized using the 4-31G basis set. The intrinsic reaction coordinate was then followed down from the transition state to the products and reactants using the 4-31G basis set. The wavefunctions were then re-calculated using the 6-31G** basis set and the optimized geometries. These better quality wavefunctions were used to calculate the atomic properties and plot the molecular graphs for each configuration along the reaction coordinate. The wavefunction was also used to plot the Laplacian of the charge density. The relative reactivities of formamide and protonated formamide were determined from an analysis of the topology of the Laplacian of the charge density.

Chapter 1

A review of amide bond hydrolysis

The kinetics of the acid catalyzed and the base catalyzed amide hydrolysis reactions were first studied by Ried in 1899. He noted that amide hydrolysis is very similar to ester hydrolysis. In the hydroxide catalyzed reaction the rate of hydrolysis is proportional to both the concentration of the amide and the concentration of the hydroxide ion (Ried, 1899). Ried showed that at low concentrations of strong acid the rate of the acid catalyzed reaction depends on the concentration of the acid and the concentration of the amide. This evidence implies that the acid catalyzed reaction follows a bimolecular mechanism because it is very unlikely that the conjugate acid of the amide would cleave heterolytically to an acylium ion under these weakly acidic conditions. The rate of hydrolysis in the acid catalyzed reaction reaches a maximum at a certain acid concentration which depends on the acid and the amide. This experimental observation also supports the hypothesis that the rate-limiting step

involves the reaction of the protonated amide with water. Increasing the acid concentration increases the concentration of the protonated amide and hence the rate. However, if the acid concentration is increased above that at which the maximum rate occurs the activity of the water decreases causing the rate to decrease (Kriebel and Holst, 1938).

In nonenzymatic reactions the intermediates and transition states are usually formed preferentially in their lowest energy configuration and conformation. This conformation is often not the most labile one. In the enzymatic reaction, however, the active site of the enzyme often changes the substrate geometry in such a way that the stereoelectronic effects favour a fast and specific reaction. In the specific case of the hydrolysis of an amide bond, the enzyme may lock the amide into an unstable conformation which leads to a selective weakening of the C-N bond. If an inhibitor binds to the enzyme the catalytic groups of the enzyme may distort the geometry of the intermediate in such a way that the C-O bond is selectively weakened and the reaction reverts back to the reactants. In neutral amides a protonation of the nitrogen atom leads to a weakening of the C-N bond while leaving the C-O bond

unaffected whereas protonation of the oxygen atom weakens both the C-N and C-O bonds (Lehn and Wipff, 1980). In spite of the fact that the C-N bond may be considerably lengthened and weakened due to anomeric type interactions, these interactions also lower the energy of the protonated species and therefore slow down the reaction. This is because if two configurations react via the same transition state then the more stable configuration will react slower.

The initial step in an acid catalyzed hydrolysis is the rapid protonation, which is then followed by a slower rate-limiting step. There are two pathways which this second step may follow; it can decompose spontaneously (A1 hydrolysis) or it may be attacked by a water molecule (A2 hydrolysis). The A2 hydrolysis mechanism is much more common in amide hydrolysis. In the A2 mechanism the planar protonated amide is attacked by water and a tetrahedral intermediate is formed in the rate-determining step. The energy of the tetrahedral intermediate is often much higher than that of the reactants. Although the polar effects in the A2 mechanism are very weak, if the substituents are suitably placed they can exert very strong steric effects (Ingold, 1953).

Formamide is like most carboxylic acid amides in that it does not undergo hydrolysis in neutral media, however, it is hydrolyzed in either basic or acidic solutions. In the base enhanced hydrolysis of formamide a stable tetrahedral intermediate is formed which then reacts through a proton transfer reaction accompanied by the cleavage of the C-N bond (Tomasi et al., 1974). The intermediate is strongly stabilized with respect to the reactants and is placed at the bottom of a well in the potential energy surface.

The mechanism of the acid catalyzed hydrolysis of formamide is not as well understood, especially at low acid concentrations. In concentrated mineral acid the reaction is believed to involve the formation of a nitrogen protonated intermediate which decomposes in the rate-limiting step to ammonia and the formyl ion. The formyl ion, once formed, reacts rapidly with water to give the corresponding carboxylic acid and ammonia. If the protonation is on the oxygen atom of formamide instead of the nitrogen atom then the lower energy oxygen-protonated isomer will be formed but the mechanism by which it reacts is still not known with certainty (Csizmadia, 1973).

If the nitrogen atom is much more basic than the oxygen atom then the concentration of the N-protonated amide will be much greater than that of the O-protonated amide in acidic solution. NMR studies on dimethylformamide in aqueous strong acids (Fraenkel and Niemann, 1958) give evidence in favour of the oxygen atom being the major site of protonation. The NMR spectrum of pure liquid dimethylformamide shows two peaks of equal area for the N-methyl groups. From this it is concluded that the two methyl groups have different environments because of the restricted rotation about the C-N bond. These two peaks remain unchanged when sulfuric acid is added and by assuming that the rotation about the C-N bond would still be restricted in the O-protonated form while in the N-protonated form it would be free to rotate, it is concluded that the O-protonated form predominates in strong acid solutions. Studies using N-methylformamide also support this conclusion. The NMR signal from the N-methyl protons is a doublet, which is attributed to spin-spin coupling with the single hydrogen atom which is bonded to the nitrogen atom. In basic or weakly acidic solutions this doublet collapses to a single peak but then reappears again as a doublet in strongly acidic solu-

tions (Fraenkel and Niemann, 1958). This evidence rules out the possibility of an NH_2Me^+ group, which would be present if protonation was on the nitrogen atom. These NMR studies, however, provide only indirect evidence in favor of the oxygen atom as being the site of protonation. Direct evidence has been obtained using anhydrous fluorosulphuric acid and low temperatures (Gillespie and Birchall, 1962). At low temperatures (below -80°C) the rate of exchange of the captured proton with the solvent is slowed down sufficiently so that a separate signal for this proton appears in the NMR spectrum. This new peak, which appears at low field, is attributed to the $\text{C}=\text{OH}^+$ group.

The fact that amides protonate mainly on the oxygen atom in strongly acidic solutions does not, however, preclude the possibility that in dilute acid solutions the predominant site of protonation may be the nitrogen atom. The site of protonation of amides in dilute acidic solutions has not been studied as extensively as that in strong acidic solutions and it may be possible that the protonation sites are different in the two media. Kinetic studies (Smith and

Yates, 1972) using acyl ammonium and acyl pyridium salts as model ions for N-protonated amides and imidate salts as model ions for O-protonated amides provide evidence that amides protonate predominantly on oxygen in dilute aqueous acids. These models were used as substrates in hydrolysis reactions and the rate constants were measured. The N-protonated models reacted between 10^3 and 10^6 times faster than the O-protonated model ions at both high and low acid concentration. From these results it is reasonable that an N-protonated amide would react at least 10^3 times faster than the O-protonated form. This is based on the observation that the imidates hydrolyze at a rate very similar to that of the amides (Edward and Meacock, 1957). If amides in dilute acid protonate exclusively on the nitrogen atom then the hydrolysis would proceed through the very reactive N-protonated form. The rate constants for amides in dilute acid show that amides are between 10^3 and 10^6 times less reactive than expected if protonation were on the nitrogen atom, implying that in dilute acidic solutions amides protonate mainly on the oxygen atom.

The fact that amides protonate predominantly at the oxygen atom does not imply that the acid catalyzed hydrolysis of an amide proceeds exclusively through an O-protonation mechanism. Although the O-protonated isomer predominates it is possible that amides may also react through an N-protonated form which may be present in very low concentrations. Since the N-protonated form is much more reactive its concentration would have to be around 10^5 times less (Smith and Yates, 1972) than that of the O-protonated form in order to have agreement with the kinetic data on amide hydrolysis. An estimate of the relative pK 's of protonated amides (Fersht, 1971) show that the O-protonated isomer is favored by a factor of 10^7 .

If the hydrolysis of an amide can follow either pathway then the pathway followed will depend on the conditions, such as pH, and the particular amide being hydrolyzed. The amides of highly basic amines would therefore be expected to favour the N-protonation pathway. The contribution of the N-protonation pathway to the overall hydrolysis has been estimated using N-acetyltrialkylammonium salts as non-protonic models of the N-protonated amide (Williams, 1976). The pK_a of

the corresponding N-protonated amide was estimated from the acid catalyzed proton exchange rate and by using this the overall rate constant for the hydrolysis of the N-protonated amide was calculated. By comparing the rate constants for the hydrolysis of the N-acetylammonium salts with the rate constants of the N-protonated amides it was shown that the rate constant for the N-protonation pathway does not account for the observed rate. In fact, even the amides of the most basic amines have only about 0.02% of their hydrolysis following the N-protonation pathway.

Studies on the effect of pH on the rate of formamide hydrolysis over the range pH1-9 (Hine et al., 1981) have determined the relative effectiveness of H^+ and OH^- as catalysts in amide hydrolysis. By measuring the rate of hydrolysis of formamide in hydrochloric acid and various aqueous buffers it has been demonstrated that hydroxide ions are about ten times more effective than hydrogen ions in catalyzing amide hydrolysis. This is also true for ester hydrolysis, where the minimum in the pH-rate profile for the hydrolysis of simple esters occurs in the range between pH4-pH6 rather than at neutrality (Bender, 1960).

Structural distortion of an amide unit away from planarity has been shown to markedly alter the reactivity of amides towards nucleophilic attack (Brown et al., 1991). The rate of attack of nucleophiles on the C=O unit is accelerated by amidic distortions that involve rotation about the N-C bond and N-pyramidalization. These distortions also result in a lengthening of the C-N bond and a slight shortening of the C=O bond. It is expected that structural or electronic perturbations might lead to a larger variation in the C-N than C=O bond length because the C=O force constant is inherently larger than the C-N force constant. As the degree of molecular distortion increases, so does the extent of protonation, however this increase in the concentration of the protonated intermediate is not the sole reason for the accelerated hydrolysis. Thus the distortion of the amide unit not only increases the susceptibility of of the C=O unit but also increases the basicity of the amide. In particular, the basicity of the nitrogen atom is increased to a greater extent than that of the oxygen atom (Brown and Somayaji, 1986).

Chapter 2

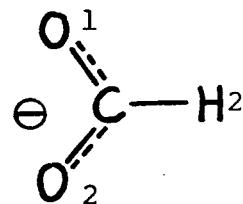
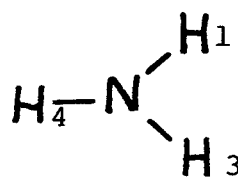
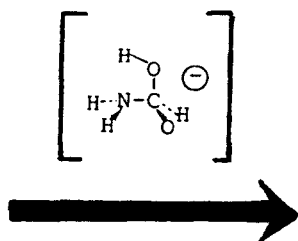
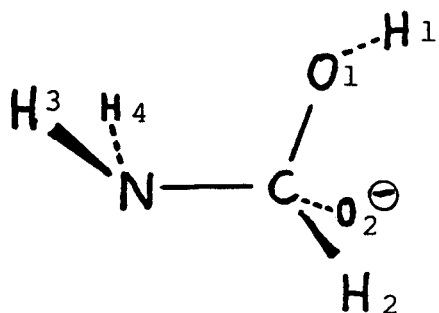
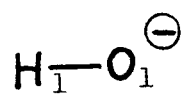
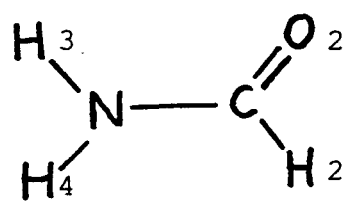
The reaction of formamide with hydroxide ion

The reaction of formamide with OH^- is an example of a nucleophilic substitution reaction. Unlike basic catalysis in which the catalyst reacts via an acid/base reaction with hydrogen and the OH^- is regenerated, in the nucleophilic reaction the OH^- reacts via a nucleophilic attack on a carbon atom. In this base enhanced reaction the nucleophile reacts with the substrate and an unstable intermediate is formed, which then reacts to give the products.

The mechanism of the reaction of formamide with hydroxide ion was previously studied using ab initio SCF-LCAO-MO calculations and the STO-3G basis set (Tomasi et al., 1975). The geometries used in these early studies were obtained from constrained optimizations in which some of the parameters, such as the two N-H bond lengths and the two C-N-H bond angles were held fixed and equal to each other. Since the energy effects caused by even small geometry distortions may

Figure II.1

The scheme for the reaction of formamide with OH^- , showing the formation of the stable intermediate and the subsequent decomposition of this intermediate to the hydrogen-bonded product. The transition state is shown in brackets.



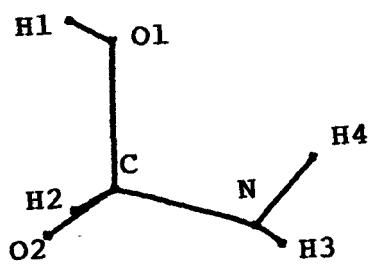
be very large this reaction has been recalculated with geometries obtained from completely free optimizations of all geometric parameters. In addition the larger 6-31G**//4-31G basis set was used and more points on the reaction path were calculated. The reaction sequence is given in Figure II.1.

The first step in the nucleophilic reaction of formamide and OH^- is the formation of a stable tetrahedral intermediate in which both the C and N atoms are pyramidalized and the C-N bond length is longer than that in formamide. This intermediate is stabilized by 38.6 kcal/mole with respect to the isolated reactants. This value is considerably less than the value of 104 kcal/mole calculated by Tomasi (Tomasi et al., 1975) and this discrepancy can be attributed to the much larger basis set used in the present study. The molecular graph of this intermediate and subsequent points on the reaction coordinate are given in Figure II.2, the corresponding energy and geometrical parameters for each of these structures is given in Table II.1 and a schematic representation of the reaction profile is given in Figure II.3.

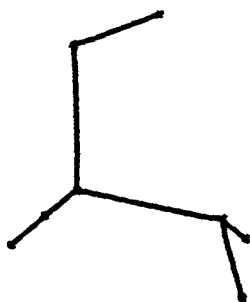
Figure II.2

The molecular graphs for a series of points along the reaction coordinate of the reaction of formamide with OH^- .

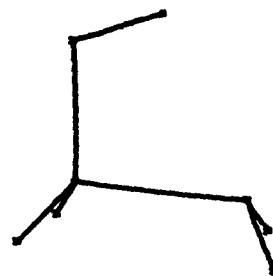
- a) the tetrahedral intermediate.
- b-d) configurations on the reaction path leading to the transition state.
- e) the transition state.
- f-h) configurations on the reaction path leading to the product.
- i) the hydrogen-bonded product.



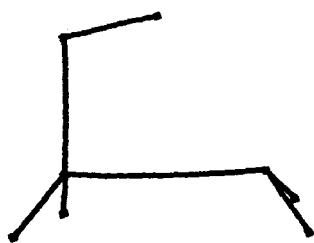
a



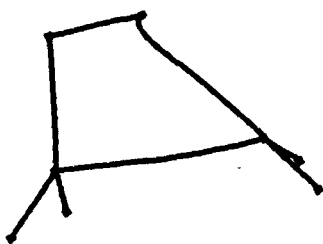
b



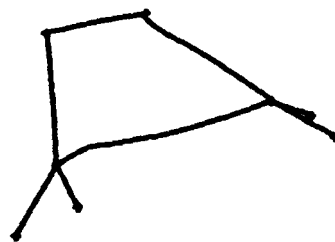
c



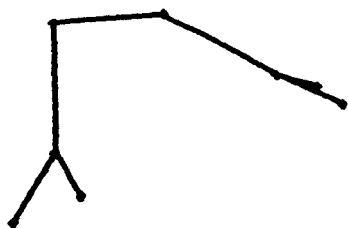
d



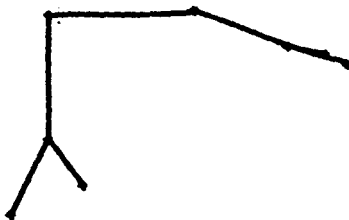
e



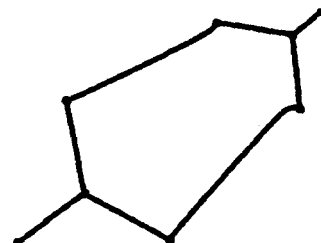
f



g



h



i

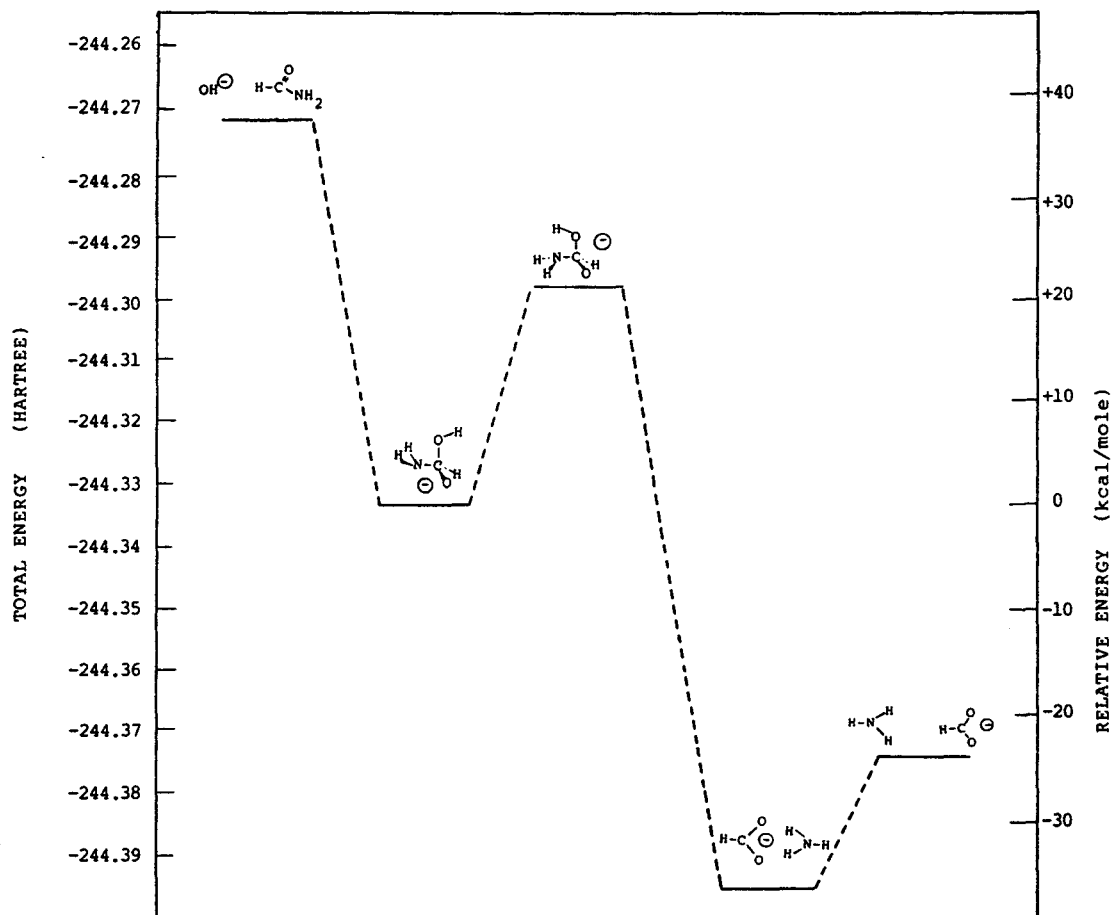
Table II.L Geometrical Parameters^a and Energies of the reaction of formamide with OH⁻.

	reagents	Intermediate configurations									Isolated products
		a	b	c	d	e	f	g	h	i	
E, hartrees	-244.2716	-244.3332	-244.3236	-244.3127	-244.2992	-244.2985	-244.3013	-244.3096	-244.3547	-244.3953	-244.3744
Δ E, kcal/mole	+38.63	0.	+6.02	+12.86	+21.32	+21.76	+20.00	+14.80	-13.48	-38.94	-25.84
Distances, Å											
C-O1		1.5232	1.4957	1.4459	1.4052	1.3845	1.3606	1.3325	1.2738	1.2551	1.2522
O1-H1	0.9844	0.9549	0.9518	0.9518	0.9634	0.9817	1.0259	1.1138	1.4865	2.4325	
N-H1		2.9448	2.1997	2.1006	1.9221	1.7724	1.5583	1.3046	1.0298	1.0021	0.9911
C-N	1.3466	1.4721	1.5201	1.7533	2.0317	2.1617	2.2790				
C-O2	1.2155	1.3151	1.3007	1.0947	1.0820	1.0780	1.0771	1.0797	1.0960	1.2528	1.2522
C-H2	1.0808	1.0937	1.1044	1.2694	1.2375	1.2269	1.2215	1.2225	1.2402	1.1066	1.1126
N-H3	0.9895	0.9998	1.0032	1.0098	1.0147	1.0155	1.0135	1.0080	0.9903	1.0007	0.9911
N-H4	0.9924	1.0006	1.0045	1.0085	1.0129	1.0141	1.0130	1.0087	0.9915	1.0043	0.9911
Angles, degrees											
C-O1-H1		103.37	107.64	105.85	102.52	100.08	97.04	94.12	92.06	106.17	
N-C-O1		105.57	102.59	97.12	88.90	83.58	77.23				
H2-C-O1		101.31	103.20	107.44	111.31	112.79	113.87	114.55	115.25	115.22	114.84
O1-C-O2		110.88	114.64	118.08	120.97	122.38	123.87	125.49	128.61	129.79	130.32
H3-N-C	121.89	112.42	105.75	103.64	106.35	108.14	109.61				
H4-N-C	119.50	108.11	110.79	109.82	114.16	117.29	120.16				
H3-N-H4	118.60	111.72	108.71	107.81	106.95	106.66	106.96	108.37	115.97	105.03	115.87
H2-C-O2	121.52	117.27	116.05	118.56	120.46	120.72	120.27	119.09	116.10	114.99	114.84
H2-C-N		107.16	104.12	97.99	90.84	87.69	85.51				
O2-C-N		113.40	114.58	113.87	115.37	116.96	119.35				
Dihedral Angle, degrees											
N-C-O1-H1		117.63	-10.85	-8.50	-6.45	-5.32	-4.23	-3.58	-3.62		

^aFor the identification of the atoms see figure II.1

Figure II.3

The computed reaction profile for the reaction of formamide with OH^- .



The next step in the reaction is the transfer of the proton from the CHOOH group to the NH₂ group and subsequent fission of the C-N bond. In order to facilitate this transfer the C-O1 bond must rotate so that the H1 atom is almost in the N-C-O1 plane and close to the nitrogen atom. The elongation of the C-N bond is accompanied by a decrease in the C-O1 bond length. It is evident from the molecular graphs that the NH₂ group moves relative to the carbon atom to facilitate the transfer. This can be seen in Table II.1, where the N-C-O1 angle is reduced from 105.57° in the intermediate (configuration a) to 83.58° at the transition state (configuration e). This also decreases the distance between the nitrogen atom and the proton being transferred. Thus the effect of the increasing C-N bond distance on the N to H1 separation during the early stages of the reaction is offset by the rotation of the C-O1 bond and the decrease in the N-C-O1 and C-O1-H1 angles. The energy of the transition state is 21.8 kcal/mole above that of the intermediate and 16.9 kcal/mole below that of the isolated reactants. Thus the reaction between OH⁻ and formamide in the gas phase is barrierless. The transition state is formed early and hence resembles the intermediate in accordance with the Hammond postulate.

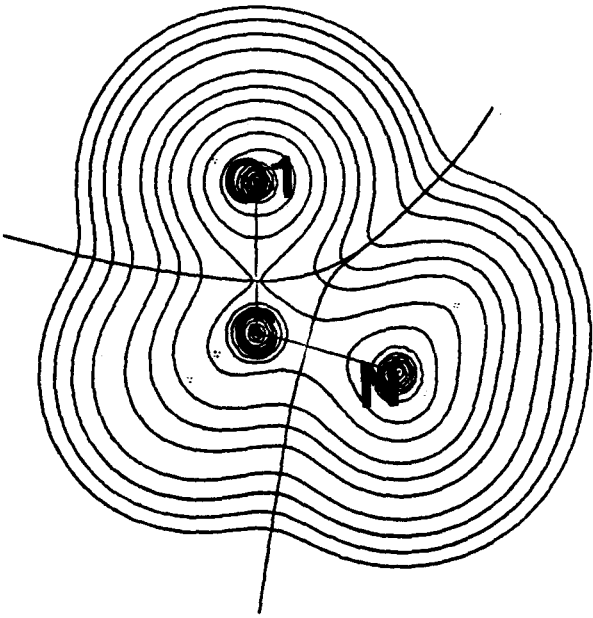
The intramolecular hydrogen transfer proceeds through a bifurcation mechanism in which the proton being transferred is bonded simultaneously to the nitrogen and oxygen atoms resulting in the formation of a four-membered ring. The C-N bond then breaks thereby opening the ring while leaving the O-H bond intact. The O-H bond breaks much later in the reaction and it is not until configuration h that there is any substantial increase in the O-H bond length that would suggest bond breakage has started. After the fission of the O1-H1 bond a new minimum is formed which is almost symmetrical. It is composed of formate anion and ammonia connected by two hydrogen bonds of length 2.4325 Å and 2.2354 Å and the angle made by these two hydrogen atoms and the nitrogen atom being 105.03°. This structure is 13.1 kcal/mole more stable than the isolated products.

The contour diagram of the charge density in the plane formed by the N,C and O1 nuclei is given for each configuration along the reaction coordinate in Figure II.4. The contour diagrams of $\rho(r)$ for configurations b through h show the gradual depletion of charge between the C and N nuclei and the accumulation

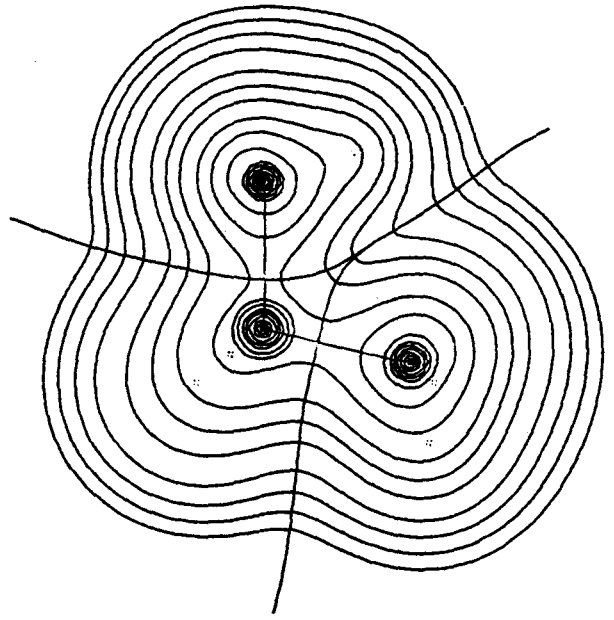
Figure II.4

The contour maps of the charge density for a series of points along the reaction coordinate of the reaction of formamide with OH^- . The maps are in the plane of the N,C and O1 nuclei and overlaid with those bond paths connecting nuclei in this plane. The projections of the interatomic surfaces onto the plane are shown for each bond path.

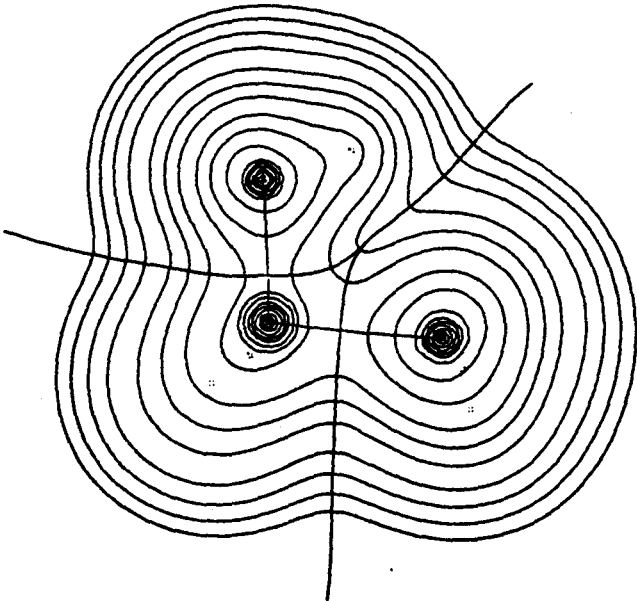
- a) the tetrahedral intermediate.
- b-d) configurations on the reaction path leading to the transition state.
- e) the transition state.
- f-h) configurations on the reaction path leading to the product.
- i) the hydrogen-bonded product.



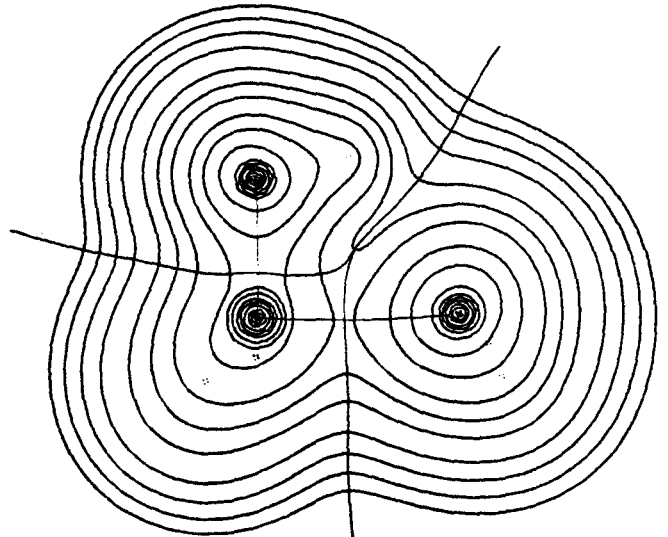
a



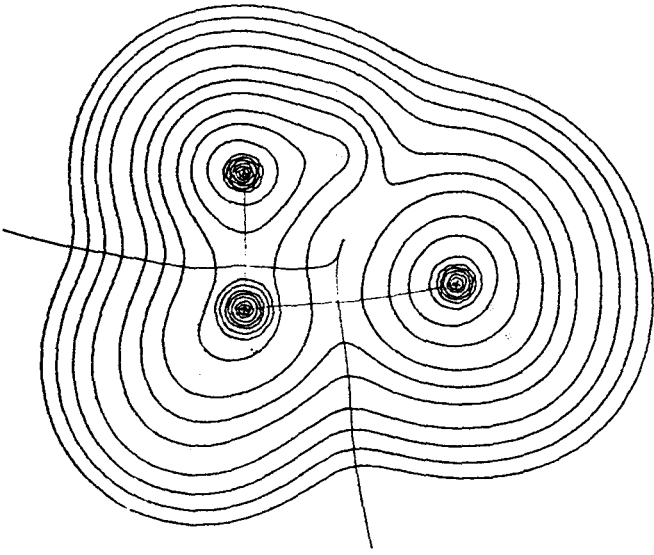
b



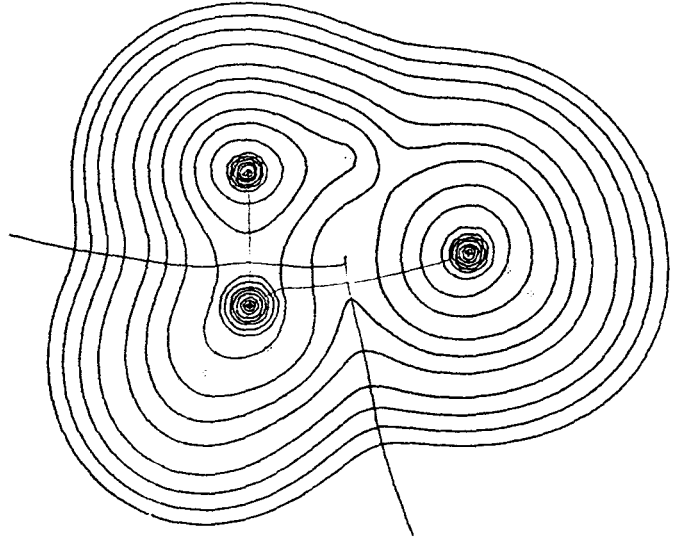
c



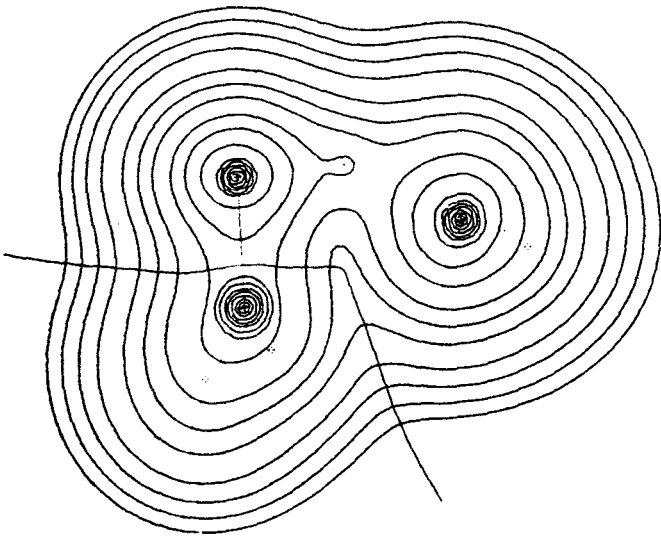
d



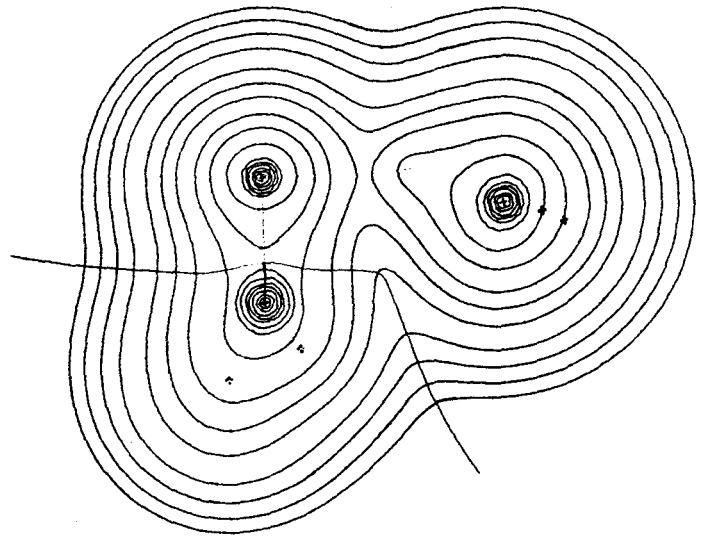
e



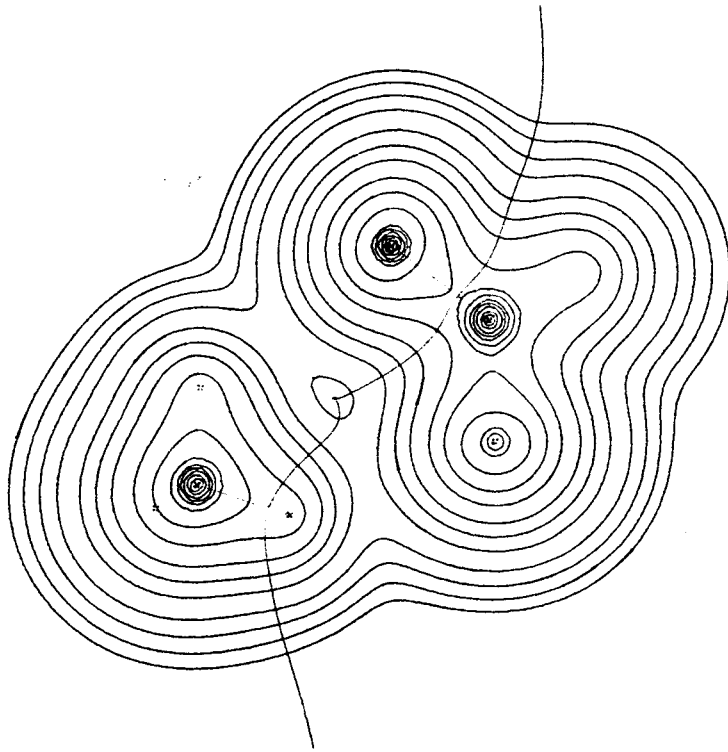
f



g



h



i

Table II.2

Values of ρ and $\nabla^2\rho$ at the critical points in $\rho(r)$ for the reaction of formamide with OH^- .

Bond ^a	property ^b	reactants	intermediate	transition state	product	isolated products
C-N	ρ_b	0.3334	0.2696	0.0549		
	$\nabla^2\rho_b$	-0.7721	-0.9539	0.0927		
C-O2	ρ_b	0.4158	0.3549	0.4068	0.3809	0.3833
	$\nabla^2\rho_b$	0.1529	-0.8586	0.0491	-0.0841	-0.0651
C-O1	ρ_b		0.2015	0.2903	0.3829	0.3833
	$\nabla^2\rho_b$		-0.3805	-0.6055	-0.0691	-0.0651
O1-H1	ρ_b	0.3470	0.3791	0.3372	0.0111	
	$\nabla^2\rho_b$	-1.6717	-2.2437	-2.2870	0.0391	
C-H2	ρ_b	0.3074	0.2970	0.3115	0.2834	0.2782
	$\nabla^2\rho_b$	-1.2721	-1.1550	-1.2942	-1.0648	-1.0241
N-H3	ρ_b	0.3605	0.3589	0.3387	0.3552	0.3582
	$\nabla^2\rho_b$	-2.0186	-1.8947	-1.6345	-1.9541	-1.9378
N-H4	ρ_b	0.3640	0.3574	0.3370	0.3560	0.3582
	$\nabla^2\rho_b$	-2.0275	-1.9120	-1.5862	-1.8613	-1.9378
O2-H3	ρ_b				0.0159	
	$\nabla^2\rho_b$				0.0481	
N-H1	ρ_b			0.0469	0.3560	0.3582
	$\nabla^2\rho_b$			0.1588	-1.8613	-1.9378
ring	ρ_b			0.0406	0.0067	
	$\nabla^2\rho_b$			0.2041	0.0321	

^a For the numbering of atoms see fig. II.1
^b The units of ρ are e/a_0^3 , the units of $\nabla^2\rho$ are e/a_0^5 .

of charge between the N and H1 nuclei. The values of ρ at the bond critical points, given in Table II.2, also indicate the weakening of the C-N bond and strengthening of the N-H1 bond. The value of ρ at the C-N bond critical point is 0.33 au in formamide, however it decreases during the reaction and at the transition state the value of ρ at this critical point is 0.05 au. The value of ρ at the N-H1 bond critical point increases from 0.05 au at the transition state to 0.36 au in the isolated products. The contour diagram of the hydrogen bonded product given in Figure II.4i and shows the ring critical point lying between the two hydrogen bonds.

The changes in the atomic populations and atomic energies relative to their values in the reactants are given for the stationary points in the reaction in Table II.3 and Table II.4 respectively. The relative populations show that on formation of the tetrahedral intermediate charge is transferred out of the OH⁻ group and the nitrogen atom and transferred to the HCO group. In the intermediate the energy of the hydroxyl oxygen atom (O1) is decreased with respect to that of the free hydroxide ion whereas the energy of

Table II.3

Changes in the atomic populations for the reaction of formamide with OH^- relative to their values in the isolated reactants.

reactants	Atom ^a	Intermediate	transition state	product	isolated products
4.0522	C	0.0892	-0.0559	-0.1849	-0.1981
8.4803	N	-0.2551	-0.2427	-0.2305	-0.3613
9.3539	O1	-0.0809	0.0528	0.1215	0.1254
9.3704	O2	0.1041	0.0851	0.1048	0.1089
0.6464	H1	-0.2346	-0.3516	-0.1154	-0.0195
1.0296	H2	0.1266	0.0441	0.1357	0.1578
0.5424	H3	0.1337	0.2397	0.1435	0.0845
0.5248	H4	0.1229	0.2291	0.0436	0.1021

^a for the numbering of atoms see fig. II.1

Table II.4

Changes in the atomic energies^a for the reaction of formamide with OH⁻ relative to their values in the isolated reactants.

reactants	Atom ^b	Intermediate	transition state	product	isolated products
-36.5794	C	0.0231	0.1398	0.1960	0.2109
-55.2578	N	0.2955	0.5837	0.3980	0.4858
-74.8680	O1	-0.4680	-0.6860	-0.6745	-0.6847
-75.5897	O2	0.1785	-0.0112	0.0516	0.0371
-0.4641	H1	0.1076	0.1903	0.0429	-0.0104
-0.6587	H2	-0.0644	-0.0318	-0.0450	-0.0503
-0.4334	H3	-0.0692	-0.1063	-0.0088	-0.0411
-0.4207	H4	-0.0634	-0.1053	-0.0840	-0.0538

^a in au.

^b for the numbering of atoms see fig. II.1

the carbon atom is increased with respect to its energy in formamide. The energy of the hydrogen atom being transferred (H1) increases at the transition state, as does that of the carbon and nitrogen atoms. However, it is the increase in the energy of the nitrogen atom that makes the dominant contribution to the energy barrier in passing from the stable intermediate to the products. In the formation of the hydrogen bonded product, charge density is transferred to the two oxygen atoms from the two hydrogen atoms to which they are hydrogen bonded.

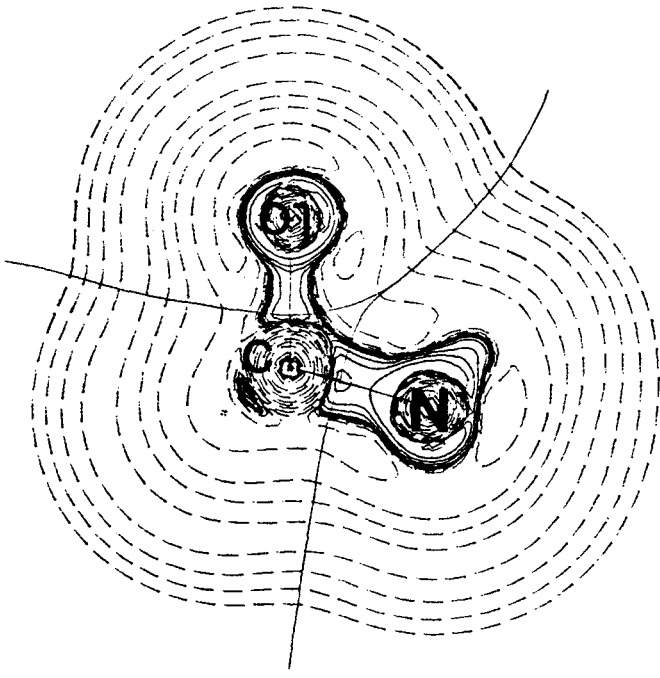
If the Lewis model is invoked to explain some of the conformational changes in the early part of the reaction leading to the transition state, then the NH_2 group distorts in such a way that the nitrogen atom's lone pair of electrons is pointed in the direction of the transferring hydrogen atom. Discussions of bonding and reactivity based upon models that invoke the existence of localized electron pairs, bonded and nonbonded, cannot be related to the form of the charge density itself. The model of localized electron pairs is, however, evident in the form of a function related to $\rho(r)$, its Laplacian distribution. A maximum in $-\nabla^2\rho(r)$

indicates that electronic charge is locally concentrated in that region of space even though the charge density itself exhibits no corresponding maximum. The points where $-\nabla^2\rho$ attains its minimum values locate the "holes" in the valence shell of charge concentration (VSCC), which since they give direct access to the core of the atom, are the sites of nucleophilic attack. The contour diagram of $\nabla^2\rho$ in the plane of the C,N and O1 nuclei is given in Figure II.5 for the points along the reaction coordinate. The changes in the magnitude and orientation of the nonbonded (3,-3) critical point in $\nabla^2\rho$ on the nitrogen atom is of particular interest in the early stages of the reaction prior to the transfer of the hydrogen atom. The values of $\nabla^2\rho$ at this critical point are given in Table II.5 for the configurations on the reaction path leading up to the transition state. The angle formed between the H1 nucleus, the critical point and the N nucleus is also tabulated. This angle is very important because it gives the orientation of the critical point with respect to the two nuclei. The closer this angle is to 180° , the greater the degree of colinearity shared between this critical point and the two nuclei.

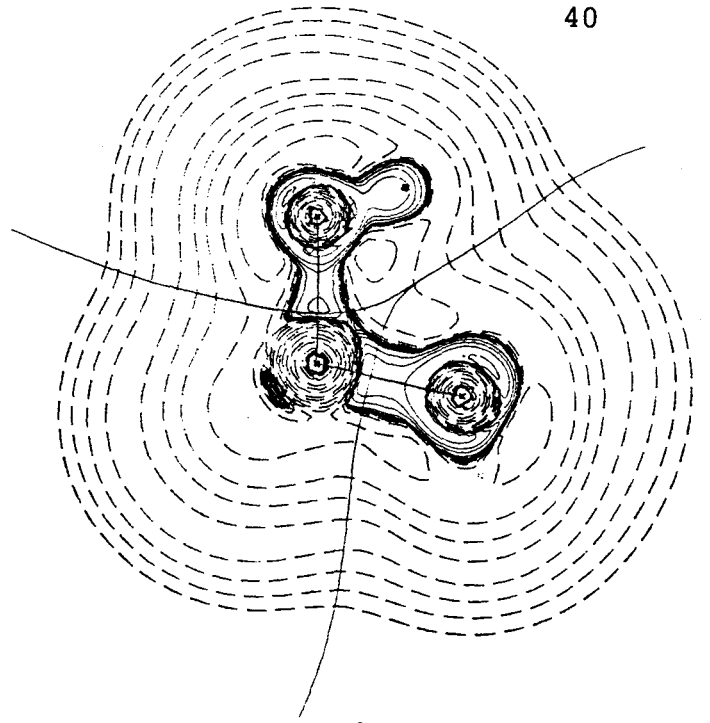
Figure II.5

The contour maps of the Laplacian of the charge density for a series of points along the reaction coordinate of the reaction of formamide with OH^- . The maps are in the plane of the N,C and O1 nuclei and overlaid with those bond paths connecting nuclei in this plane. The projections of the interatomic surfaces onto the plane are shown for each bond path. Dashed contours denote positive values.

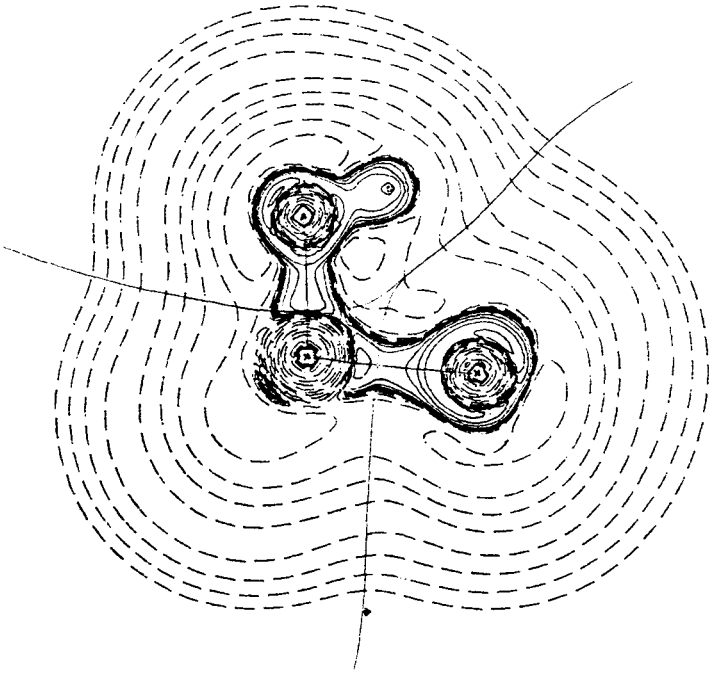
- a) the tetrahedral intermediate.
- b-d) configurations on the reaction path leading to the transition state.
- e) the transition state.
- f-h) configurations on the reaction path leading to the product.
- i) the hydrogen-bonded product.



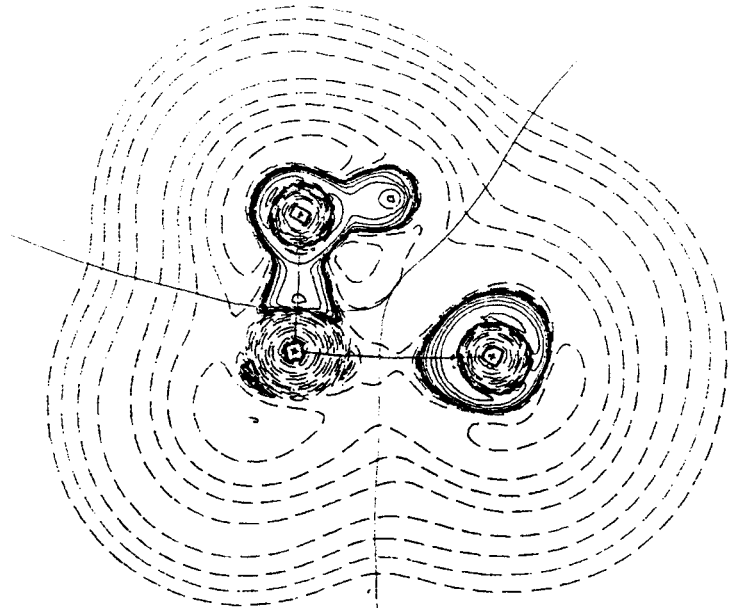
a



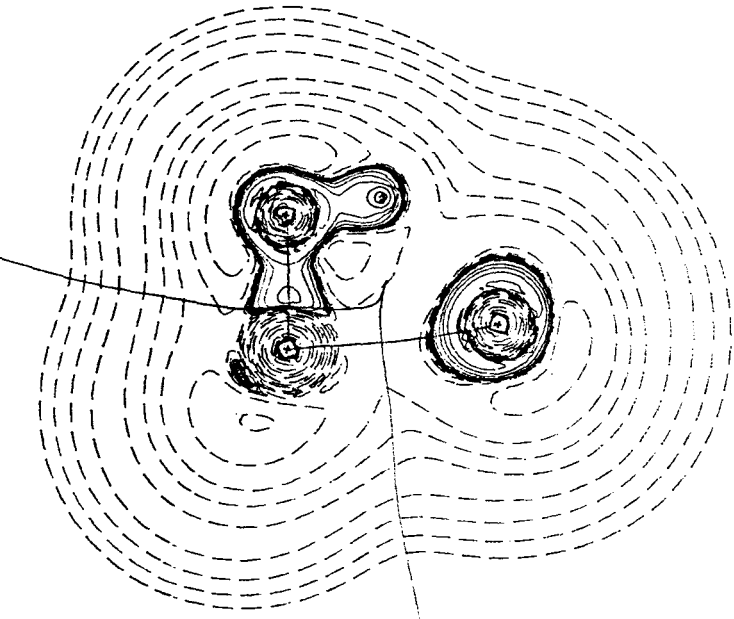
b



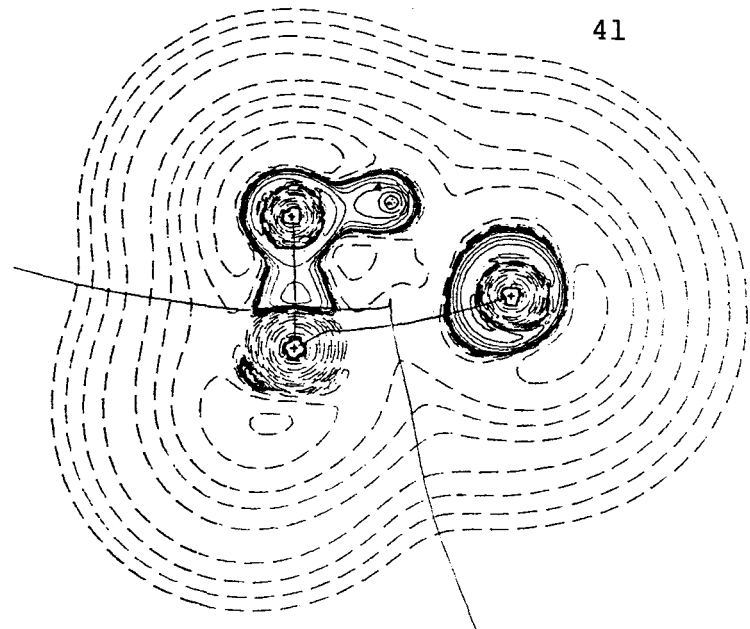
c



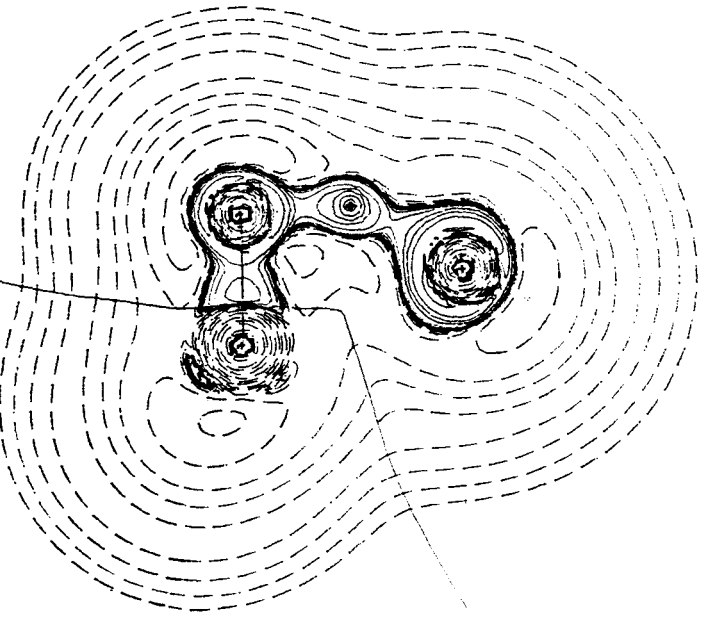
d



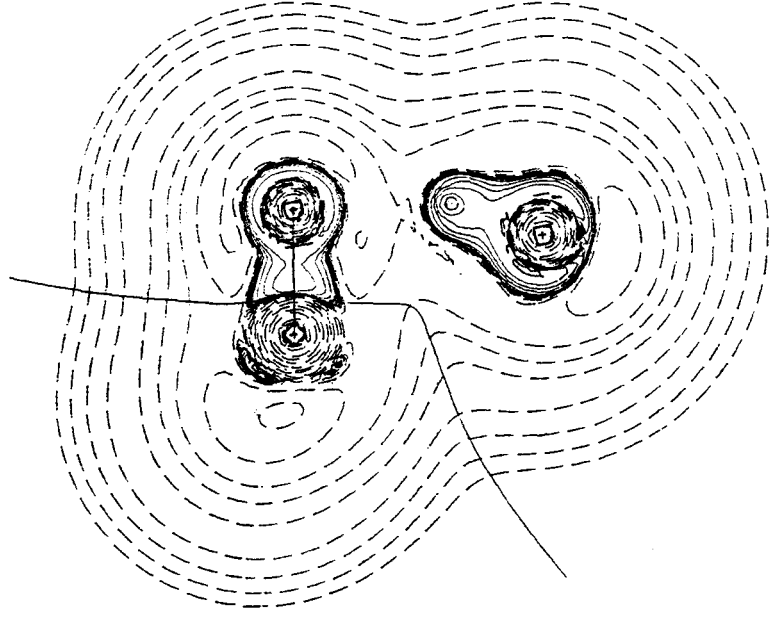
e



f



g



h

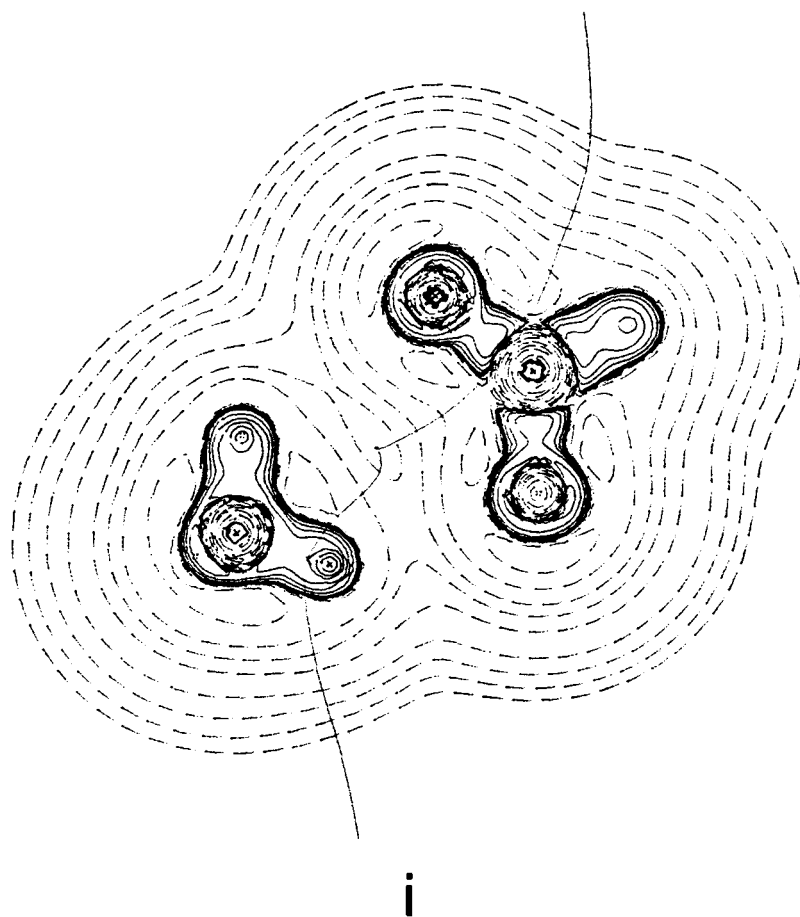


Table II.5

The properties of the nonbonded (3,-3) critical point (cp) in $\nabla^2\rho$ at the nitrogen atom of the $\text{HC}(\text{O}^-)\text{OHNH}_2$ intermediate during the initial stages of the hydrogen transfer from OH^- .

	formamide	a	b	c	d	transition state e
$\nabla^2\rho$ ^a	-2.129	-3.170	-3.149	-2.996	-2.714	-2.562
$r(\text{N}), \text{\AA}$	0.400	0.389	0.390	0.392	0.395	0.397
$r(\text{H1}), \text{\AA}$		3.269	1.981	1.888	1.711	1.555
$\angle \text{N-cp-H1}$ ^b			119.62	117.96	116.88	117.19
$\angle \text{C-N-cp}$	80.95	107.77	110.52	111.15	108.33	105.36
$\angle \text{C-N-H1}$			61.82	59.50	56.31	54.42

^a The units of $\nabla^2\rho$ are $e/a_0^5 = 24.100e/\text{\AA}^5$

^b All angles are in degrees.

When formamide reacts with OH^- to form the stable intermediate the NH_2 group pyramidalizes as evident in figure II.2a. This pyramidalization has the effect of increasing the magnitude of the nonbonded charge concentration in the VSCC of the nitrogen atom which in turn facilitates the transfer of the hydrogen atom. During the transfer the nonbonded (3,-3) critical point moves further from the nitrogen nucleus and the magnitude of the local charge concentration decreases. The reason for these changes is that during the hydrogen transfer the nonbonded (3,-3) critical point of nitrogen is changing to a bonded (3,-3) critical point. In general the nonbonded charge concentrations are considerably greater than the bonded concentrations when on the same atom because the bonded charge concentration is shared between two nuclei. In addition, the radial curvature of $-\nabla^2\rho$, the curvature perpendicular to the surface of the sphere of charge concentration, is always greater for the bonded than for the nonbonded charge concentrations. When configuration h is reached the hydrogen transfer is complete and a new nonbonded (3,-3) critical point is created at the oxygen atom from what was formerly a bonded (3,-3) critical point.

Chapter 3

The acid catalyzed hydrolysis of formamide

A: hydrolysis with protonation on the nitrogen.

Unlike the reaction of formamide with OH^- , there have been no thorough theoretical studies of the acid catalyzed hydrolysis of formamide. The mechanism of the acid catalyzed hydrolysis of formamide is still not well understood from either a theoretical or an experimental standpoint. Although much work has been done to determine the predominant site of protonation, very little has been done to determine the details of the mechanism after this initial protonation step. An extended Hückel molecular orbital study (EHMO) on the N-protonation pathway found the reaction leading to separated formic acid and ammonium ion to be exothermic by 32.5 kcal/mole with the formyl ion being a minimum in the reaction (Csizmadia et al., 1968). In this mechanism the protonation takes place on the nitrogen atom followed by the heterolytic cleavage of the C-N bond yielding ammonia and the formyl ion, HCO^+ . The

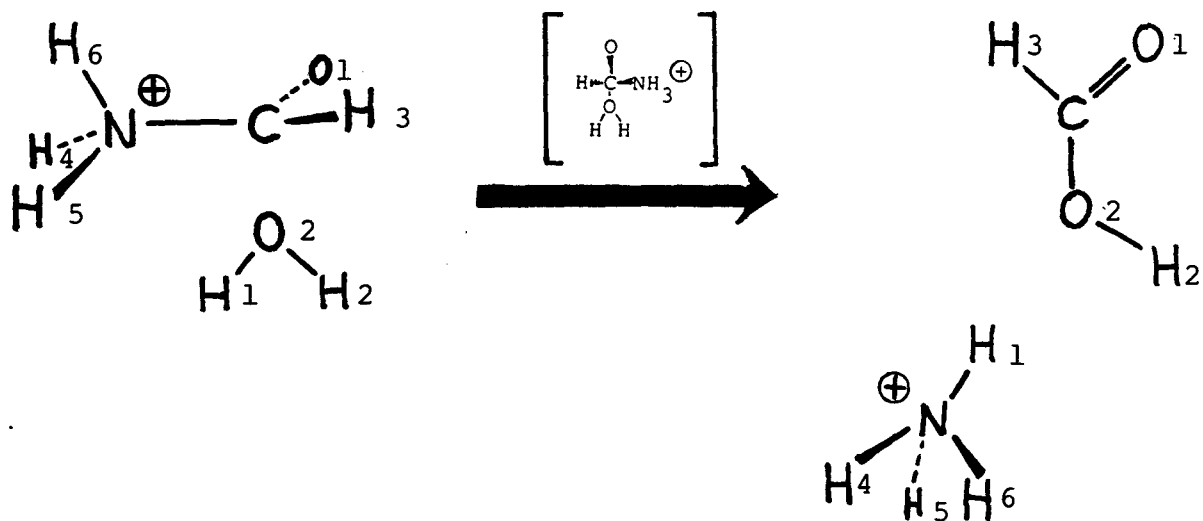
formyl ion then reacts with a water molecule to give protonated formic acid, which subsequently reacts with the free ammonia molecule to give the final products. The EHMO method predicts the nitrogen atom to be the predominant site of protonation, contrary to the experimental results. An ab initio study of this reaction mechanism (Hopkinson and Csizmadia, 1973) gave a very different reaction profile from that obtained using the EHMO method. In the ab initio calculations the heterolytic cleavage of N-protonated formamide is predicted to be endothermic by 67.3 kcal/mole, which is in sharp contrast to the exothermic prediction of the EHMO calculation. The formyl ion is then attacked by water giving protonated formic acid and ammonia. The final products, formic acid and NH_3 , lie 107.9 kcal/mole below that of the formyl ion, H_2O and NH_3 , whereas the EHMO calculations give the opposite energy ordering. The ab initio calculations also correctly predict the oxygen atom to be the predominant site of protonation. No energy barriers were calculated, however it was assumed that the formation of the formyl ion is the slow step. This assumption can be justified by the fact that the formyl ion, like all acylium ions, is stable only as a salt with SbF_6^- ions or in oleum solutions (Deno et al., 1968) and quickly picks up water in

most acidic solutions to produce the corresponding carboxylic acid. Since only the N-protonated formamide ion is involved in the rate-limiting step the mechanism outlined above is unimolecular.

It is also possible that the reaction may follow a bimolecular mechanism. Since the N-protonated formamide ion decomposes slowly it will exist for an appreciable time and it is therefore possible that N-protonated formamide may react with a water molecule before the C-N bond has had a chance to break. In this mechanism the hydrolysis would take place in a single step in which the oxygen atom of the water molecule would form a bond with the carbon atom while the C-N bond is breaking. This mechanism would involve the passage through a transition state in which the carbon atom is bonded to both the nitrogen atom and the oxygen atom from the water molecule. Therefore in order to be complete, a study of the hydrolysis of N-protonated formamide must consider both of these two possible reaction pathways. The actual mechanism followed will depend on the relative energy barriers of the two pathways.

Figure III.A.1

The reaction scheme for the hydrolysis of N-protonated formamide to the hydrogen-bonded product. The transition state is shown in brackets.



The initial protonation reaction in which the proton binds to the nitrogen atom of formamide is calculated to be exothermic by 13.4 kcal/mole. This value is considerably less than the value of 22.3 kcal/mole reported previously (Hopkinson and Csizmadia, 1973). This discrepancy is due to the fact that a much larger basis set has been used in the present calculation. After this initial protonation step the reaction can then follow either the unimolecular or the bimolecular reaction mechanism, the latter possibility will be discussed first.

An outline of the bimolecular reaction scheme is given in Figure III.A.1. As a water molecule approaches N-protonated formamide the energy of the system increases. The preferred orientation of approach for the water molecule is approximately perpendicular to the plane of the N-protonated formamide molecule and with the oxygen atom of the water molecule approaching the carbon atom at a right angle to the C-N bond. A transition state is reached when the oxygen atom of the water molecule is 1.70 \AA from the carbon nucleus. At this point the energy of the system is 10.7 kcal/mole above that of the isolated N-protonated

Figure III.A.2

The molecular graphs for a series of points along the reaction coordinate of the hydrolysis of N-protonated formamide.

- a-d) configurations on the reaction path leading to the transition state.
- e) the transition state.
- f-h) configurations on the reaction path leading to the product.
- i) the hydrogen-bonded product.

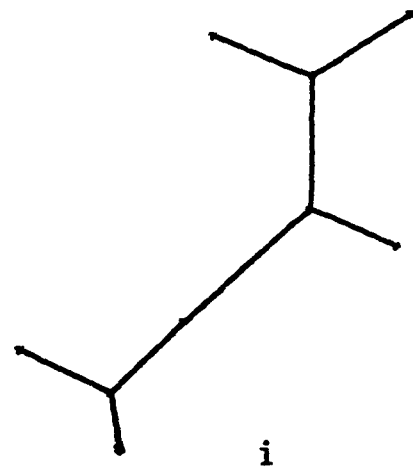
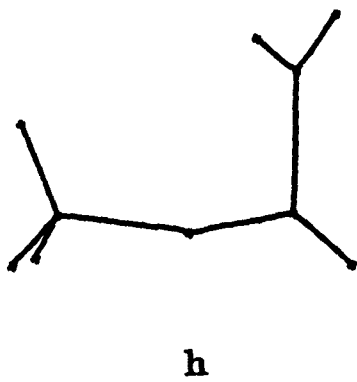
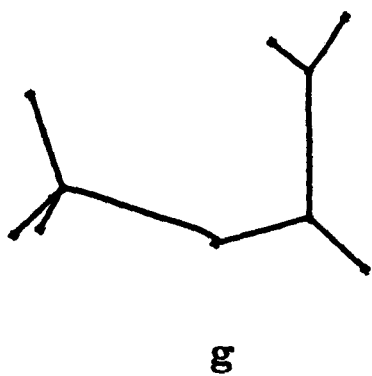
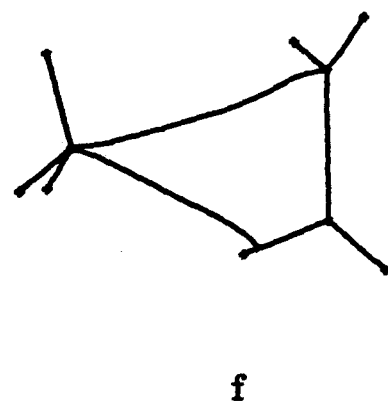
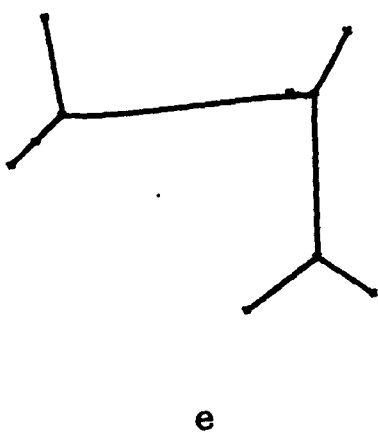
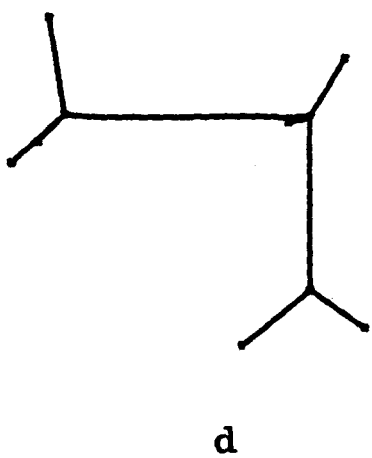
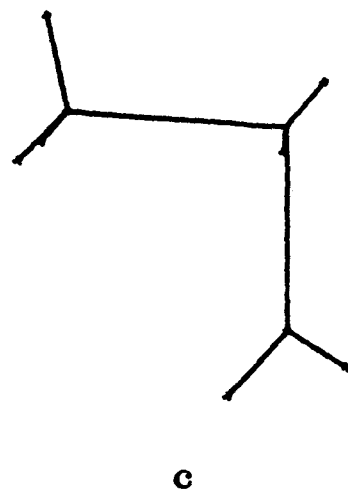
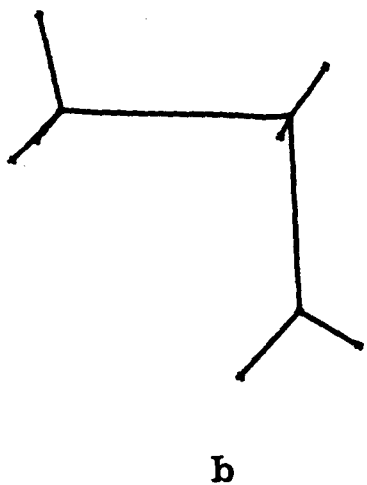
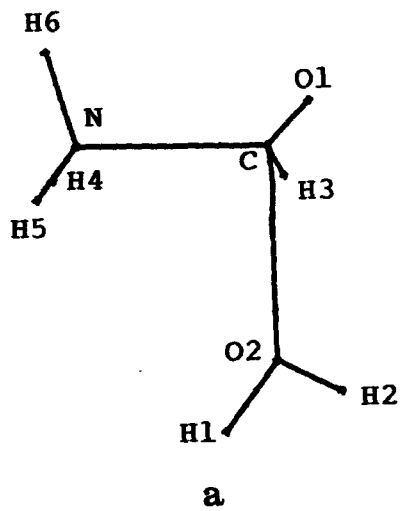


Table III.A.1

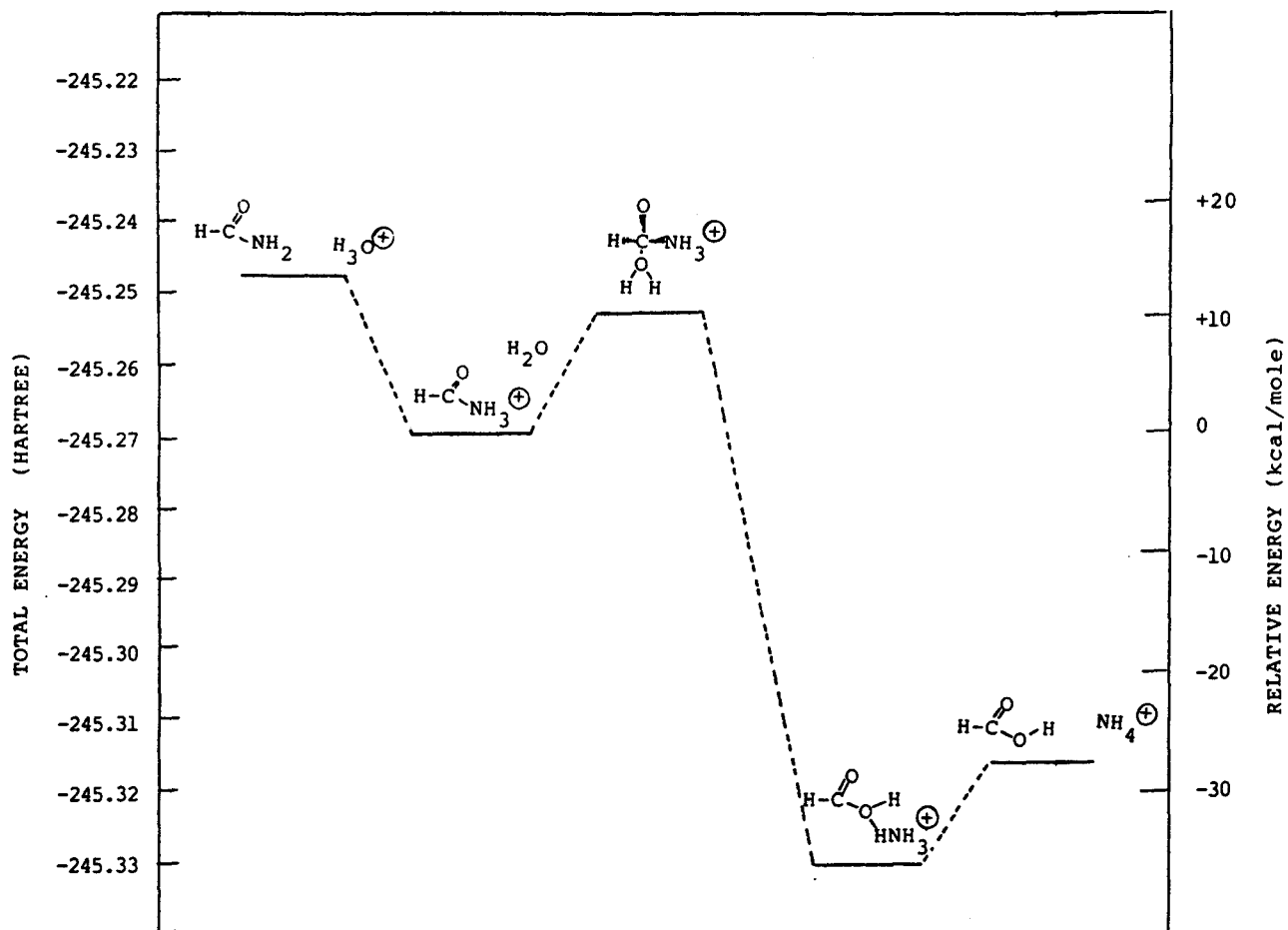
Geometrical Parameters^a and Energies of the reaction of N-protonated formamide with water

	reagents ^b	Intermediate configurations									Isolated products
		a	b	c	d	e	f	g	h	i	
E, hartrees	-245.2697	-245.2700	-245.2610	-245.2580	-245.2532	-245.2527	-245.2570	-245.2635	-245.2752	-245.3263	-245.3137
ΔE , kcal/mole	0.	+0.19	+5.46	+7.34	+10.35	+10.66	+7.96	+3.89	-3.45	-35.44	-27.59
Distances, Å											
C-O2		2.2447	2.1281	2.0388	1.8124	1.6993	1.5460	1.4983	1.4564	1.3846	1.3417
C-N	1.5282	1.9658	2.2339	2.3473	2.5134	2.5817	2.7276				
O2-H1	0.9566	0.9540	0.9541	0.9544	0.9561	0.9578	0.9712	1.0056	1.0915	1.7326	
C-O1	1.1755	1.1358	1.1217	1.1203	1.1295	1.1389	1.1554	1.1621	1.1693	1.1856	
C-H3	1.0521	1.0590	1.0561	1.0558	1.0575	1.0593	1.0635	1.0657	1.0681	1.0712	1.0723
N-H6	1.0155	1.0039	1.0029	1.0026	1.0025	1.0027	1.0047	1.0062	1.0075	1.0095	1.0116
N-H4	1.0145	1.0057	1.0039	1.0036	1.0033	1.0032	1.0037	1.0040	1.0050	1.0093	1.0116
N-H5	1.0145	1.0055	1.0035	1.0029	1.0025	1.0026	1.0045	1.0063	1.0083	1.0095	1.0116
O2-H2	0.9566	0.9553	0.9557	0.9562	0.9588	0.9606	0.9629	0.9627	0.9618	0.9609	0.9564
N-H1									1.3466	1.0352	1.0116
Angles, degrees											
N-C-O2		92.08	94.21	94.07	90.25	86.42	72.91				
O2-C-H3		80.45	83.97	87.60	96.15	100.37	105.45	106.41	107.56	110.92	110.45
O2-C-O1		105.67	106.86	107.76	111.81	113.96	117.43	119.26	120.88	122.27	124.56
O1-C-H3	129.07	148.25	158.28	159.21	150.95	145.17	137.08	134.32	131.51	126.81	124.99
H1-O2-H2	111.20	110.66	111.27	111.92	114.29	115.85	119.79	122.27	124.37	115.95	
H6-N-H5	111.49	110.60	110.06	109.80	109.39	109.17	108.48	108.29	108.07	109.16	109.50
H6-N-H4	108.76	109.74	109.54	109.43	109.12	108.92	108.40	108.27	108.14	109.14	109.50
H5-N-H6	111.50	110.30	110.18	110.15	110.11	108.94	109.03	108.21	107.83	109.35	109.50
H6-C-N	107.79	106.11	104.51	99.30	95.77	87.30					
Dihedral Angle, degrees											
N-C-O2-H1		37.23	35.08	33.84	29.88	26.63	15.67	9.89	5.70		

^a For the identification of the atoms see figure III.A.1

Figure III.A.3

The computed reaction profile for the acid-catalyzed hydrolysis of formamide with protonation on the Nitrogen atom.



formamide and water molecules, however it is still below that of formamide and H_3O^+ by 2.8 kcal/mole. If the intrinsic reaction coordinate is followed down from this transition state it leads to a hydrogen bonded product of NH_4^+ and formic acid with an energy lying 48.8 kcal/mole below that of the isolated formamide molecule and H_3O^+ ion.

The molecular graphs of the reactants, products and some of the configurations along the reaction path are given in Figure III.A.2. The corresponding energies and geometries for each of these structures is given in Table III.A.1 and the energy profile for this reaction is given in Figure III.A.3. As the distance between the oxygen atom of the water molecule and the carbon atom decreases, the C-N bond length increases. At the same time one of the O-H bonds in the water molecule also increases, slowly before the transition state but then very rapidly after the transition state. This hydrogen atom is eventually transferred to the nitrogen atom. The other O-H bond in the water molecule does not change during the reaction however the H-O-H angle increases steadily. The geometry of the NH_3 group remains constant throughout the reaction with none of the N-H bond lengths changing by more than 0.01 Å.

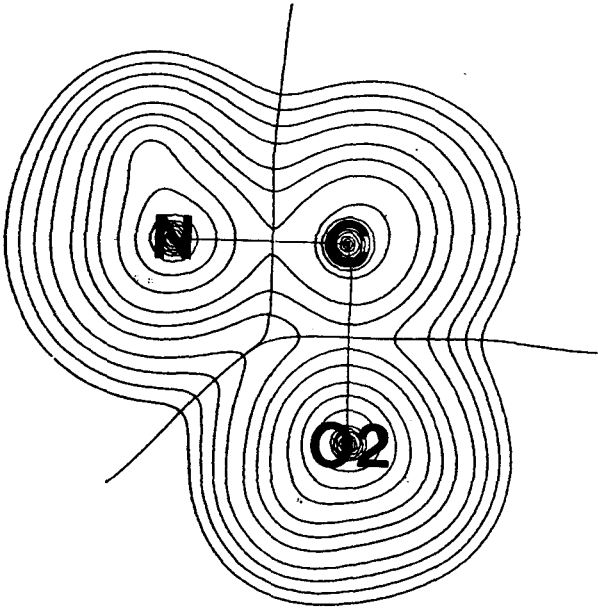
and none of the H-N-H bond angles changing by more than 3° . Therefore this step of the reaction can be considered as an ammonia transfer reaction in which the NH_3 group is transferred from the carbon atom to one of the hydrogen atoms of the water molecule. Throughout the course of the reaction there is a steady decrease in the dihedral angle formed by the N,C,O2 and H1 nuclei. This dihedral angle, which is given in Table II.A.1, is very important because it indicates not only the degree to which these four atoms lie in a plane but also the relative orientation of the hydrogen atom being transferred with respect to the nitrogen atom. When all four atoms are in a plane and the hydrogen and nitrogen atoms are on the same side of the C-O2 bond this dihedral angle is 0° . In the hydrogen bonded product all of these atoms lie in a plane. The energy required to separate the hydrogen-bonded product into isolated formic acid and NH_4^+ is 7.6 kcal/mole. It is interesting to note that since the energy of the transition state is below that of the isolated H_3O^+ and formamide molecules, the hydrolysis of formamide via the N-protonation pathway is a barrierless process.

The contour diagram of the charge density in the plane formed by the N,C and O₂ nuclei is given in Figure III.A.4 for all the selected points along the reaction path. These contour diagrams show the gradual buildup of charge density between the oxygen nucleus of the water molecule and the carbon nucleus along with the gradual depletion of charge between the carbon and nitrogen nuclei. This buildup of charge between the carbon and oxygen atoms is evident from the values of ρ at the bond critical point between these nuclei given in Table III.A.2. The value of ρ at this critical point increases from 0.12 au in the transition state to 0.30 au in the isolated products. In the steps leading to the transition state the value of ρ at the bond critical point between the carbon and nitrogen nuclei decreases sharply indicating that the breaking of this bond occurs before the transition state is reached. At configuration f a nonplanar four-membered ring is formed with the C,N,H₁ and O₂ atoms. At configuration g the C-N bond path breaks leaving the nitrogen atom bonded to one of the hydrogen atoms of the water molecule. At this point the hydrogen atom is still closer to the oxygen atom than the nitrogen atom however in the subsequent two configurations this hydrogen atom is transferred to the nitrogen atom.

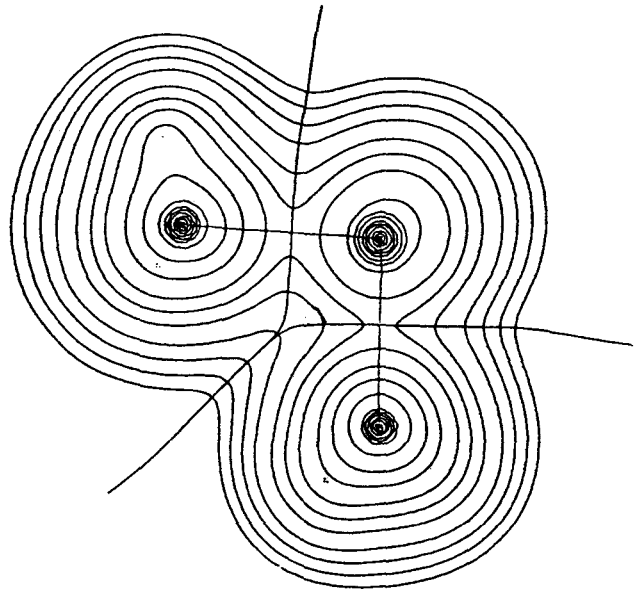
Figure III.A.4

The contour maps of the charge density for a series of points along the reaction coordinate of the hydrolysis of N-protonated formamide. The maps are in the plane of the N,C and O2 nuclei and overlaid with those bond paths connecting nuclei in this plane. The projections of the interatomic surfaces onto the plane are shown for each bond path.

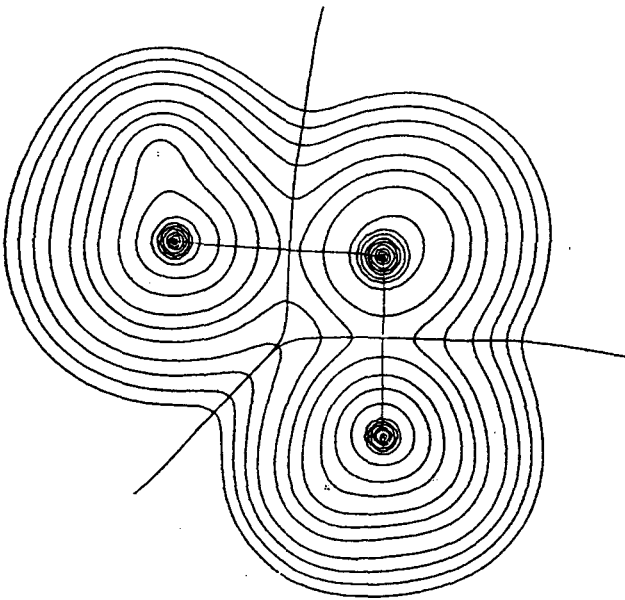
- a-d) configurations on the reaction path leading to the transition state.
- e) the transition state.
- f-h) configurations on the reaction path leading to the product.
- i) the hydrogen-bonded product.



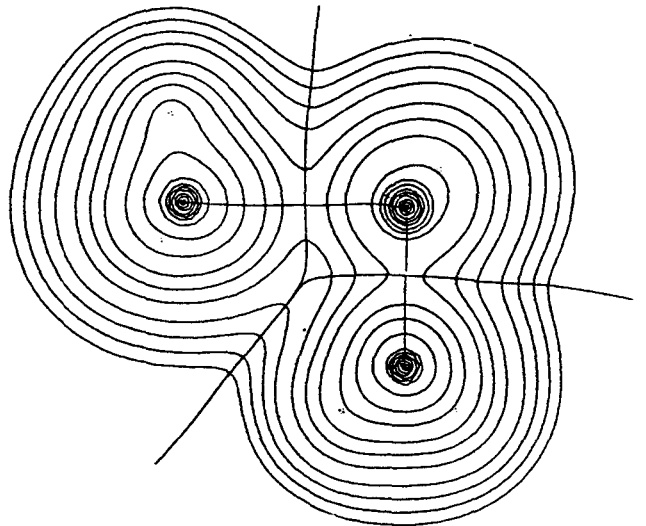
a



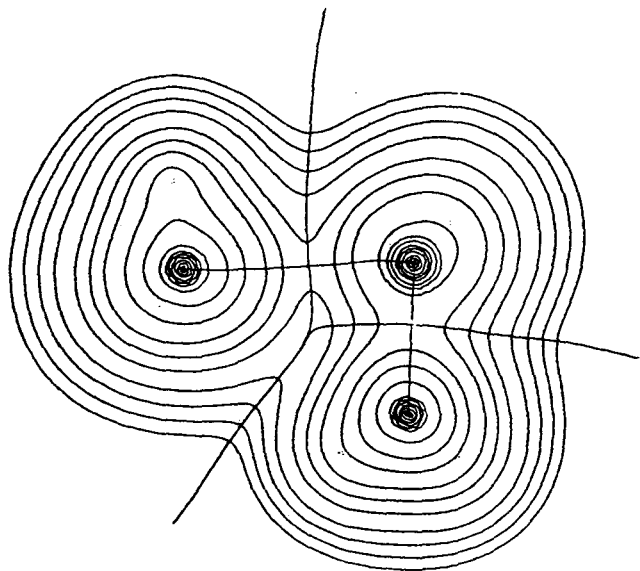
b



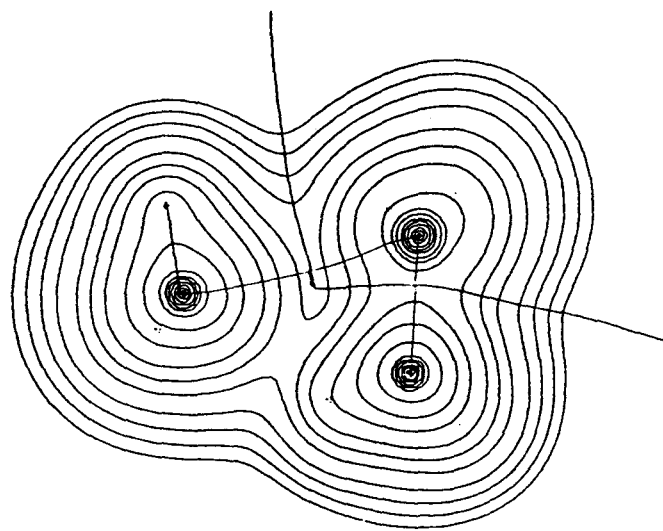
c



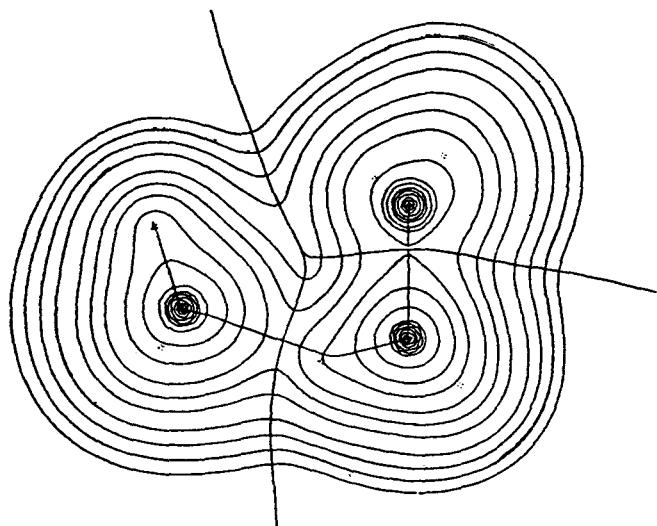
d



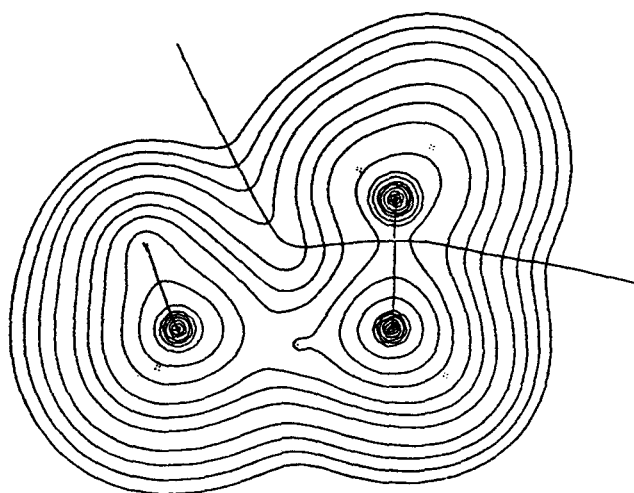
e



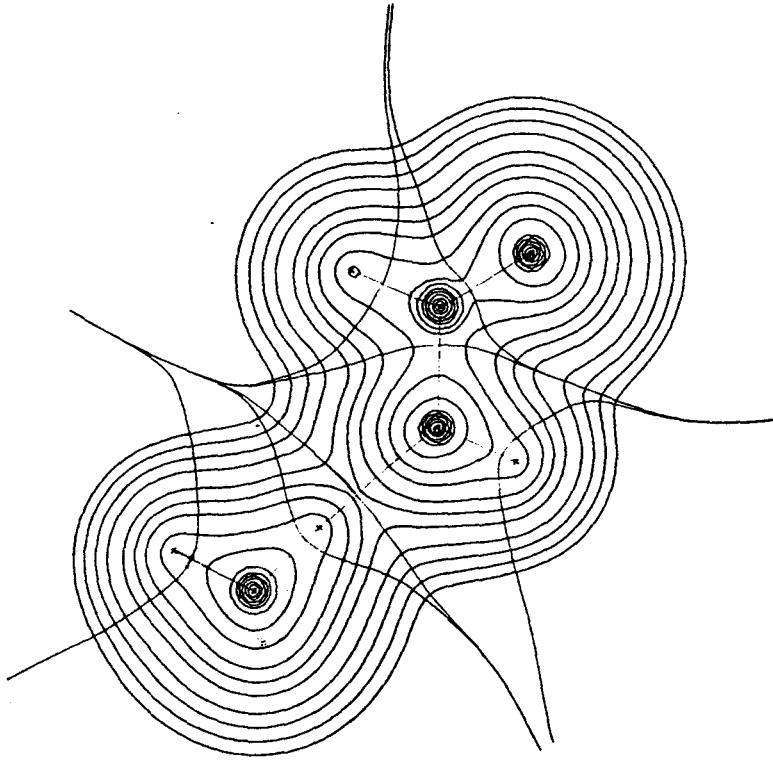
f



g



h



i

Table III.A.2

Values of ρ and $\nabla^2\rho$ at the critical points in $\rho(r)$ for the reaction of N-protonated formamide with water.

Bond ^a	property ^b	reactants ^c	transition state	product	isolated products
C-N	ρ_b	0.2291	0.0228		
	$\nabla^2\rho_b$	-0.6721	0.0673		
C-O1	ρ_b	0.4475	0.4840	0.4420	0.4285
	$\nabla^2\rho_b$	0.7524	1.0411	0.4906	0.3355
C-O2	ρ_b		0.1182	0.2679	0.3018
	$\nabla^2\rho_b$		0.0513	-0.1551	-0.1306
O2-H1	ρ_b	0.3814	0.3597	0.0380	
	$\nabla^2\rho_b$	-2.3606	-2.5945	0.1329	
O2-H2	ρ_b	0.3814	0.3556	0.3646	0.3732
	$\nabla^2\rho_b$	-2.3606	-2.5692	-2.4409	-2.4245
C-H3	ρ_b	0.3161	0.3247	0.3174	0.3169
	$\nabla^2\rho_b$	-1.4359	-1.6588	-1.4009	-1.3819
N-H4	ρ_b	0.3458	0.3547	0.3513	0.3492
	$\nabla^2\rho_b$	-2.0165	-1.9556	-2.0388	-2.0420
N-H5	ρ_b	0.3468	0.3548	0.3515	0.3492
	$\nabla^2\rho_b$	-2.0079	-1.9542	-2.0387	-2.0420
N-H6	ρ_b	0.3468	0.3548	0.3513	0.3492
	$\nabla^2\rho_b$	-2.0079	-1.9529	-2.0388	-2.0420
N-H1	ρ_b			0.3227	0.3492
	$\nabla^2\rho_b$			-1.8928	-2.0420

^a For the numbering of atoms see fig. III.A.1

^b The units of ρ are e/a^3 , the units of $\nabla^2\rho$ are e/a^5 .

^c N-protonated formamide and water at infinite separation.

The relative atomic populations at the stationary points in the reaction are given in Table III.A.3. In the steps leading up to the transition state charge is transferred out of the carbon atom. This trend is continued for the steps leading down to the products. The relative atomic energies, given in Table III.A.4, show that it is the NH_3 group that makes the dominant contribution to the activation barrier of the reaction.

The contour diagrams of $-\nabla^2\rho$ in the plane formed by the N,C and O2 nuclei are given in Figure III.A.5 for the points along the reaction coordinate. The carbon atom in N-protonated formamide has two (3,+1) critical points in $\nabla^2\rho$ above and below the plane of the CHO group. These two critical points are "holes" in the VSCC and it is through these holes that the nucleophile will attack the carbon atom. Before the transition state is reached this hole in the VSCC no longer exists and is instead replaced by a bonded charge concentration. This is because a bond is being formed in the region between the carbon atom and the water molecule. The value of $\nabla^2\rho$ at the (3,+1) critical point being attacked is given in Table III.A.5 for the points along the reaction coordinate leading to the

Table III.A.3

Changes in the atomic populations for the reaction of N-protonated formamide with water relative to their values in the isolated reactants^a.

reactants ^a	Atom ^b	transition state	product	isolated products
4.3290	C	-0.0768	-0.2649	-0.3191
8.2653	N	-0.0123	0.0117	-0.0297
9.2172	O1	0.0386	0.1300	0.1483
9.2511	O2	0.0400	0.0605	0.0760
0.3744	H1	-0.1002	-0.0037	0.0667
0.3744	H2	-0.1042	-0.0611	-0.0377
0.8478	H3	-0.1359	0.0850	0.1169
0.4532	H4	0.1321	0.0260	0.0043
0.4573	H5	0.1040	0.0040	-0.0162
0.4368	H6	0.1117	0.0079	-0.0121

^a N-protonated formamide and water at infinite separation.

^b for the numbering of atoms see fig.III.A.1

Table III.A.4

Changes in the atomic energies^a for the reaction of N-protonated formamide with water relative to their values in the isolated reactants^b.

reactants ^b	Atom ^c	transition state	product	isolated products
-36.7638	C	0.0746	0.1969	0.2288
-55.1449	N	0.2242	0.0034	0.0785
-75.6469	O1	-0.1419	-0.0325	-0.0288
-75.3474	O2	-0.1380	-0.2064	-0.2621
-0.3376	H1	0.0684	0.0127	-0.0322
-0.3376	H2	0.0727	0.0430	0.0245
-0.5740	H3	0.0596	-0.0433	-0.0599
-0.4396	H4	-0.0636	-0.0061	0.0063
-0.4422	H5	-0.0624	-0.0034	0.0100
-0.4351	H6	-0.0863	-0.0172	-0.0047

^a in au.

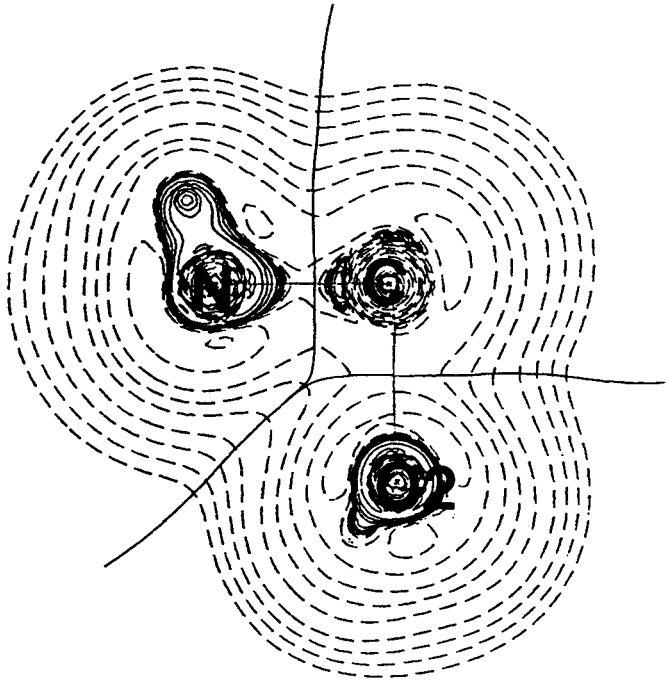
^b N-protonated formamide and water at infinite separation.

^c for the numbering of atoms see fig. III.A.1

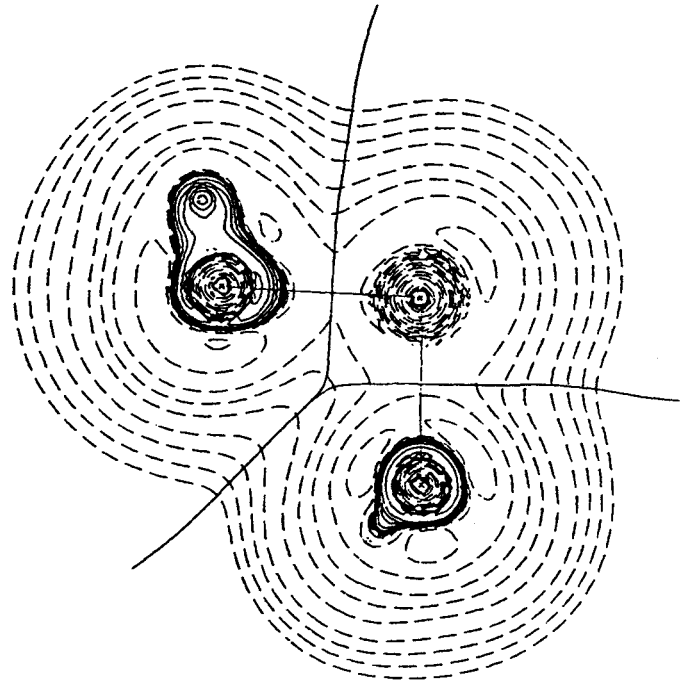
Figure III.A. 5

The contour maps of the Laplacian of the charge density for a series of points along the reaction coordinate of the hydrolysis of N-protonated formamide. The maps are in the plane of the N,C and O2 nuclei and overlaid with those bond paths connecting nuclei in this plane. The projections of the interatomic surfaces onto the plane are shown for each bond path. Dashed contours denote positive values.

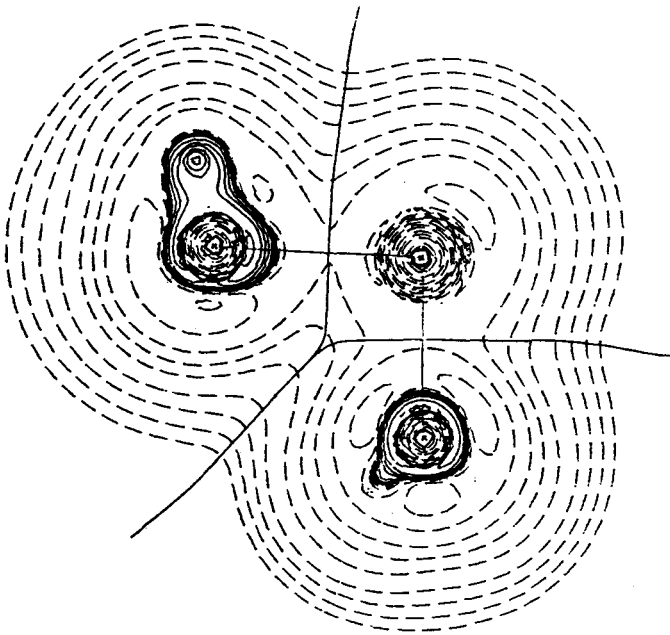
- a-d) configurations on the reaction path leading to the transition state.
- e) the transition state.
- f-h) configurations on the reaction path leading to the product.
- i) the hydrogen-bonded product.



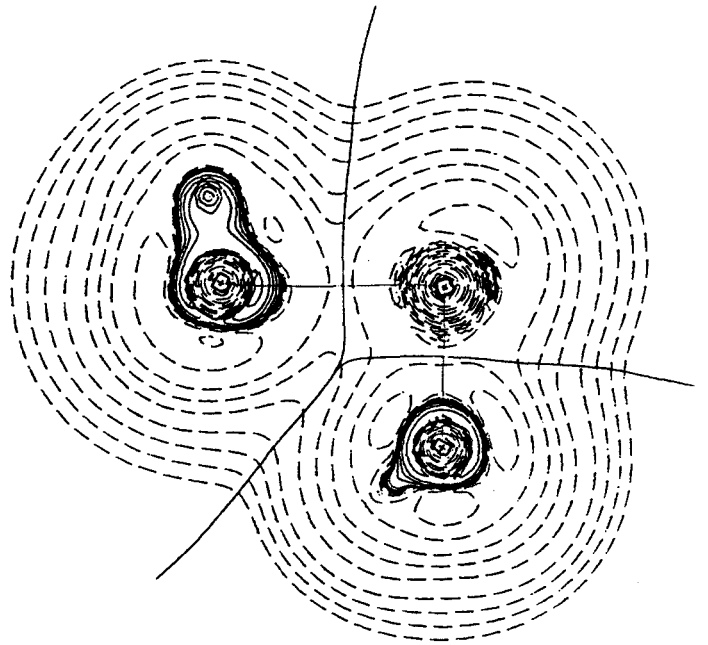
a



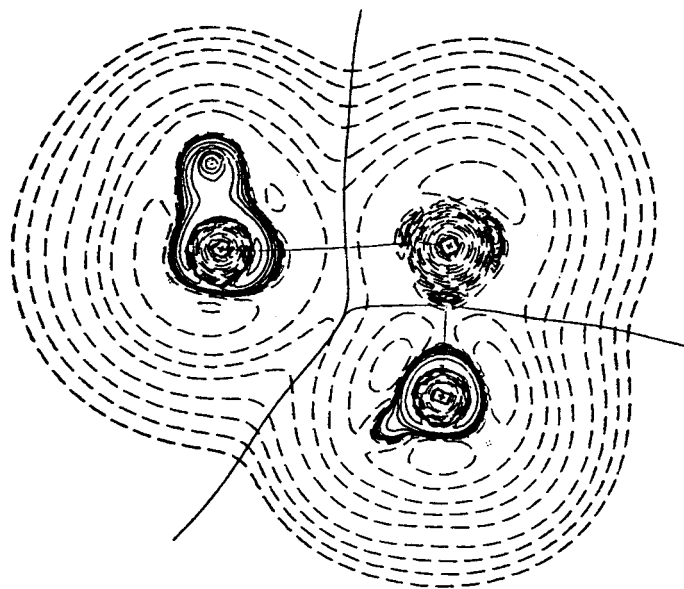
b



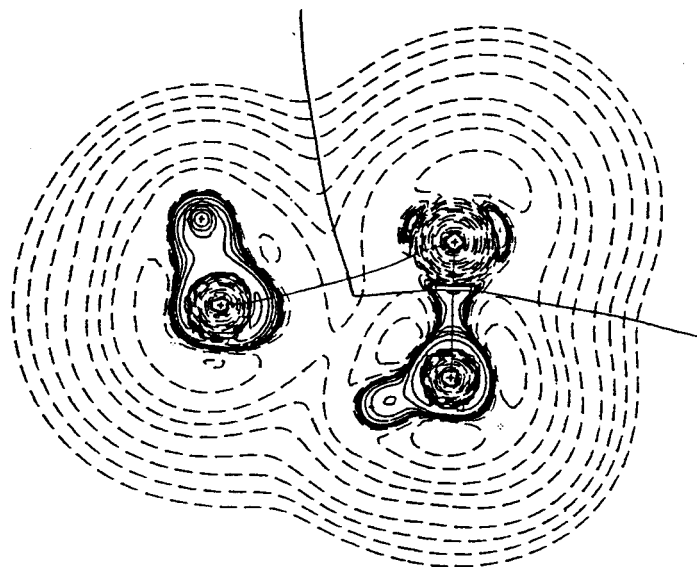
c



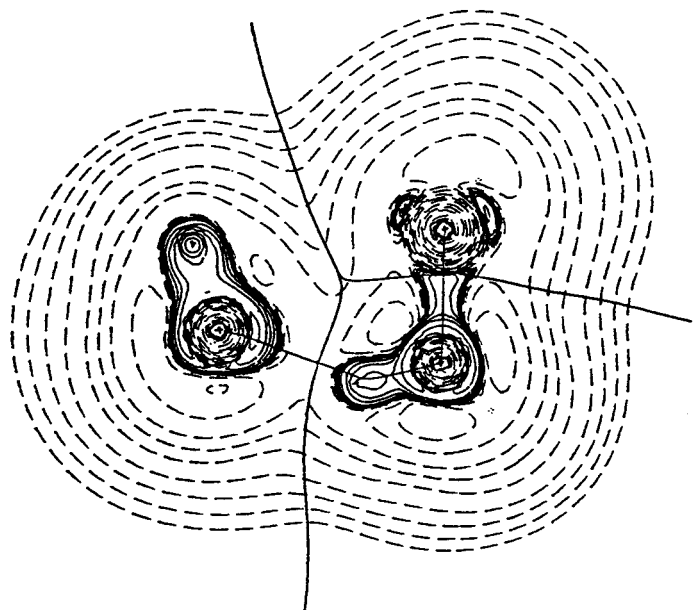
d



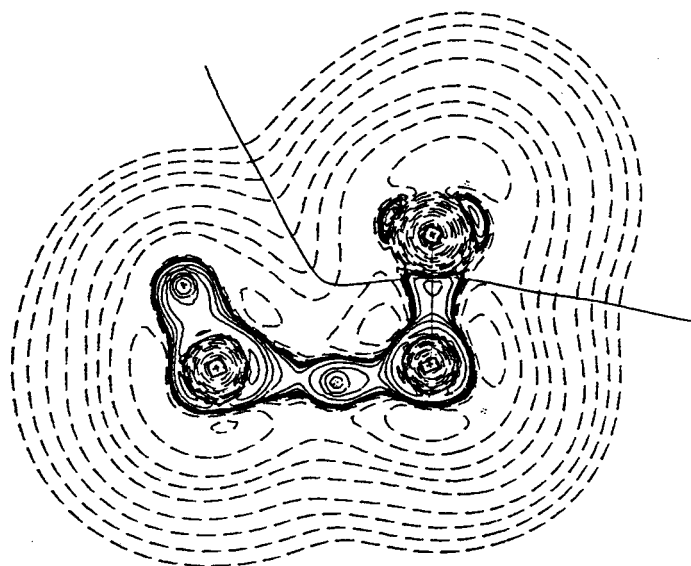
e



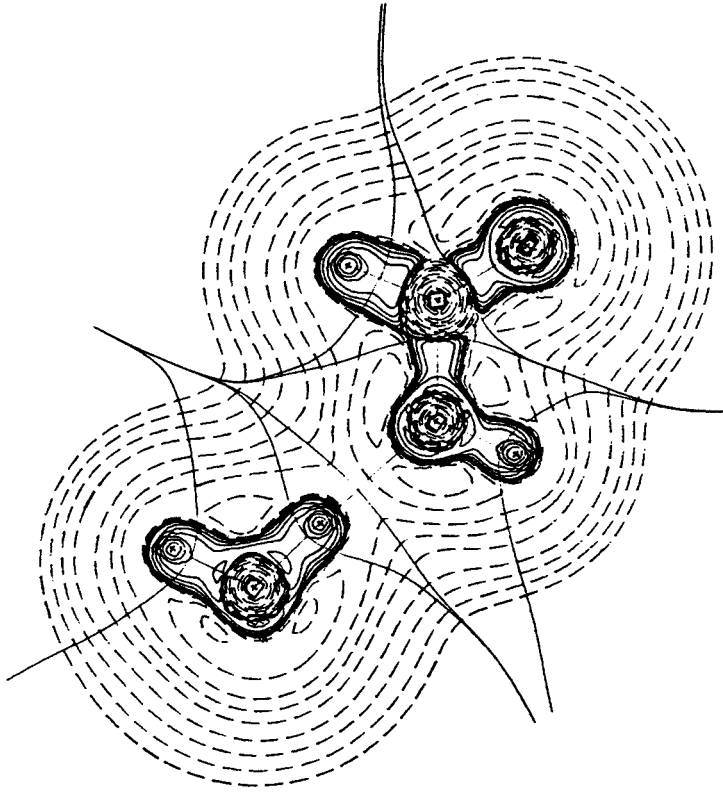
f



g



h



i

Table III.A.5

The properties of the (3,+1) critical point (cp) in $\nabla^2\rho$ at the carbon atom of N-protonated formamide during the initial steps of reaction with water.

	N-protonated formamide	a	b	c
$\nabla^2\rho$ ^a	0.093	0.092	0.089	0.087
$r(\text{C}), \text{\AA}$	0.551	0.563	0.567	0.568
$r(\text{O}2), \text{\AA}$		1.748	1.672	1.627
$\angle \text{C-cp-O}2$ ^b		147.62	138.10	127.87
$\angle \text{N-C-cp}$	93.16	95.69	102.31	101.63
$\angle \text{N-C-O}2$		92.08	94.21	94.27

^a The units of $\nabla^2\rho$ are $e/a_0^5 = 24.100e/\text{\AA}^5$

^b All angles are in degrees.

Table III.A.6

The properties of the nonbonded (3,-3) critical point (cp) in $\nabla^2\rho$ at the oxygen atom of water during the initial steps of the attack on N-protonated formamide.

	water	a	b	d	transition state e
$\nabla^2\rho^a$	-6.584	-6.337	-6.288	-6.072	-5.978
$r(O2) \text{ \AA}$	0.335	0.336	0.336	0.336	0.336
$r(C) \text{ \AA}$		2.142	2.013	1.717	1.620
$\angle C\text{-cp-O2}^b$		103.61	105.65	101.34	97.95

^a The units of $\nabla^2\rho$ are $e/a_0^5 = 24.100e/\text{\AA}^5$

^b All angles are in degrees.

transition state. The oxygen atom of the incoming water molecule makes an angle with the C-N bond which is almost identical to the angle the (3,+1) critical point makes with this bond. The value of $\nabla^2\rho$ at this critical point gradually decreases because as the water molecule gets closer charge becomes locally concentrated in the region between the carbon atom and the oxygen atom of the water molecule and hence the hole in the VSCC of the carbon atom gradually gets filled in. Likewise the magnitude of $\nabla^2\rho$ at the nonbonded (3,-3) critical point on the oxygen atom of the water molecule, given in Table III.A.6, is gradually decreased. This can be attributed to the fact that as the new C-O bond is being formed this nonbonded charge concentration is being changed to a bonded charge concentration, which is generally smaller in magnitude.

In the bimolecular reaction mechanism the water molecule is involved in the rate-limiting step. This is consistent with experimental studies (Hine et al., 1981) in which a small water term appears in the rate equation. However, since only a very small percentage of the formamide molecules hydrolyze via the N-protonation pathway it is possible that this water term is due to the O-protonated hydrolysis and the N-protonation

mechanism actually follows a unimolecular mechanism. In order to test the plausibility of this hypothesis the unimolecular hydrolysis mechanism was calculated and the fission reaction of N-protonated formamide into NH_3 and formyl ion was found to be endothermic by 55.1 kcal/mole. However this is more than five times the activation barrier of the bimolecular reaction of N-protonated formamide with water. Therefore it is very unlikely that the hydrolysis of N-protonated formamide will follow this pathway when the much more energetically favorable bimolecular mechanism is available. For this reason there is no need to investigate the unimolecular hydrolysis mechanism of formamide any further.

B: hydrolysis with protonation on the oxygen.

When the acid catalyzed hydrolysis of formamide follows the pathway in which the proton binds to the oxygen atom, the reaction involves a more complex mechanism than that of the N-protonation pathway. This is expected because in the latter mechanism the protonated reactant already has a good leaving group, namely the NH_3 group. In the case of O-protonated formamide, however, this leaving group must be created in a step prior to C-N bond fission. Thus the hydrolysis of O-protonated formamide is by necessity a multi-step reaction.

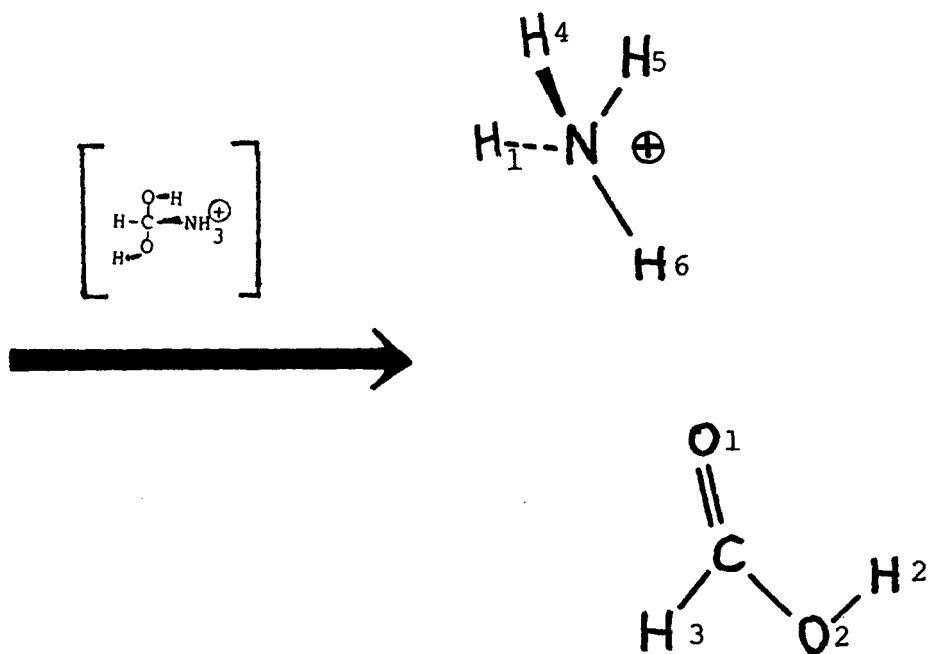
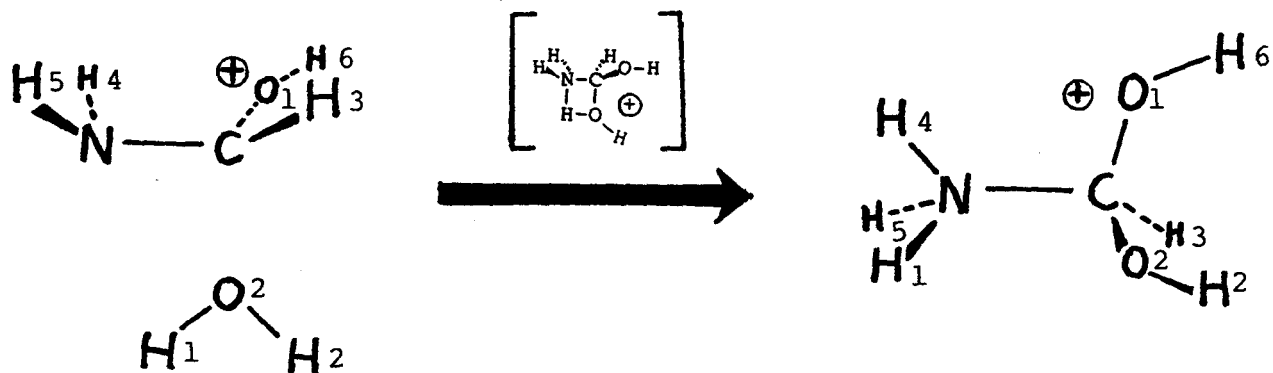
Although some theoretical studies have been made to determine the mechanism of the hydrolysis of N-protonated formamide, no reliable theoretical studies have been made on a possible O-protonation pathway. The only theoretical study of this mechanism has been one using the EHMO method (Csizmadia et al., 1968), which has been shown to be completely unreliable when applied to chemical reactions. The fact that there have been no ab initio studies of this mechanism is

very surprising in light of the fact that experimental studies have shown that the acid catalyzed hydrolysis of amides occurs mainly through an O-protonation pathway.

In the EHMO study on the O-protonation pathway it was found that in the first step of the reaction an intermediate is formed in which the water molecule is bonded to the carbon atom of O-protonated formamide. This intermediate is destabilized by 75.0 kcal/mole with respect to the isolated O-protonated formamide and water molecules. A proton then leaves the water molecule forming a tetrahedral intermediate with two OH groups bonded to the carbon atom. Another proton then protonates the nitrogen atom forming the NH_3 group which then separates from the intermediate. The NH_3 molecule then reacts with the keto-oxygen protonated formic acid ion to give NH_4^+ and formic acid. Although it was demonstrated in the discussion on the N-protonation hydrolysis that the EHMO approach is completely unreliable for even the simplest chemical reaction, ie. protonation, this may be a possible mechanism. For this reason the first part of the study on the hydrolysis of O-protonated formamide involved trying to find

Figure III.B.1

The reaction scheme for the hydrolysis of O-protonated formamide showing the formation of the intermediate and the subsequent decomposition of this intermediate to the hydrogen-bonded product. The transition states are shown in brackets.



this intermediate in which the water molecule is bonded to the carbon atom of O-protonated formamide. However a thorough investigation of the potential energy hypersurface of this reaction failed to find any such minimum. What was found, however, was that as the water molecule approached the carbon atom a bond was formed with the carbon and then a hydrogen atom was transferred from the water molecule to the nitrogen atom in one step. Following the hydrogen atom transfer step a stable tetrahedral intermediate was formed. This intermediate decomposed to give a hydrogen-bonded product in the last step of the reaction. The reaction scheme is outlined in Figure III.B.1.

The molecular graphs for a series of structures on the reaction coordinate are given in Figure III.B.2 and the corresponding energy and geometry at each of these points is given in Table III.B.1 and Table III.B.2. The energy profile for this reaction mechanism is given in Figure III.B.3. During the approach of the water molecule there are two important differences between this reaction and the reaction of water with N-protonated formamide. The first is that in this reaction the C-N bond elongates only slightly in contrast to the reaction of N-protonated formamide in

Figure III.B.2

The molecular graphs for a series of points along the reaction coordinate of the hydrolysis of O-protonated formamide.

- a-c) configurations on the reaction path leading to the first transition state.
- d) the first transition state.
- e) configuration on the reaction path leading to the intermediate.
- f) the stable intermediate.
- g) configuration on the reaction path leading to the second transition state.
- h) the second transition state.
- i-k) configurations on the reaction path leading to the product.
- l) the hydrogen-bonded product.

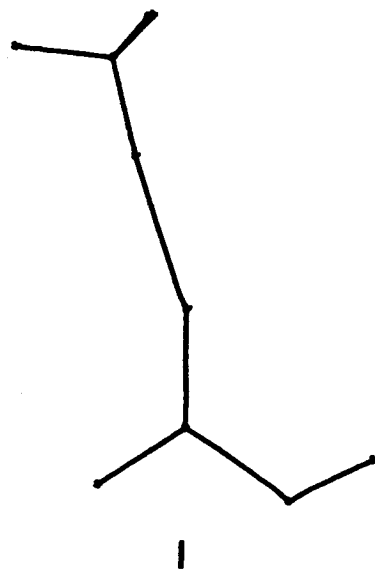
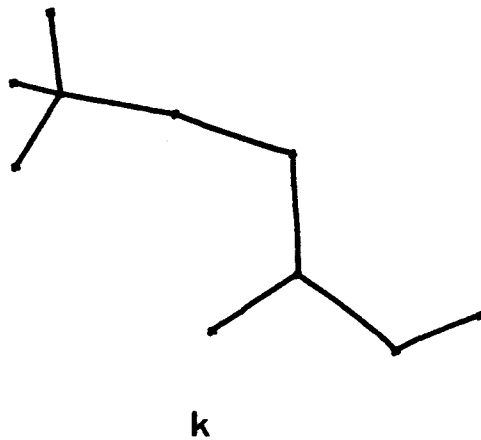
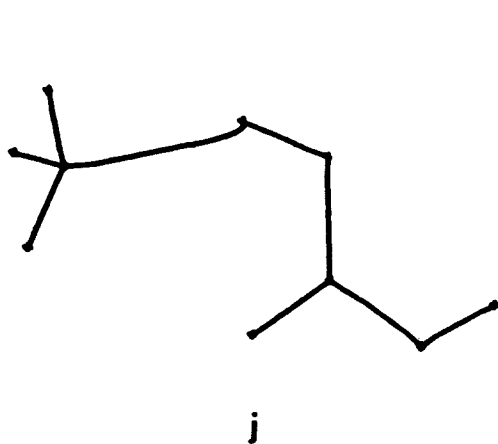
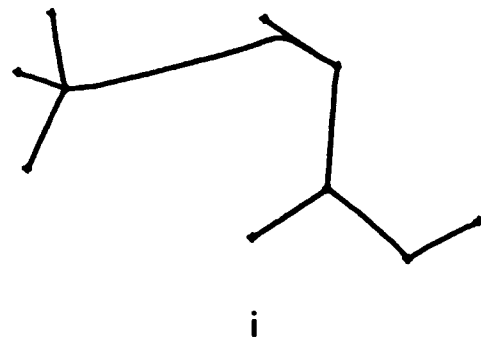
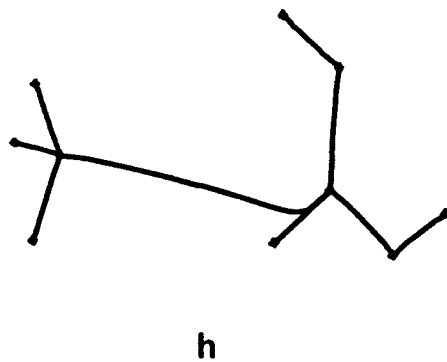
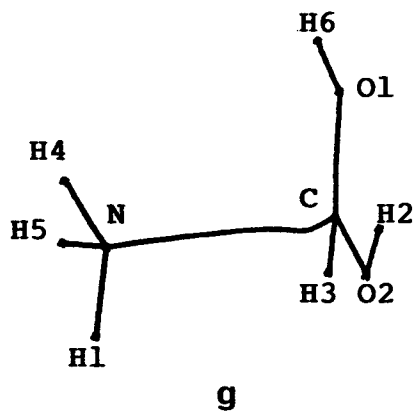
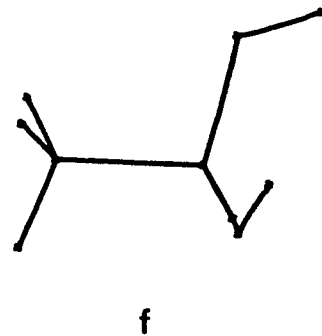
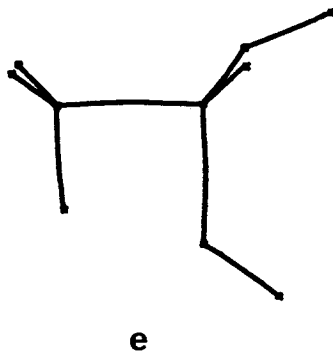
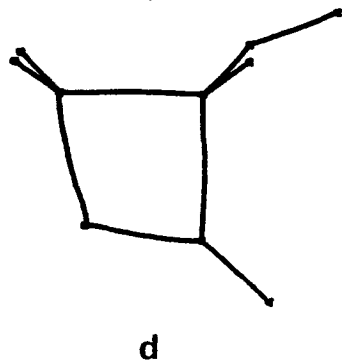
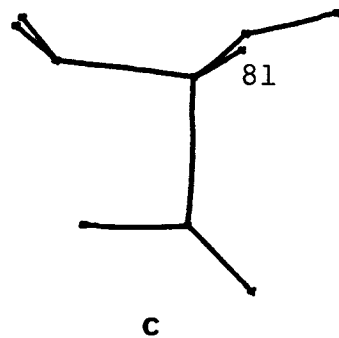
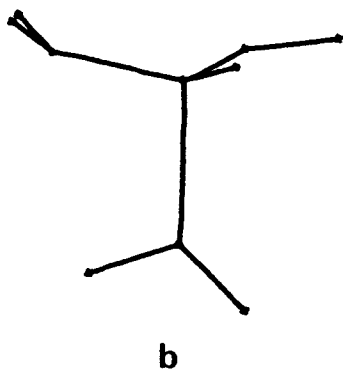
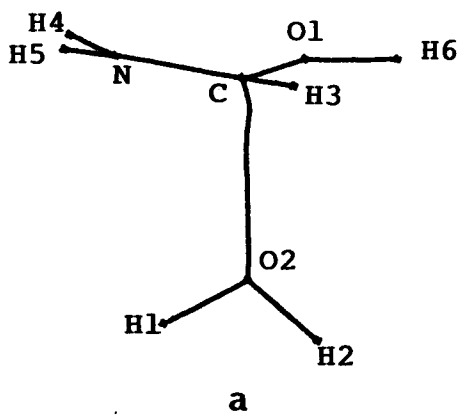


Table III.B.1 Geometrical Parameters^a and Energies for the reaction of O-protonated formamide with water leading to the tetrahedral intermediate.

	reagents ^b					Intermediate	
		a	b	c	d	e	f
E, hartrees	-245.3048	-245.3138	-245.2861	-245.2556	-245.2430	-245.2754	-245.3163
E, kcal/mole	0	-5.66	+11.73	+30.85	+38.76	+18.44	-7.21
Distances, Å							
C-O2		2.0868	1.7002	1.5491	1.5070	1.4430	1.3756
C-N	1.2781	1.2946	1.3544	1.4278	1.4511	1.4848	1.5262
O2-H1	0.9566	0.9547	0.9583	1.0756	1.1876	1.4686	
O2-H2	0.9566	0.9549	0.9576	0.9579	0.9572	0.9557	0.9557
C-H3	1.0717	1.0650	1.0699	1.0712	1.0712	1.0721	1.0736
C-O1	1.2905	1.3028	1.2230	1.2460	1.3475	1.3545	1.3690
O1-H6	1.0020	0.9545	0.9546	0.9548	0.9547	0.9545	0.9572
N-H4	0.9980	0.9983	0.9986	1.0031	1.0053	1.0088	1.0101
N-H5	1.0020	0.9947	0.9955	1.0002	1.0024	1.0057	1.0098
N-H1		2.8000	2.3054	1.7333	1.3881	1.0639	1.0123
Angles, degrees							
C-O2-H1		115.77	108.94	92.02	82.92	75.29	
H1-O2-H2	111.20	110.87	116.10	132.17	142.36	154.32	
N-C-O2		101.86	100.73	94.35	89.93	89.70	102.14
H4-N-C	120.65	119.97	115.91	113.28	113.16	112.71	110.08
H5-N-C	121.99	121.79	118.83	117.10	117.16	117.16	111.26
N-C-H3	120.03	119.88	117.15	115.19	115.87	114.19	107.43
N-C-O1	118.74	116.95	113.69	110.56	110.29	108.24	106.42
C-O1-H6	121.53	119.85	119.27	119.17	119.13	119.08	116.81
C-O2-H2		131.74	132.88	132.35	130.22	124.36	118.18
H4-N-H5	117.35	117.89	115.69	112.61	111.81	111.12	110.14
Dihedral Angle, degrees							
H1-O2-C-N		6.27	5.71	4.34	3.46	2.43	

^a For the identification of the atoms see figure III.B.1

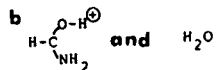


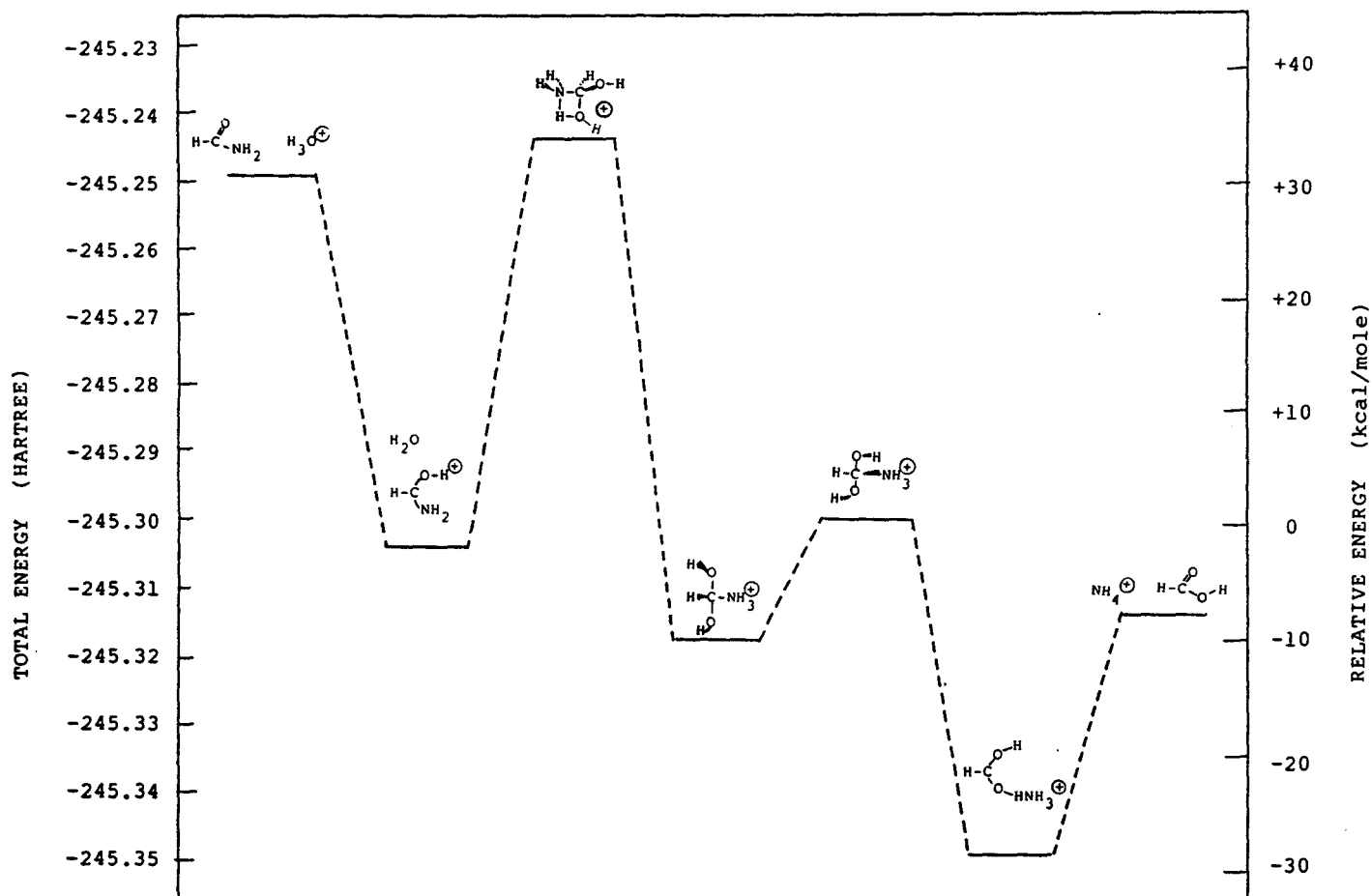
Table III.B.2 Geometrical Parameters^a and Energies for the decomposition of the tetrahedral intermediate in the reaction of O-Protonated formamide with water.

	Intermediate							Isolated products
	f	g	h	i	j	k	l	
E, hartrees	-245.3163	-245.3001	-245.2984	-245.3024	-245.3076	-245.3254	-245.3472	-245.3137
ΔE , kcal/mole	0.	+10.16	+11.23	+8.72	+5.43	-5.71	-19.38	+1.63
Distances, Å								
C-O2	1.3756	1.2854	1.2706	1.2626	1.2561	1.2286	1.2197	1.2002
C-N	1.5262	2.3405	2.7708	2.8833				
O1-H6	0.9557	0.9573	0.9548	0.9678	0.9856	1.2574	1.6369	
C-H3	1.0736	1.0622	1.0629	1.0652	1.0668	1.0745	1.0714	1.0723
C-O1	1.3790	1.2750	1.2651	1.2656	1.2671	1.2872	1.3092	1.3417
O2-H2	0.9572	0.9627	0.9650	0.9651	0.9647	0.9615	0.9578	0.9560
N-H4	1.0101	1.0033	1.0027	1.0035	1.0037	1.0070	1.0084	1.0016
N-H5	1.0098	1.0031	1.0026	1.0034	1.0041	1.0065	1.0079	1.0116
N-H1	1.0123	1.0032	1.0024	1.0037	1.0051	1.0090	1.0084	1.0116
N-H6		3.1102	2.7447	2.2029	1.8823	1.1880	1.0376	1.0116
Angles, degrees								
N-C-O1	106.42	100.24	87.08					
C-O1-H6	116.81	120.17	121.39	121.57	121.56	120.71	160.25	
C-O2-H2	118.18	121.48	119.83	115.83	112.56	111.24	118.39	114.91
H1-N-C	108.34	103.31	99.32					
H4-N-C	110.08	108.67	110.07					
H5-N-C	111.26	115.45	118.51					
C-N-H3	115.08	62.13	59.18					
H4-N-H5	110.14	109.70	109.23	108.65	108.38	107.88	109.46	109.49
Dihedral Angle, degrees								
H6-O1-C-N	20.93	72.28	42.47	25.74	17.72	4.34	0.00	

^aFor the identification of the atoms see figure III.B.1

Figure III.B.3

The computed reaction profile for the acid-catalyzed hydrolysis of formamide with protonation on the oxygen atom.



which there was a very marked lengthening of this bond. This suggests that the C-N bond is not being broken in this step of the reaction but only weakened. The second major difference is that during the approach of the reactants in the N-protonated formamide hydrolysis the geometry of the water molecule did not change. On approaching O-protonated formamide, however, there are very dramatic changes to the geometry of the water molecule. In particular, the stretching of the one O-H bond and widening of the H-O-H angle suggests that the formation of the new C-O bond and hydrogen transfer to the nitrogen occur in one concerted step. Another important feature of this early stage of the reaction is that the approaching water molecule causes a pyramidalization of the NH₂ group. This causes the magnitude of the nonbonded maximum in the VSCC of nitrogen facing the water molecule to increase. The pyramidalization of the NH₂ group also changes the position of this nonbonded (3,-3) critical point in $\nabla^2\rho$ and the combination of these two features greatly enhance the basicity of the nitrogen atom. As the water molecule approaches O-protonated formamide it does so such that one of the hydrogen atoms (H1) is almost in the plane of the N,C and O2 nuclei. This is illustrated by the values of

the H1-O2-C-N dihedral angle, given in Table III.B.1, which decreases as the water molecule approaches the carbon atom. The effect of this is to decrease the distance between this hydrogen atom and the nitrogen atom as much as possible thereby maximizing the interactions between these two atoms. The actual hydrogen transfer is an intramolecular acid/base reaction in which the main interaction involved is the attraction of the H^+ ion to the nonbonded maximum in the VSCC of the nitrogen atom. A four-membered ring is formed at the transition state in which one of the hydrogen atoms of the water molecule is bonded to both the oxygen and the nitrogen atoms. The energy barrier for this step is 38.8 kcal/mole and since this energy is 3.3 kcal/mole above that of the isolated formamide and H_3O^+ , the hydrolysis of formamide via the O-protonation mechanism is not a barrierless process. Following this transition state a tetrahedral intermediate is formed which is stabilized by 7.2 kcal/mole with respect to the O-protonated formamide and water molecules. It is interesting to note that the C-N bond length in this intermediate is almost exactly the same as that of N-protonated formamide, the two bond lengths differing by only 0.0020 Å. The next step of the mechanism is the transfer of the NH_3 group to one of the hydroxyl

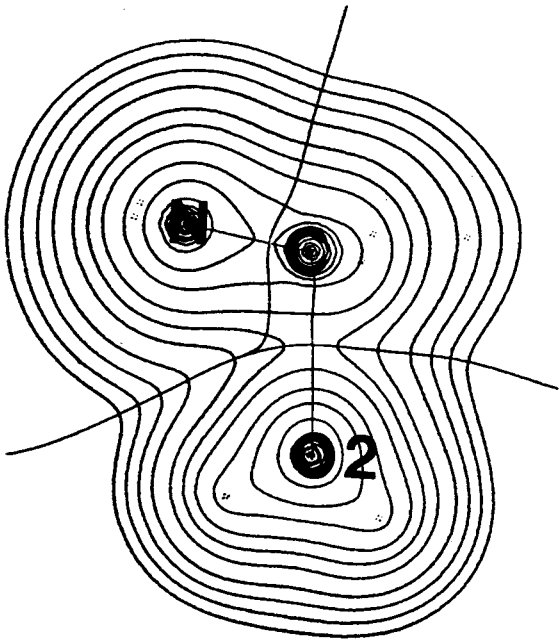
hydrogen atoms. In order to facilitate this transfer there is a rotation about one of the C-O bonds (C-O1) until the hydroxyl hydrogen atom (H6) is about 40° out of the plane formed by the C,N and O1 nuclei. This dihedral angle, which is given in Table III.B.2, decreases until the hydrogen-bonded product is formed. The NH_3 group is transferred through a series of conflict mechanisms, first from the carbon to the oxygen atom (O1) and then to the hydrogen atom (H6). Throughout this part of the reaction the HC(OH)OH group gradually begins to adopt a planar geometry as illustrated in the molecular graphs of the final four structures on the reaction coordinate for this reaction (Figures III.B.2g-III.B.2l). Since the energy barrier for this step of the reaction is only 11.2 kcal/mole it is not a rate-limiting step in the overall reaction. The final hydrogen-bonded product is stabilized by 26.6 kcal/mole with respect to the isolated O-protonated formamide and water molecules. An additional 21.0 kcal/mole of energy is required to break the hydrogen-bonded product into its two components.

The contour diagrams of $\rho(r)$ are given in Figure III.B.4 for each configuration calculated on the reaction coordinate of this mechanism. In the contour diagrams for the first four configurations the gradual buildup of charge between the C and O2 nuclei is evident, however, unlike the case for water approaching N-protonated formamide, there is no large decrease in the charge density between the C and N nuclei. In the contour diagrams for the configurations following the intermediate the gradual decrease in the charge density between the C and N nuclei becomes evident. In addition there is a very small buildup in the charge density between the C and O1 nuclei. This charge buildup is also evident from the values of ρ at the bond critical point between these two nuclei given in Table III.B.3. The values of ρ at the bond critical point between the carbon and nitrogen nuclei decreases slowly during the first part of the reaction leading to the stable intermediate, but then decreases sharply during the decomposition of the intermediate. This implies that most of the C-N bond breaking occurs in the second step of the reaction.

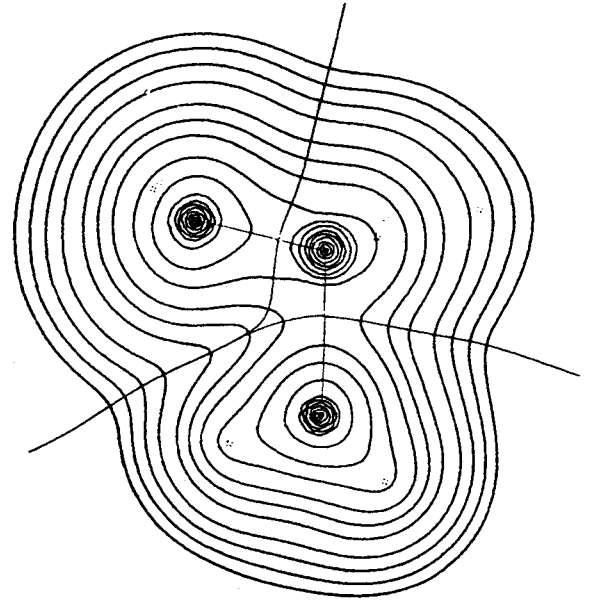
Figure III.B.4

The contour maps of the charge density for a series of points along the reaction coordinate of the hydrolysis of O-protonated formamide. Maps a-e are in the plane of the N,C and O2 nuclei and maps f-l are in the plane of the C,N and O1 nuclei. The maps are overlaid with those bond paths connecting nuclei in this plane. The projections of the interatomic surfaces onto the plane are shown for each bond path.

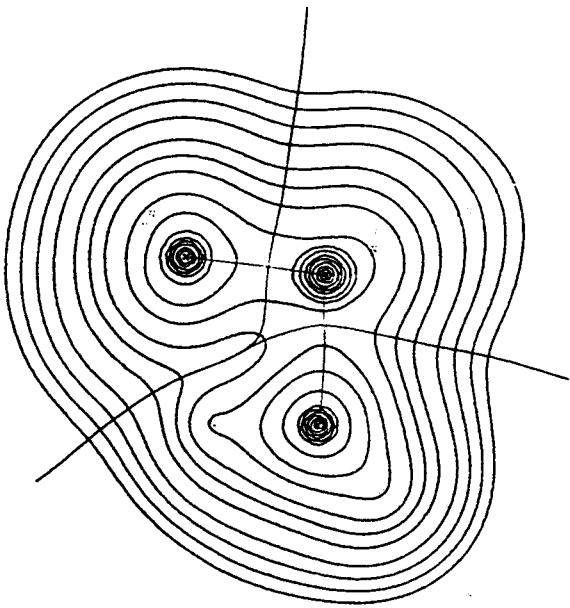
- a-c) configurations on the reaction path leading to the first transition state.
- d) the first transition state.
- e) configuration on the reaction path leading to the intermediate.
- f) the stable intermediate.
- g) configuration on the reaction path leading to the second transition state.
- h) the second transition state.
- i-k) configurations on the reaction path leading to the product.
- l) the hydrogen-bonded product.



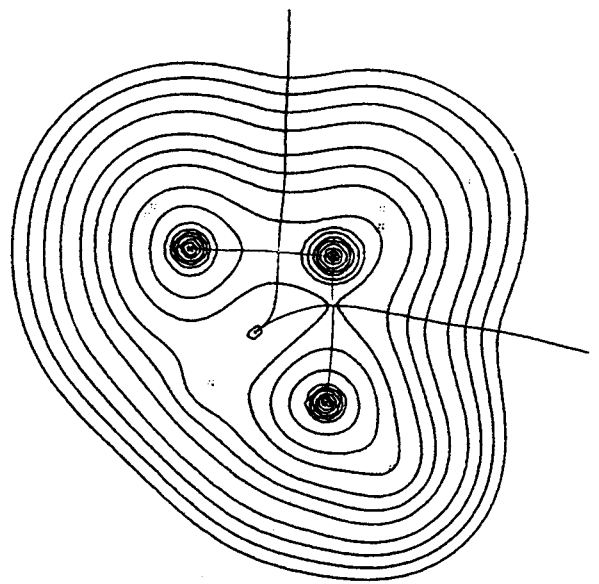
a



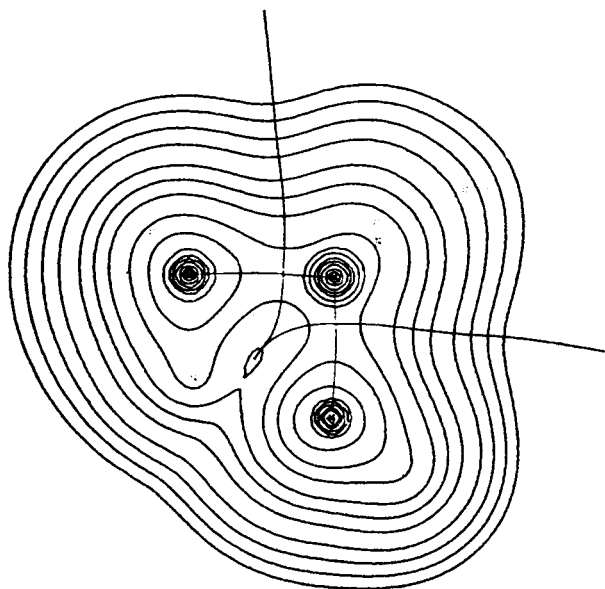
b



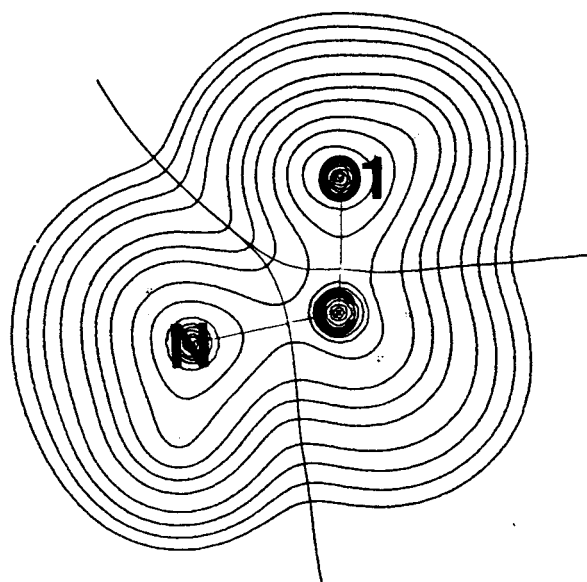
c



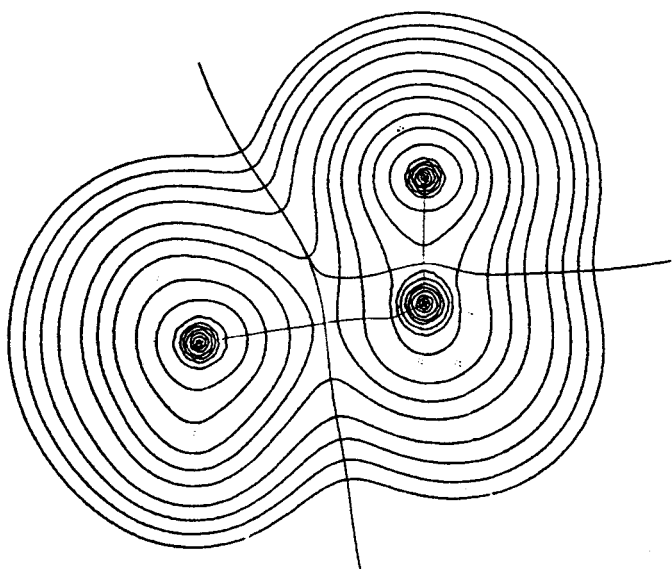
d



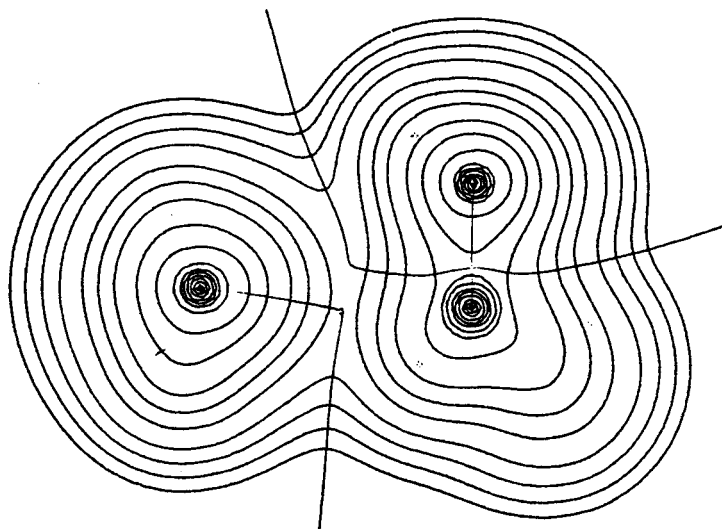
e



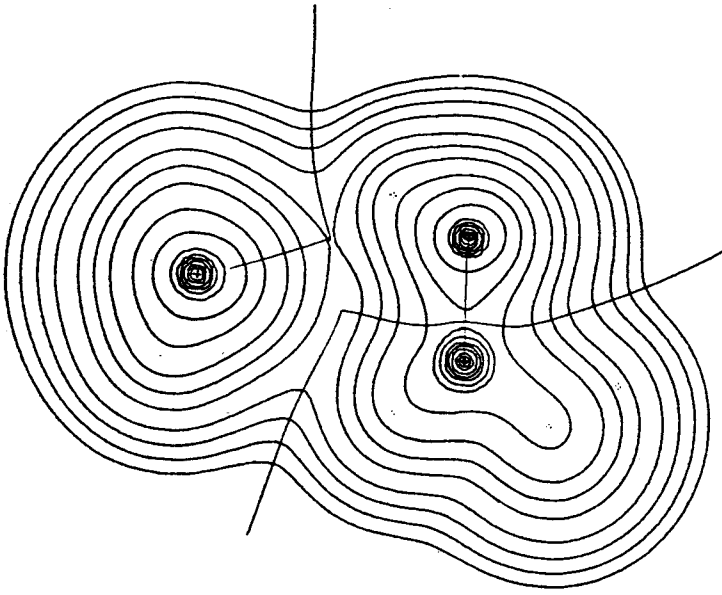
f



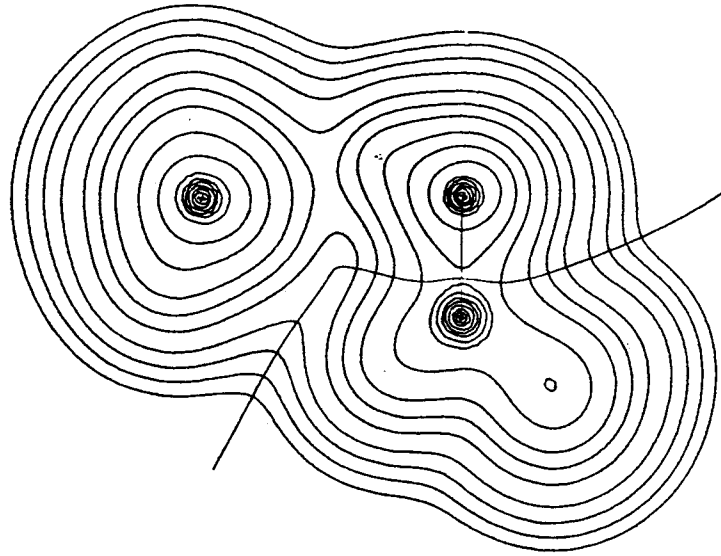
g



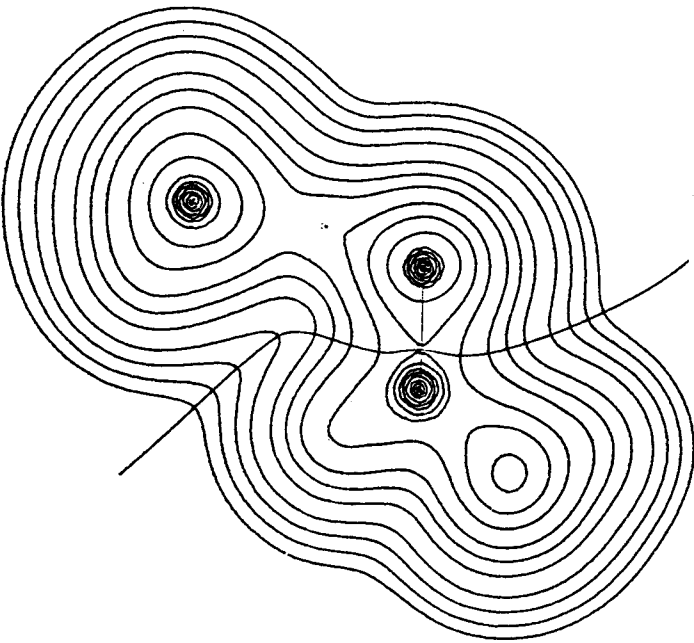
h



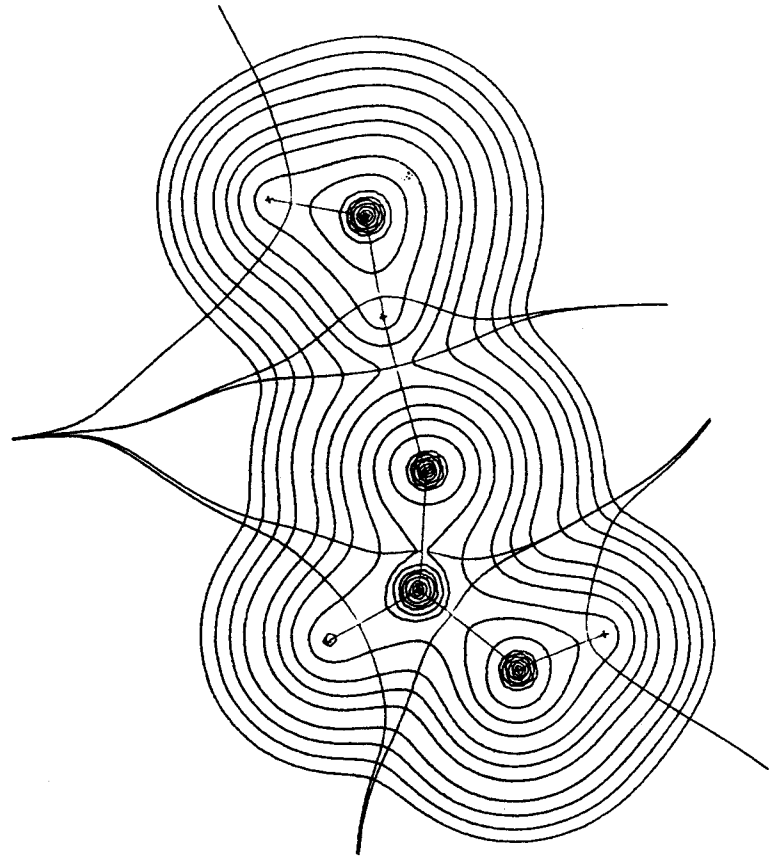
i



j



k



l

Table III.B.3

Values of ρ and $\nabla^2\rho$ at the critical points in $\rho(r)$ for the reaction of O-protonated formamide with water.

Bond ^a	property ^b	reactants ^c	transition state	intermediate	transition state	product	isolated products
C-N	ρ_b	0.3906	0.2956	0.2311	0.0175		
	$\nabla^2\rho_b$	-0.8035	-1.1320	-0.6703	0.0647		
C-O1	ρ_b	0.3433	0.3127	0.3013	0.3610	0.4056	0.4285
	$\nabla^2\rho_b$	-0.0752	-0.4691	-0.5532	-0.0395	0.1751	0.3355
C-O2	ρ_b		0.2011	0.2952	0.3636	0.3268	0.3018
	$\nabla^2\rho_b$		-2.9834	-0.5381	0.0352	-0.0741	-0.1306
O2-H1	ρ_b	0.3814	0.1674				
	$\nabla^2\rho_b$	-2.3606	-0.5089				
O2-H2	ρ_b	0.3814	0.3586	0.3667	0.3530	0.3675	0.3732
	$\nabla^2\rho_b$	-2.3606	-2.5179	-2.4680	-2.5518	-2.4799	-2.4245
C-H3	ρ_b	0.3204	0.3238	0.3240	0.3318	0.3217	0.3169
	$\nabla^2\rho_b$	-1.4798	-1.4498	-1.4331	-1.6704	-1.4556	-1.3819
O1-H6	ρ_b	0.3612	0.3684	0.3663	0.3580	0.0435	
	$\nabla^2\rho_b$	-2.6038	-2.4935	-2.4304	-2.6290	0.1719	
N-H4	ρ_b	0.3518	0.3518	0.3532	0.3549	0.3532	0.3492
	$\nabla^2\rho_b$	-2.0397	-2.0063	-2.0532	-1.9515	-2.0450	-2.0420
N-H5	ρ_b	0.3557	0.3549	0.3537	0.3547	0.3526	0.3492
	$\nabla^2\rho_b$	-2.0622	-2.0177	-2.0508	-1.9507	-2.0418	-2.0420
N-H1	ρ_b		0.1208	0.3507	0.3546	0.3526	0.3492
	$\nabla^2\rho_b$		-1.4121	-2.0326	-1.9489	-2.0418	-2.0420
N-H6	ρ_b					0.3181	0.3492
	$\nabla^2\rho_b$					-1.8780	-2.0420
ring	ρ_b		0.0777				
	$\nabla^2\rho_b$		0.4906				

^a For the numbering of atoms see fig. III.B.1

^b The units of ρ are e/a_0^3 , the units of $\nabla^2\rho$ are e/a_0^5 .

^c O-protonated formamide and water at infinite separation.

The relative atomic populations and relative atomic energies are given in Table III.B.4 and Table III.B.5 respectively. The relative atomic populations show that in the reaction leading to the first transition state charge is moved from the nitrogen atom to the carbon atom. The amount of charge transferred is almost the same as that transferred between these two atoms in the reaction of formamide with OH^- . The relative atomic energies show that although the nitrogen atom makes a significant contribution to the activation barrier it makes a much greater contribution to the energy barrier of the second transition state. The energy of the oxygen atom of the water molecule is lowered considerably during the reaction and this offsets the large energy increase of the nitrogen atom.

The contour diagram of the Laplacian of the charge density is given in Figure III.B.5 for each configuration calculated in the reaction. As evident from these diagrams, the hole in the VSCC of the carbon atom has already been filled with a local concentration of charge by the time configuration c is reached. In configuration c a new (3,-1) critical point in $\nabla^2\rho$ is present in the same region that was previously occupied

Table III.B.4

Changes in the atomic populations for the reaction of O-protonated formamide with water relative to their values in the isolated reactants^a.

reactants	Atom ^b	transition state	intermediate	transition state	product	isolated products
4.1577	C	0.1949	0.0337	-0.0964	-0.1606	-0.1478
8.5258	N	-0.2255	-0.2861	-0.2711	-0.2495	-0.2902
9.3281	O1	-0.0093	-0.0171	0.0172	0.0966	0.0374
9.2511	O2	0.0271	0.0669	0.0794	0.0764	0.0760
0.3745	H1	-0.0757	0.0883	0.1964	0.0948	0.0667
0.3745	H2	-0.0931	-0.0691	-0.1072	-0.0642	-0.0377
0.8402	H3	0.0622	0.0901	-0.0762	0.0641	0.1245
0.4362	H4	0.0389	0.0249	0.1356	0.0343	0.0049
0.4399	H5	0.0500	0.0299	0.1304	0.0294	0.0012
0.2724	H6	0.0301	0.0403	-0.0076	0.0783	0.1687

^a O-protonated formamide and water at infinite separation.

^b for the numbering of atoms see fig. III.B.1

Table III.B.5

Changes in the atomic energies^a for the reaction of O-protonated formamide with water relative to their values in the isolated reactants^b.

reactants ^d	Atom ^c	transition state	intermediate	transition state	product	isolated products
-36.6652	C	-0.0969	0.0225	0.1007	0.1455	0.1301
-55.3957	N	0.2646	0.2262	0.4914	0.2522	0.3293
-75.6373	O1	0.0397	0.0659	-0.0806	-0.0243	-0.0384
-75.3474	O2	-0.1867	-0.2118	-0.3611	-0.2971	-0.2624
-0.3376	H1	0.0915	-0.0447	-0.1054	-0.0497	-0.0322
-0.3376	H2	0.0631	0.0448	0.0740	0.0424	0.0245
-0.5733	H3	-0.0397	-0.0569	0.0277	-0.0345	-0.0605
-0.3678	H4	-0.0229	-0.0153	-0.0758	-0.0205	-0.0020
-0.3725	H5	-0.0282	-0.0158	-0.0703	-0.0149	0.0027
-0.2706	H6	-0.0225	-0.0263	0.0062	-0.0413	-0.0992

^a in au.

^b O-protonated formamide and water at infinite separation.

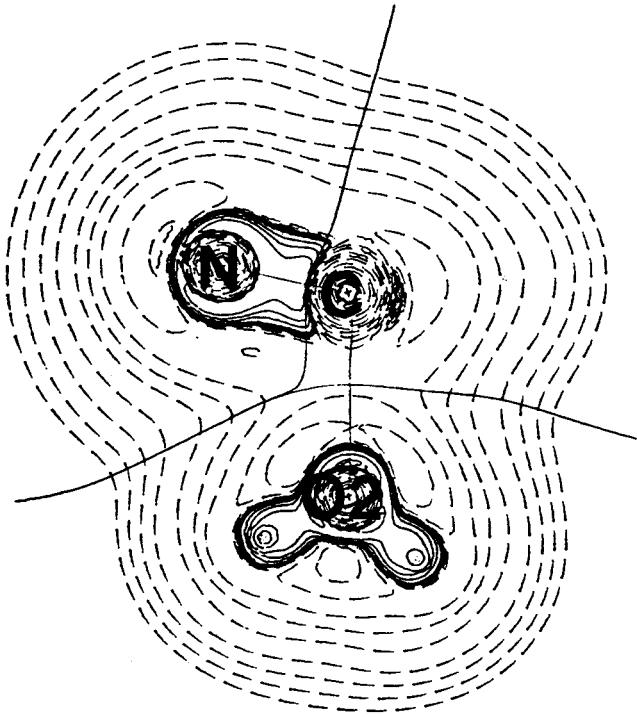
^c for the numbering of atoms see fig. III.B.1

Figure III.B. 5

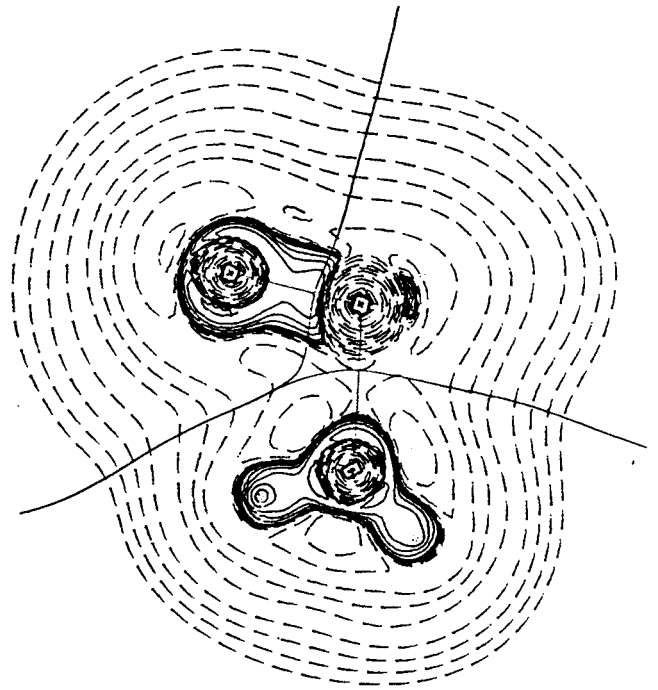
The contour maps of the Laplacian of the charge density for a series of points along the reaction coordinate of the hydrolysis of O-protonated formamide. Maps a-e are in the plane of the N,C and O2 nuclei and maps f-l are in the plane of the C,N and O1 nuclei. The maps are overlaid with those bond paths connecting nuclei in this plane.

The projections of the interatomic surfaces onto the plane are shown for each bond path. Dashed contours denote positive values.

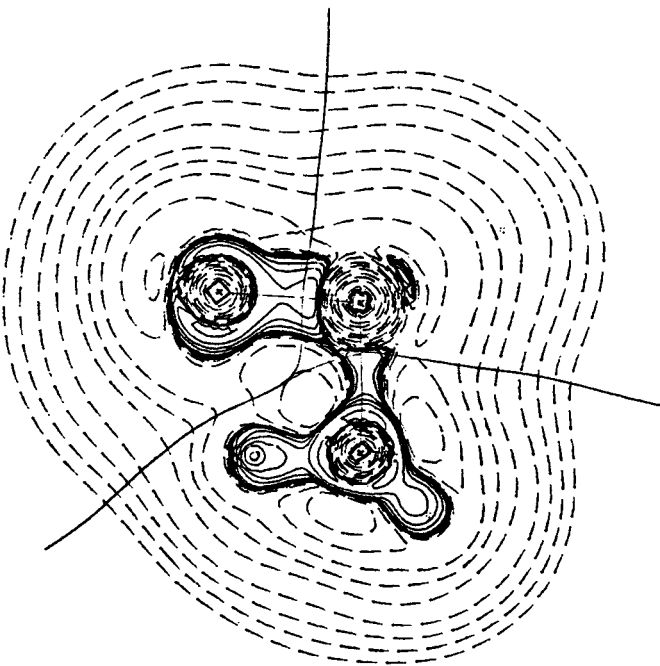
- a-c) configurations on the reaction path leading to the first transition state.
- d) the first transition state.
- e) configuration on the reaction path leading to the intermediate.
- f) the stable intermediate.
- g) configuration on the reaction path leading to the second transition state.
- h) the second transition state.
- i-k) configurations on the reaction path leading to the product.
- l) the hydrogen-bonded product.



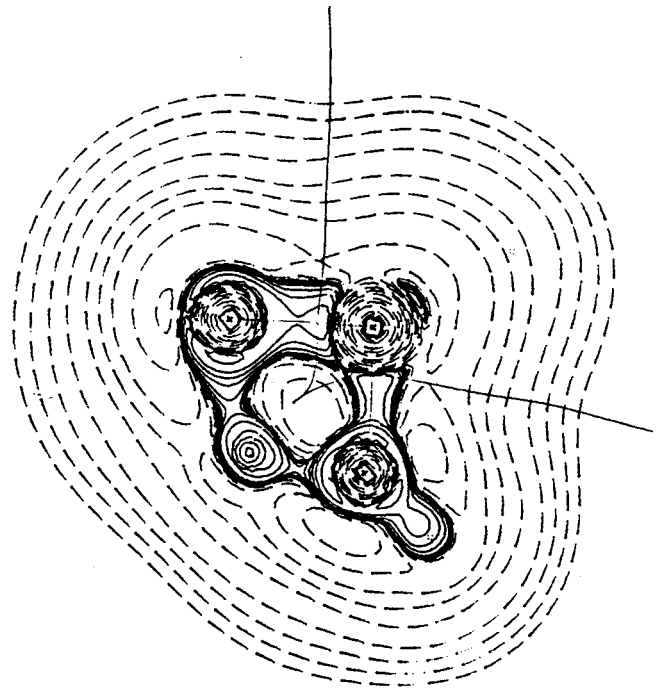
a



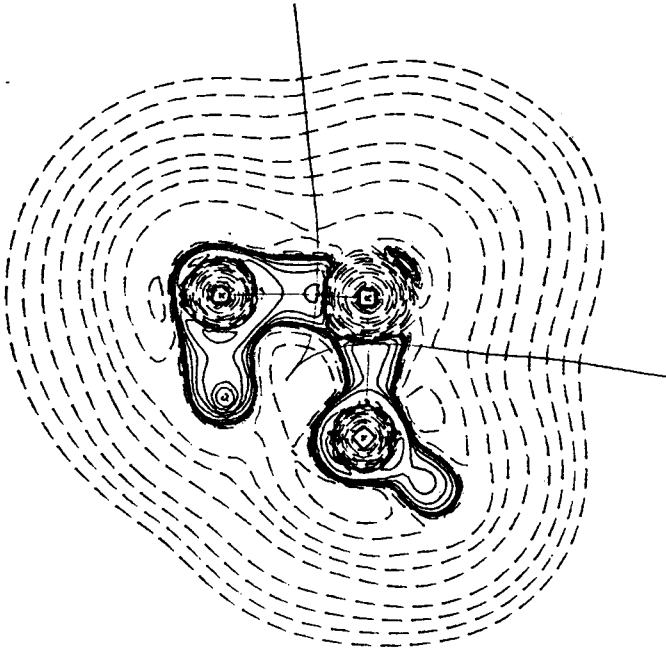
b



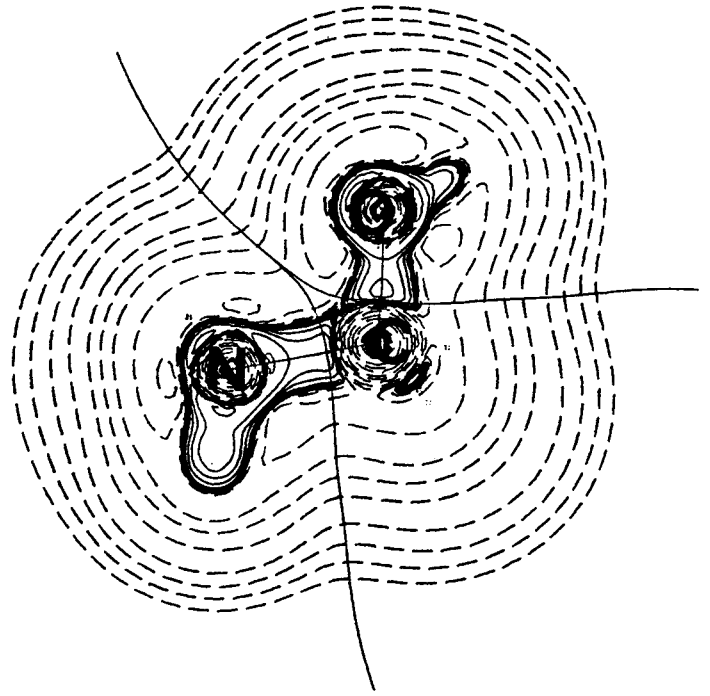
c



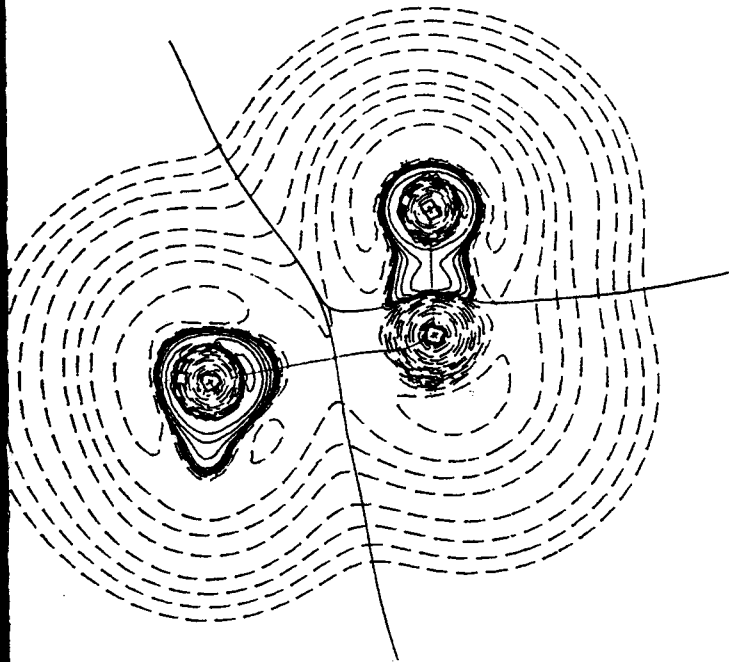
d



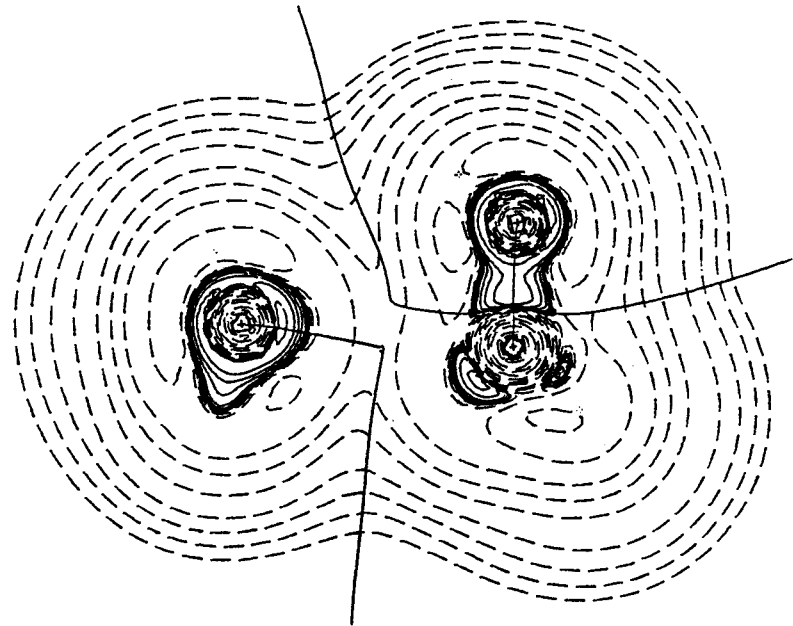
e



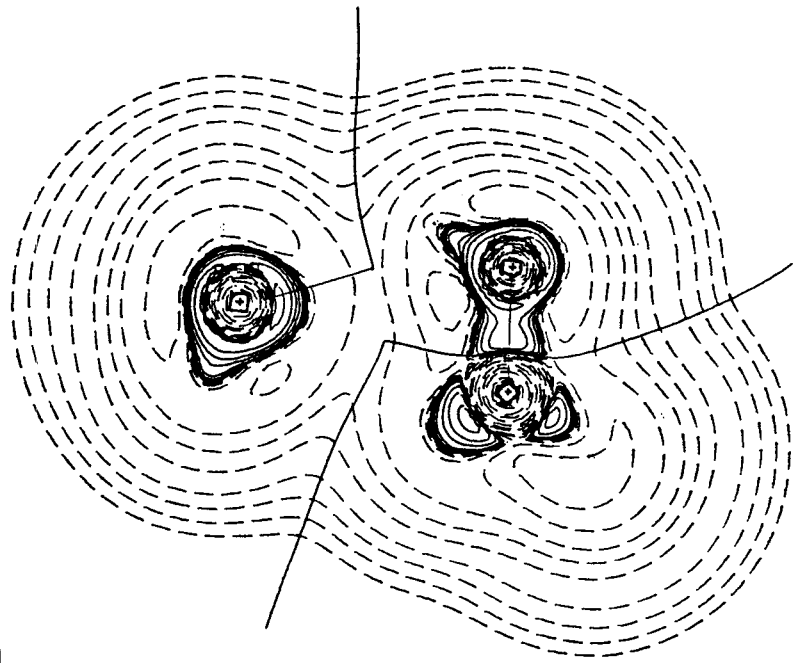
f



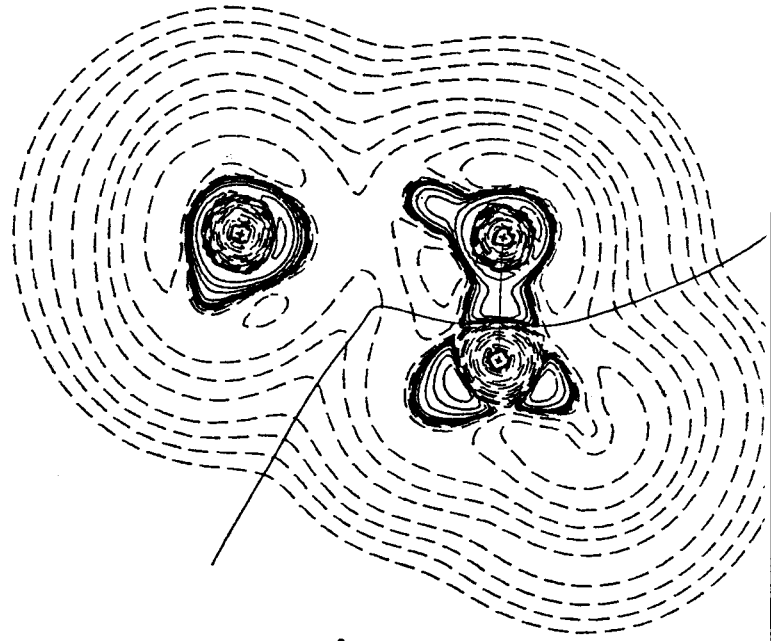
g



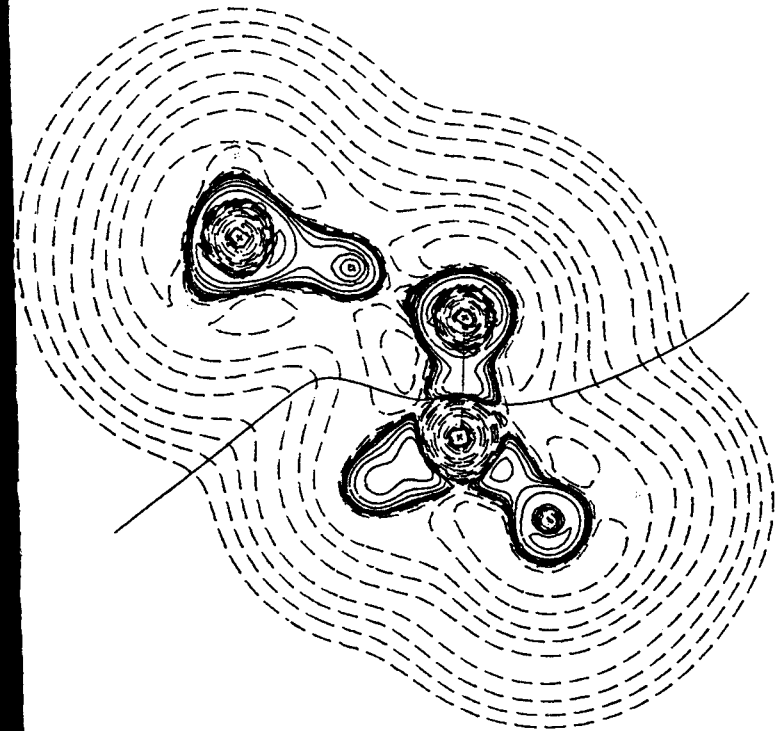
h



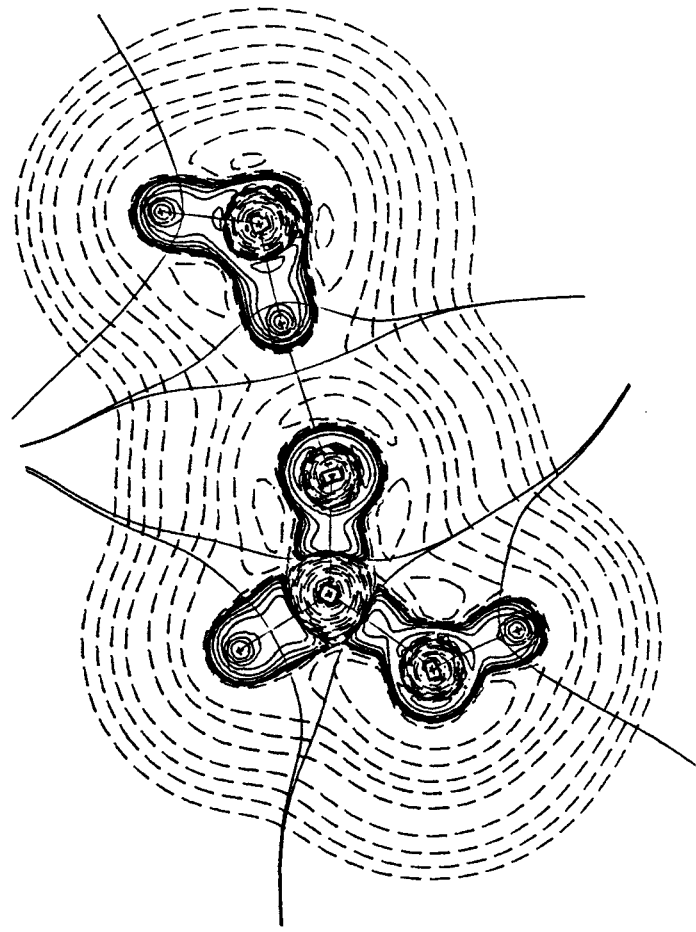
i



j



k



l

by the (3,+1) critical point. Thus the formation of the new C-O bond occurs earlier in this reaction than it does in the hydrolysis of N-protonated formamide. Table III.B.6 shows the changes in the value of $\nabla^2\rho$ at this critical point during the approach of the water molecule. The angle that this critical point makes with the C-N bond is 52.18° in O-protonated formamide, however as the water molecule approaches this angle is increased to 83.95°. Such changes in the position of a (3,+1) critical point on the approach of a nucleophile are not uncommon, especially in cases where a planar carbonyl group becomes pyramidalized. During the nucleophilic attack the hole in the VSCC of the carbon atom is being attacked by one of the nonbonded charge concentrations on the oxygen atom of the water molecule. The values of $\nabla^2\rho$ at this nonbonded (3,-3) critical point of the oxygen atom are given in Table III.B.7. As expected, the value of $\nabla^2\rho$ at this critical point decreases during the formation of the C-O2 bond, which, in the process converts the nonbonded charge concentration into a bonded charge concentration. The values of $\nabla^2\rho$ for the nonbonded (3,-3) critical point on nitrogen, given in Table III.B.8, show an increase in the magnitude of the nonbonded charge concentration on approach of the water molecule.

Table III.B.6

The properties of the (3,+1) critical point (cp) in $\nabla^2\rho$ at the carbon atom of O-protonated formamide during the initial steps of reaction with water.

	O-protonated formamide	a	b
$\nabla^2\rho^a$	0.161	0.167	0.174
$r(\text{C}), \text{\AA}$	0.655	0.560	0.559
$r(\text{O}2), \text{\AA}$		1.495	1.375
$\angle \text{C-cp-O}2^b$		121.99	113.35
$\angle \text{N-C-cp}$	52.18	86.20	83.95
$\angle \text{N-C-O}2$		101.86	100.72

^a The units of $\nabla^2\rho$ are $e/a_0^5 = 24.100e/\text{\AA}^5$

^b All angles are in degrees.

Table III.B.7

The properties of the nonbonded (3,-3) critical point (cp) in $\nabla^2\rho$ at the oxygen atom of water during the initial steps of the attack on O-protonated formamide..

	water	a	b	c	transition state d
$\nabla^2\rho^a$	-6.584	-6.364	-6.164	-5.993	-5.971
$r(O2), \text{Å}$	0.335	0.336	0.336	0.336	0.337
$r(C), \text{Å}$		1.942	1.621	1.518	1.507
$\angle C\text{-cp-O2}^b$		111.20	97.92	88.95	83.53

^a The units of $\nabla^2\rho$ are $e/a_0^5 = 24.100e/\text{Å}^5$

^b All angles are in degrees.

Table III.B.8

The properties of the nonbonded (3,-3) critical point (cp) in $\nabla^2\rho$ at the nitrogen atom of O-protonated formamide during the initial stages of the hydrogen transfer from water.

	a	b	c	transition state d
$\nabla^2\rho^a$	-1.875	-2.633	-2.950	-2.816
$r(\text{N}), \text{\AA}$	0.402	0.393	0.392	0.397
$r(\text{H1}), \text{\AA}$	2.410	1.971	1.381	1.010
$\angle \text{N-cp-H1}^b$	164.68	145.48	150.45	159.29
$\angle \text{C-N-cp}$	79.55	66.98	98.17	71.43
$\angle \text{C-N-H1}$	69.66	68.57	73.94	78.67

^a The units of $\nabla^2\rho$ are $e/a_0^5 = 24.100e/\text{\AA}^5$

^b All angles are in degrees.

This trend is continued until the transition state is reached, at which point there is a decrease in the magnitude of this local charge concentration. The explanation for this can be seen in Figure III.B.5e, which shows that when the transition state is reached this nonbonded charge concentration is being used to form the new N-H bond with the hydrogen atom being transferred from the water molecule. An important feature of the hydrogen transfer is the fact that the angle which the transferring hydrogen atom makes with the N and C nuclei is very close to the angle formed between the C and N nuclei and the nonbonded (3,-3) critical point at the nitrogen atom. This implies that this nonbonded maximum is instrumental in attracting the hydrogen atom to the nitrogen atom, even over relatively large distances. This same conclusion is evident from the N-cp-H1 angle given in Table III.B.8, which shows that even in the early stages of the reaction there is a high degree of colinearity between the nitrogen nucleus, the (3,-3) nonbonded critical point and the nucleus of the transferring hydrogen atom.

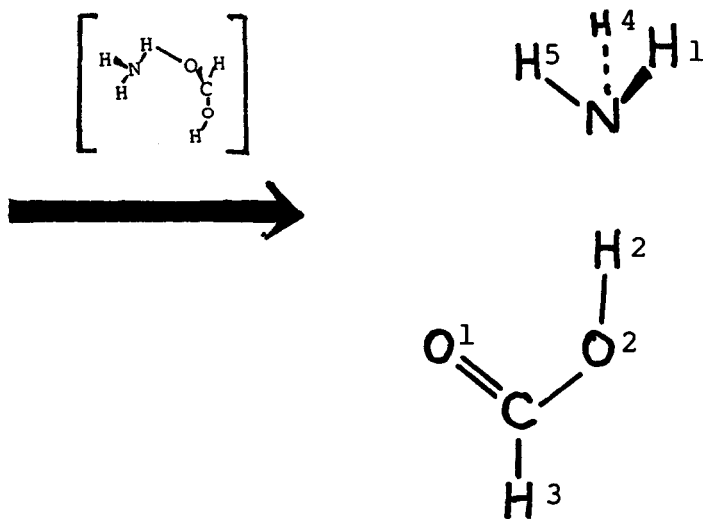
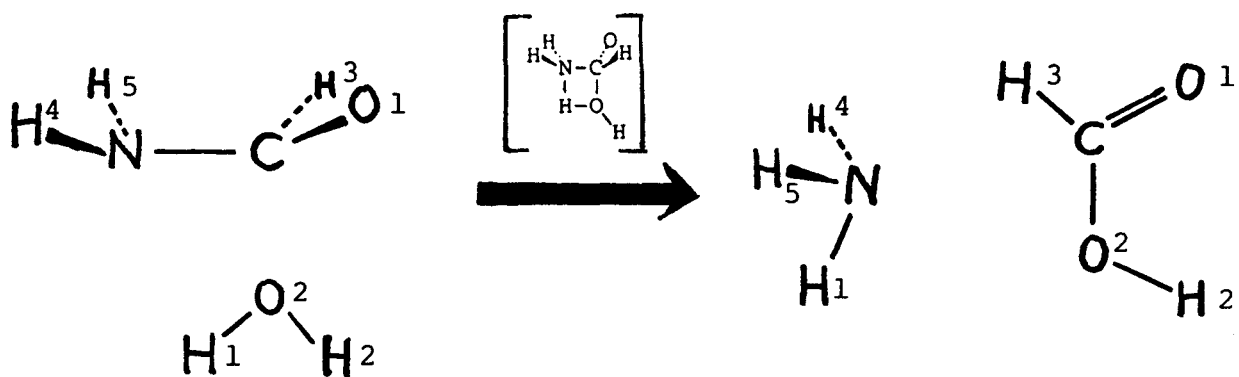
Chapter 4

The uncatalyzed hydrolysis of formamide

It is a well known experimental observation that amides do not undergo hydrolysis in neutral media (Talbot, 1972). This fact might lead one to question the purpose of studying the uncatalyzed amide hydrolysis reaction, after all, Why study a reaction that does not occur? The answer to this question is very simple; the fact that a certain reaction does not occur does not necessarily mean that there is no mechanism for it to follow. If a plausible reaction mechanism can be found for the uncatalyzed hydrolysis of formamide then this mechanism can be compared to the catalyzed reactions which do occur. Such a comparison would give valuable insight into what actually drives the catalyzed reactions forward. In searching for a possible uncatalyzed amide hydrolysis mechanism the most logical approach is to simultaneously optimize all of the geometrical parameters without any constraints while gradually moving the water molecule closer to the formamide molecule. This approach avoids the pitfalls

Figure IV.1

The reaction scheme for the hydrolysis of neutral formamide showing the formation of the intermediate and the subsequent decomposition of this intermediate to the hydrogen-bonded product. The transition states are shown in brackets.



of searching for some preconceived mechanism which, in reality may not exist. By performing unconstrained optimizations while gradually moving the reactants together the system will automatically follow the minimum energy pathway.

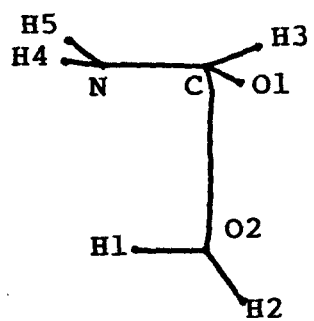
In the case of formamide and water, as the two reactants are brought together the energy of the system increases. This same observation was made in both acid catalyzed mechanisms, however, in this case the energy increases much more quickly. When the oxygen of the water molecule is within 2 \AA of the carbon atom of formamide a reaction begins and the intrinsic reaction coordinate can then be followed. An outline of the reaction scheme is given in Figure IV.1.

The molecular graphs for a series of configurations along the reaction coordinate are given in Figure IV.2 and the corresponding energy and geometry of each of these structures is given in Table IV.1 and Table IV.2. The energy profile for this reaction is given in Figure IV.3. It may at first appear that the first step of this reaction is similar to that of the reaction between O-protonated formamide and water, however

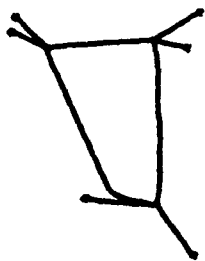
Figure IV.2

The molecular graphs for a series of points along the reaction coordinate of the hydrolysis of neutral formamide.

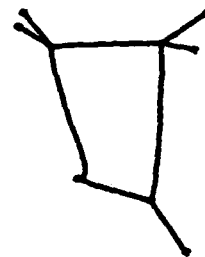
- a-c) configurations on the reaction path leading to the first transition state.
- d) the first transition state.
- e-f) configurations on the reaction path leading to the intermediate.
- g) the intermediate.
- h-i) configurations on the reaction path leading to the second transition state.
- j) the second transition state.
- k) configuration on the reaction path leading to the product.
- l) the hydrogen-bonded product.



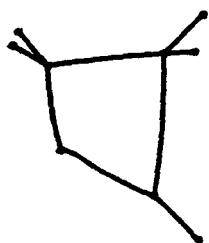
a



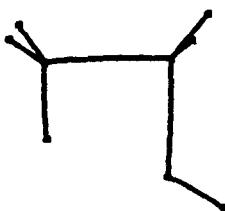
b



c



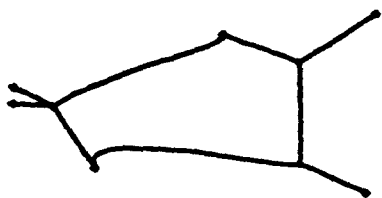
d



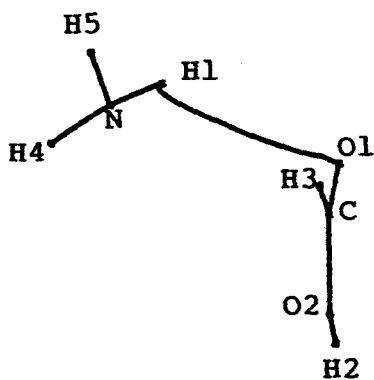
e



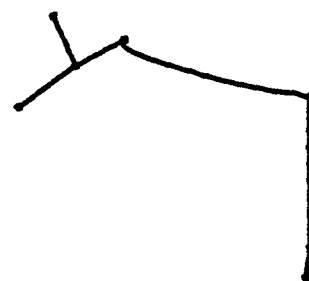
f



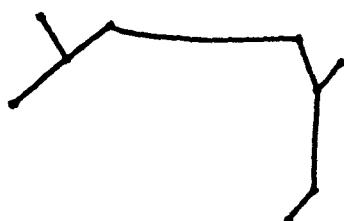
g



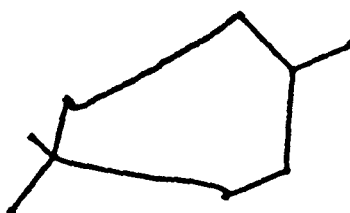
h



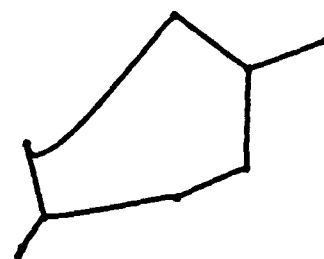
i



j



k



l

Table IV.1

Geometrical Parameters^a and Energies for the neutral hydrolysis of formamide leading to the intermediate.

	reagents	Intermediate configurations						Intermediate
		a	b	c	d	e	f	g
E, hartrees	-244.9622	-244.9580	-244.9429	-244.9226	-244.8619	-244.8886	-244.9573	-244.9660
ΔE, kcal/mole	0	+2.63	+12.10	+24.83	+62.90	+46.15	+3.07	-2.38
Distances, Å								
C-O2		2.4423	2.1920	2.1011	1.8882	1.5786	1.3578	1.3511
C-N	1.3466	1.3641	1.4064	1.4463	1.5370	1.6530	2.5291	3.2677
O2-H1	0.9506	0.9509	0.9556	1.0173	1.3761	1.6606	2.2024	2.6716
N-H1		2.4991	2.0721	1.8008	1.1291	1.0204	0.9946	0.9952
O2-H2	0.9506	0.9501	0.9470	0.9460	0.9497	0.9528	0.9560	0.9560
C-O1	1.2155	1.2154	1.2125	1.2098	1.2120	1.2358	1.2023	1.2022
C-H3	1.0808	1.0738	1.0707	1.0703	1.0701	1.0780	1.0652	1.0721
N-H5	0.9835	0.9913	0.9960	0.9983	1.0011	1.0008	0.9947	0.9941
N-H4	0.9924	0.9941	0.9470	0.9998	1.0026	1.0022	0.9947	0.9941
Angles, degrees								
H1-O2-C		89.94	84.16	77.78	68.08			
O2-C-N		90.31	86.53	84.02	79.63	86.53	84.95	
H1-O2-H2	111.20	112.29	118.27	125.55	141.08			
N-C-O1	124.75	123.18	121.07	119.07	117.29	113.86	106.55	
N-C-H3	113.72	114.06	113.59	112.98	111.18	105.13	80.60	
H4-N-C	119.50	117.38	112.75	111.17	109.86	108.21	103.71	
H5-N-C	121.89	120.32	116.84	115.84	115.64	116.65	128.46	
O1-C-H3	121.52	122.69	124.50	126.15	126.49	123.64	125.93	126.58
H4-N-H5	118.60	117.33	114.42	113.32	112.08	112.13	113.80	114.07
Dihedral Angle								
H1-O2-C-N		14.14	11.07	8.96	4.92	4.31	0.71	2.22

^a For the identification of the atoms see figure IV.1

Table IV.2

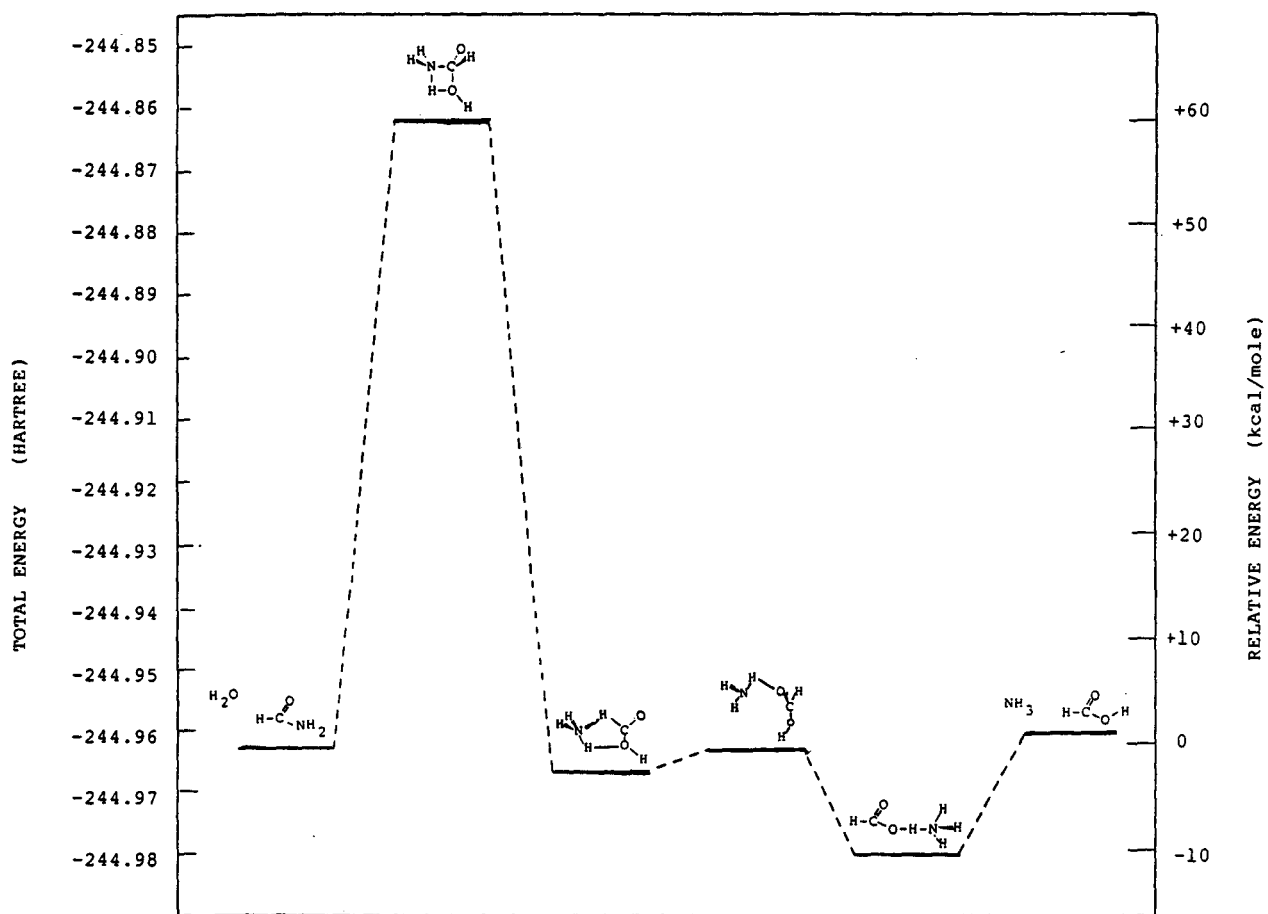
Geometrical Parameters^a and Energies for the decomposition of the intermediate in the neutral hydrolysis of formamide.

	Intermediate g	Intermediate configurations					Isolated products
		h	i	j	k	l	
E, hartrees	-244.9660	-244.9652	-244.9648	-244.9642	-244.9706	-244.9800	-244.9579
ΔE, kcal/mole	0	+0.50	+0.75	+1.13	-2.88	-8.78	+3.95
Distances, Å							
O2-H2	0.9560	0.9558	0.9557	0.9554	0.9609	0.9880	0.9560
N-H2					2.3286	1.7736	
N-H3	2.4115	3.0954	3.3098	3.7200			
N-H1	0.9952	0.9939	0.9938	0.9937	0.9958	1.0006	0.9911
N-H4	0.9941	0.9932	0.9931	0.9931	0.9945	0.9977	0.9911
N-H5	0.9941	0.9932	0.9930	0.9930	0.9940	0.9976	0.9911
C-H3	1.0721	1.0694	1.0703	1.0718	1.0735	1.0746	1.0723
C-O1	1.2022	1.2033	1.2031	1.2031	1.2062	1.2112	1.2002
C-O2	1.3511	1.3412	1.3399	1.3372	1.3303	1.3219	1.3417
O1-H4		2.5741	2.5510	2.4842	2.5143		
Angles, degrees							
C-O2-H2	114.26	114.60	114.68	114.84	114.22	114.86	114.91
O2-H2-N					129.88	164.91	
O1-C-O2	123.34	123.98	124.24	124.74	124.91	125.16	124.56
O1-C-H3	125.58	125.20	125.14	124.74	123.39	123.02	124.99
H4-N-H5	114.07	114.81	114.96	115.10	114.89	112.20	115.87
O2-C-H3	110.08	110.82	110.62	110.51	111.68	111.82	110.45
H4-O1-C		91.97	93.84	98.69			
Dihedral Angle, degrees							
C-O2-H2-N	-156.03	-95.06	-86.30	-68.27	-28.14	-1.22	

^aFor the identification of the atoms see figure IV.1

Figure IV.3

The computed reaction profile for the uncatalyzed hydrolysis of formamide.



a closer examination will reveal the fact that these two hydrolysis mechanisms have nothing in common. In order for this reaction to occur the system must surmount an activation barrier of 62.9 kcal/mole. The geometry at both the carbon and nitrogen atoms pyramidalizes on approach of the water molecule. The orientation of the approaching water molecule is such that the hydrogen atom being transferred is almost in the plane formed by the oxygen atom of the water molecule and the C-N bond. The degree to which this hydrogen atom is in the plane of these three atoms is illustrated by the small values of the H1-O2-C-N dihedral angle given in Table IV.1. The geometry of the water molecule begins to distort very early in the reaction and a three membered ring structure is formed while the oxygen atom of the water molecule is still more than 2 Å from the carbon atom. This is in contrast to the hydrolysis of O-protonated formamide which the ring structure is formed only when the oxygen nucleus is within 1.55 Å of the carbon nucleus. This three membered ring is then increased to a four membered ring in which the angle made by the carbon atom with one of the O-H bonds of the water molecule (C-O2-H1) is only 77.8°. The length of this O-H bond at this point is

extended by 0.43 \AA over its value in the isolated water molecule. Following the transfer of the hydrogen atom a rather unstable intermediate is formed with an energy lying 2.4 kcal/mole below that of the reactants. This intermediate contains a five-membered ring formed between the planar HCOOH group and one of the N-H bonds in NH_3 . The ring is slightly puckered to relieve any angle strain, which is minimal in this ring structure because the bond paths connecting the NH_3 group to the HCOOH group are very long. The two components of this intermediate have geometries almost identical to those of the isolated ammonia and formic acid molecules. This suggests that the intermediate is nothing more than a very weak interaction between these two separated molecules. This fact is demonstrated by the value of ρ_b (the value of ρ at the bond critical point) for the two bonds holding the two groups together. The value of ρ_b for the bond between the N and H3 atoms is 0.014 au which when compared to the value $\rho_b = 0.358 \text{ au}$ for the N-H bond in ammonia, clearly demonstrates the weakness of this bond. The value for the other weak bond, that between the hydroxyl oxygen atom and a hydrogen atom of the NH_3 group, is only 0.006 au , which is much less than the value $\rho_b = 0.374 \text{ au}$ for the O-H bond in the formic acid group. In order for this

Table IV.3

Values of ρ and $\nabla^2\rho$ at the critical points in $\rho(r)$ for the uncatalyzed hydrolysis of formamide.

Bond ^a	property ^b	reagents	transition state	intermediate	transition state	product	isolated products
C-N	ρ_b	0.3334	0.2283				
	$\nabla^2\rho_b$	-0.7721	-0.6796				
C-O1	ρ_b	0.4158	0.4235	0.4263	0.4260	0.4185	0.4285
	$\nabla^2\rho_b$	0.1529	0.0427	0.3212	0.2964	0.2379	0.3355
C-O2	ρ_b		0.0825	0.2937	0.3052	0.3294	0.3018
	$\nabla^2\rho_b$		0.1276	-0.1183	-0.1228	-0.1493	-0.1306
O2-H1	ρ_b	0.3814	0.1024	0.0057			
	$\nabla^2\rho_b$	-2.3606	0.1666	0.0262			
O2-H2	ρ_b	0.3844	0.3777	0.3739	0.3739	0.3285	0.3732
	$\nabla^2\rho_b$	-2.3606	-2.2465	-2.4099	-2.4313	-2.2516	-2.4245
C-H3	ρ_b	0.3074	0.3198	0.3208	0.3177	0.3149	0.3169
	$\nabla^2\rho_b$	-1.2721	-1.3951	-1.4583	-1.3890	-1.3543	-1.3819
N-H4	ρ_b	0.3605	0.3576	0.3600	0.3597	0.3584	0.3582
	$\nabla^2\rho_b$	-2.0186	-2.0271	-1.9644	-1.9799	-1.9685	-1.9378
N-H5	ρ_b	0.3640	0.3593	0.3600	0.3604	0.3583	0.3582
	$\nabla^2\rho_b$	-2.0275	-2.0197	-1.9642	-1.9594	-1.9674	-1.9378
N-H1	ρ_b		0.2376	0.3590	0.3606	0.3553	0.3582
	$\nabla^2\rho_b$		-1.1469	-1.9687	-1.9597	-1.9727	-1.9378
N-H2	ρ_b					0.0429	
	$\nabla^2\rho_b$					0.1177	
N-H3	ρ_b			0.0140			
	$\nabla^2\rho_b$			0.0394			
H1-O1	ρ_b				0.0087	0.0080	
	$\nabla^2\rho_b$				0.0351	0.0331	
ring	ρ_b		0.0565	0.0057			
	$\nabla^2\rho_b$		0.3285	0.0264			

^a For the numbering of atoms see fig. IV.1

^b The units of ρ are e/a_0^3 , the units of $\nabla^2\rho$ are e/a_0^5 .

intermediate to react further the NH_3 group must move around to the other side of the HCOOH group so that the nitrogen atom can form a strong hydrogen bond with the OH group. The barrier for this process is only 1.1 kcal/mole, however it leads to a stabilization of 8.8 kcal/mole over that of the intermediate. With such a small activation barrier to decomposition it is very unlikely that such an intermediate will ever be detected or studied experimentally. In order to facilitate the movement of the NH_3 group, the very weak bonds between the NH_3 and HCOOH molecules are broken and a new bond is formed between the keto-oxygen and one of the hydrogen atoms of the NH_3 molecule. This bond remains intact for the remainder of the reaction although it weakens continually, which is evident from the values of ρ at the critical point for this bond given in Table IV.3. In the final product the value of ρ for this O-H bond is only 0.004 au, which is much less than the value of 0.328 au for the O-H bond in the hydroxyl group of the product. The final product of the neutral hydrolysis differs considerably from that of the O-protonation pathway. The most obvious difference is that in the neutral hydrolysis the hydroxyl hydrogen atom is not removed from the oxygen. This implies that NH_3 is not a strong enough base to cause

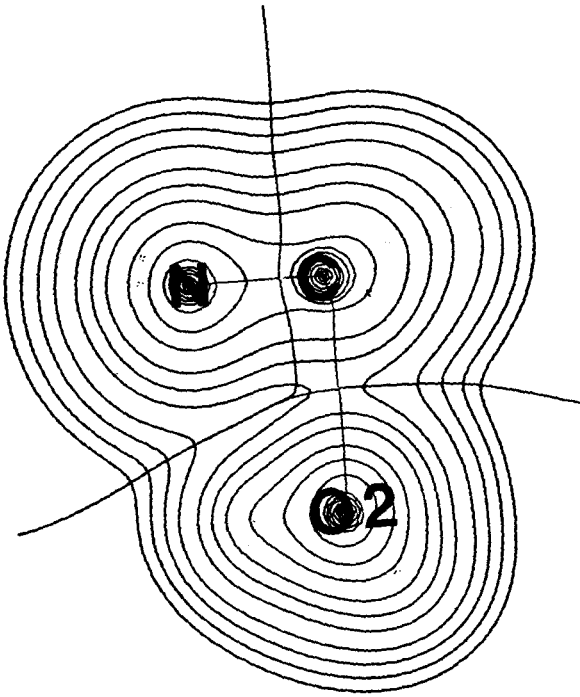
the ionization of formic acid. The energy required to separate this hydrogen-bonded product to ammonia and formic acid is 12.7 kcal/mole. If this product were separated as the NH_4^+ and HCOO^- ions then the energy required for the separation would be 157.8 kcal/mole. The hydrogen bonded product is more stable than the isolated reactants by 11.2 kcal/mole.

From the energy profile for this reaction, given in Figure IV.3, it should be obvious that the prohibitive activation barrier of 62.9 kcal/mole is the reason why formamide cannot be hydrolyzed without a catalyst. However this is only explaining one observation by using another. In order to find the real reason why the neutral hydrolysis does not occur it is necessary to look much deeper into the reaction mechanism. The contour diagrams of ρ and $\nabla^2\rho$, given in Figures IV.4 and IV.5 respectively offer a good clue of what this reason might be. From an examination of these diagrams for the first four configurations leading to the transition state it becomes evident that the water molecule is not reacting with the carbon atom at all. Instead it is reacting with the nitrogen atom in an acid/base reaction, which explains why the hydrogen

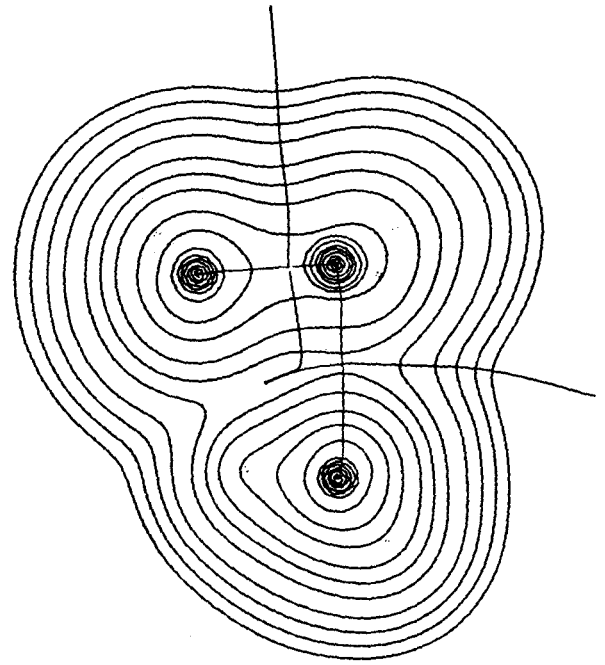
Figure IV.4

The contour maps of the charge density for a series of points along the reaction coordinate of the uncatalyzed hydrolysis of formamide. The maps are in the plane of the N,C and O₂ nuclei and overlaid with those bond paths connecting nuclei in this plane. The projections of the interatomic surfaces onto the plane are shown for each bond path.

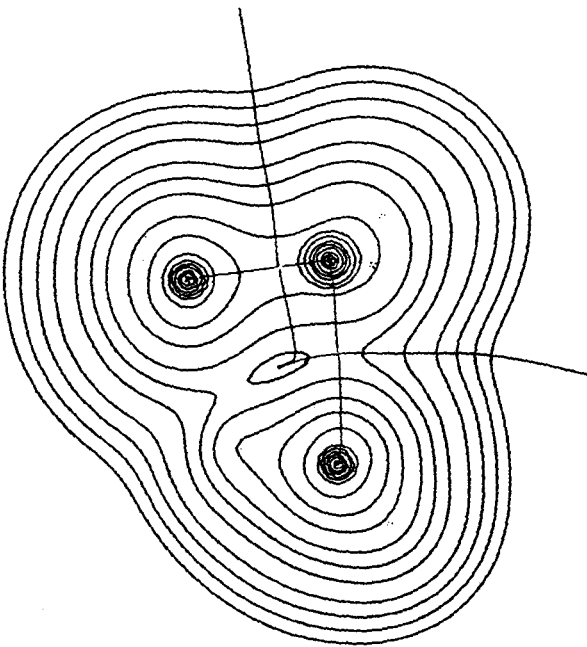
- a-c) configurations on the reaction path leading to the first transition state.
- d) the first transition state.
- e-f) configurations on the reaction path leading to the intermediate.
- g) the intermediate.
- h-i) configurations on the reaction path leading to the second transition state.
- j) the second transition state.
- k) configuration on the reaction path leading to the product.
- l) the hydrogen-bonded product.



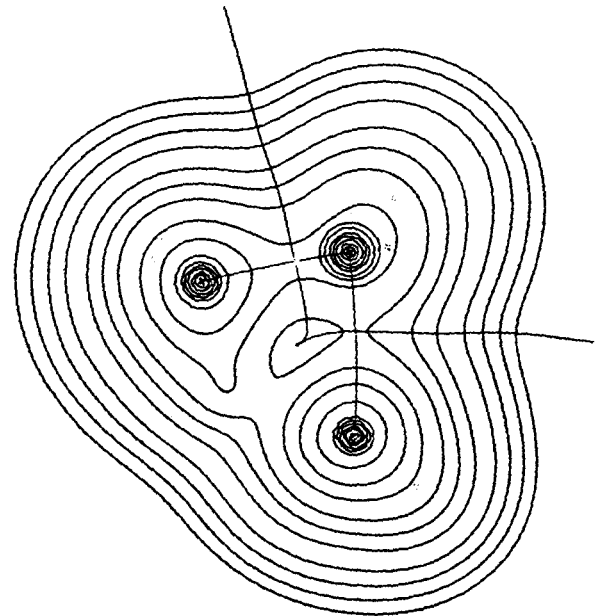
a



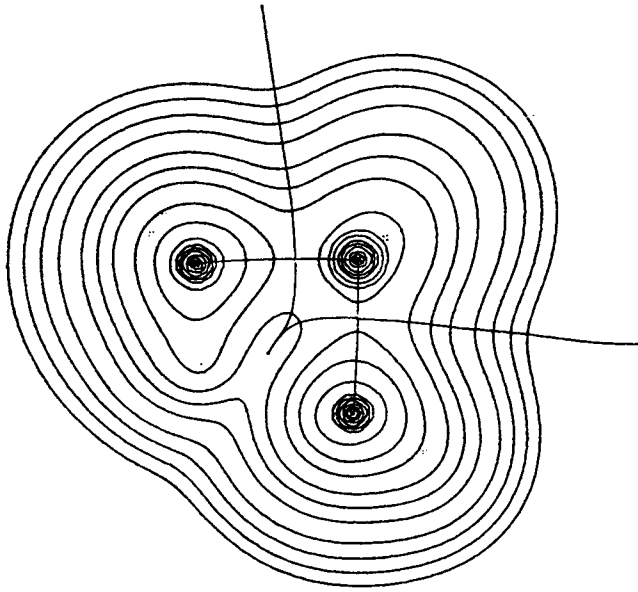
b



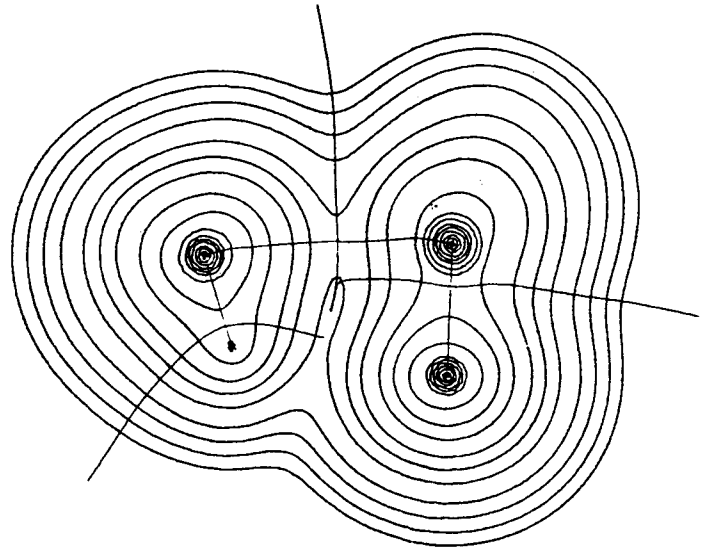
c



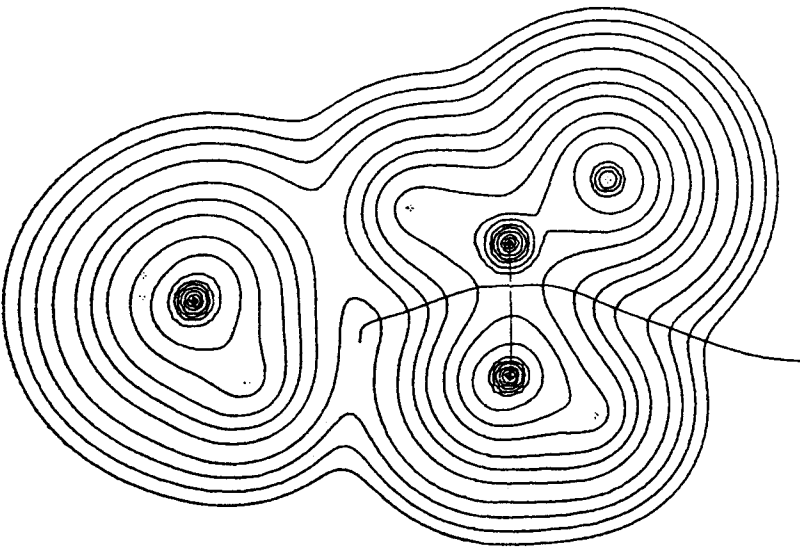
d



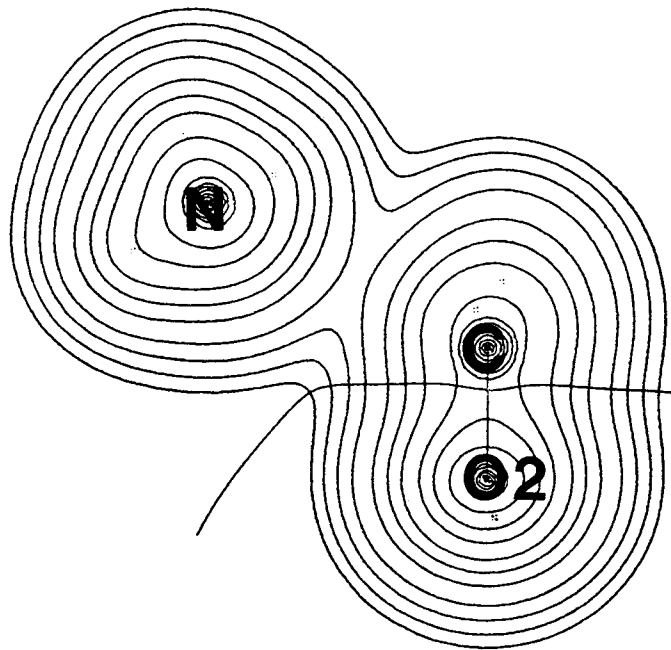
e



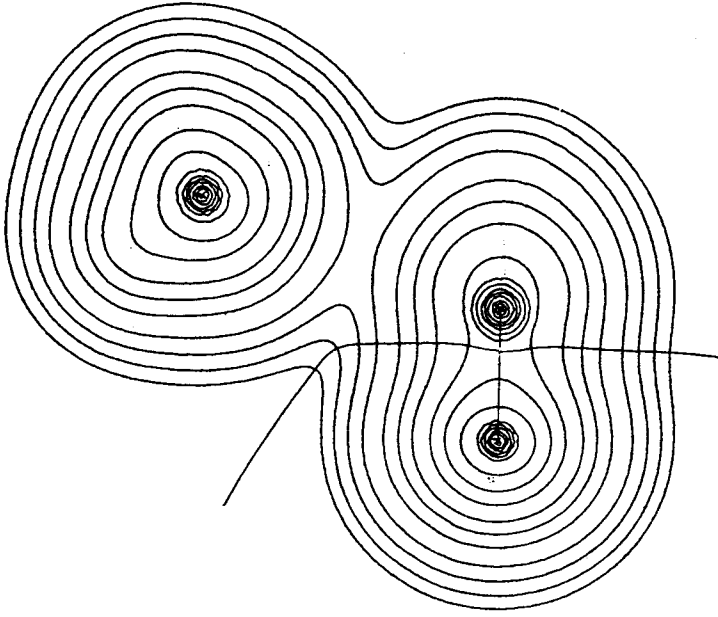
f



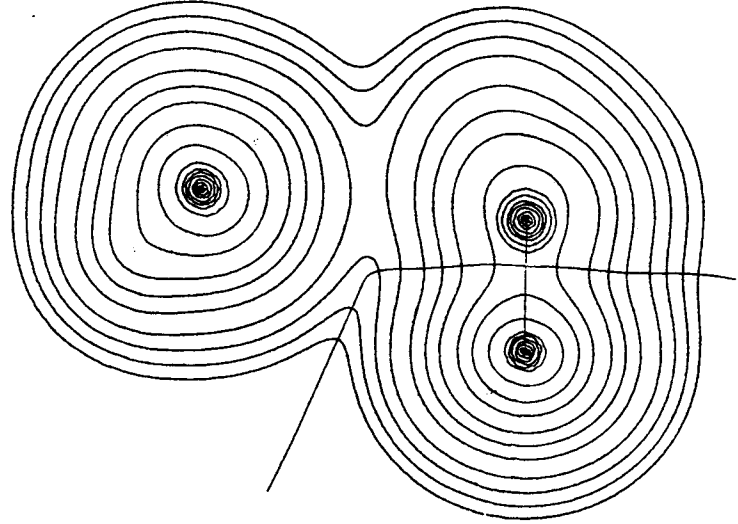
g



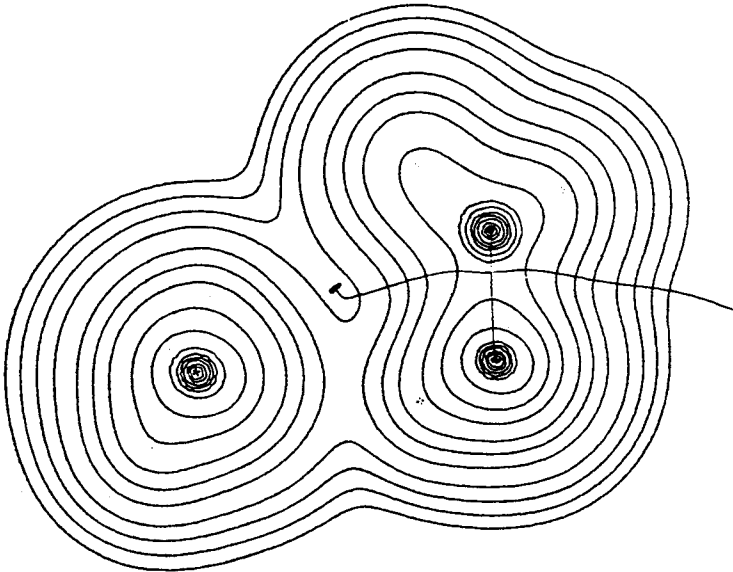
h



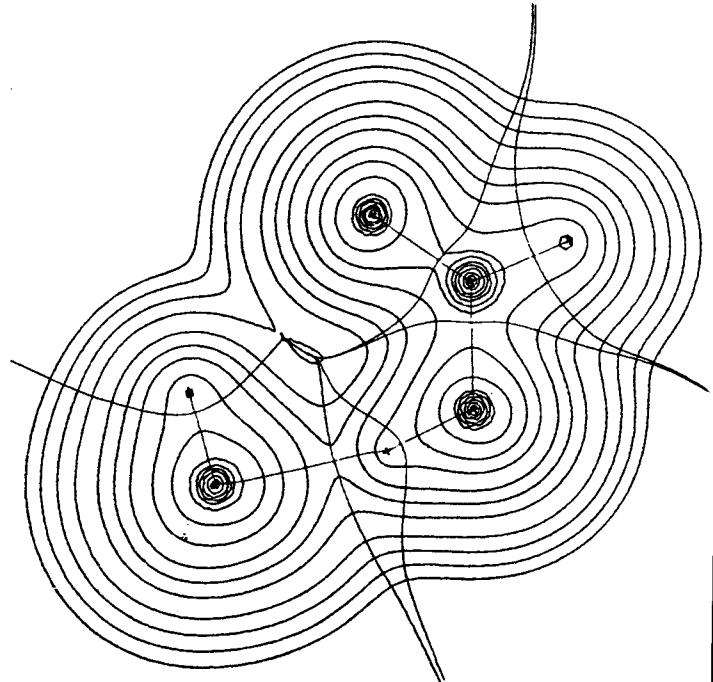
i



j



k

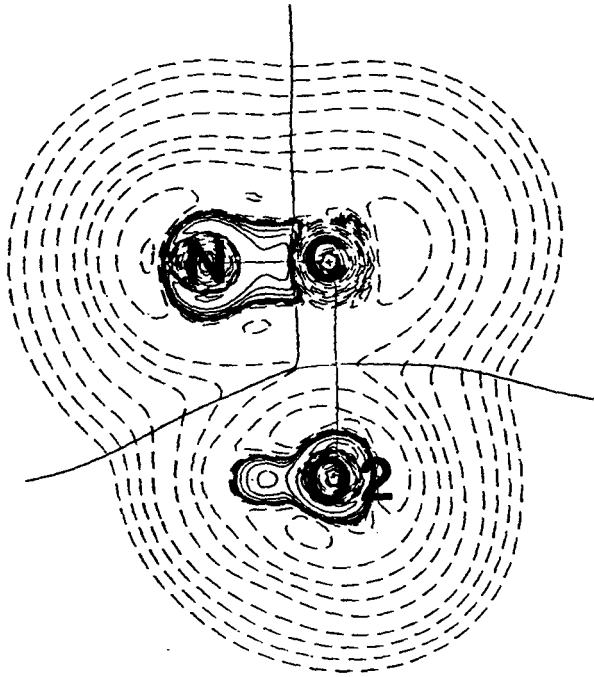


l

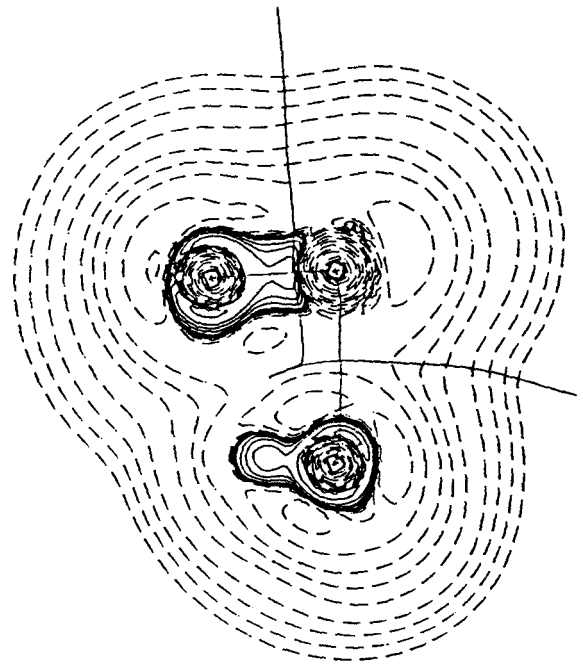
Figure IV.5

The contour maps of the Laplacian of the charge density for a series of points along the reaction coordinate of the uncatalyzed hydrolysis of formamide. The maps are in the plane of the N,C and O2 nuclei and overlaid with those bond paths connecting nuclei in this plane. The projections of the interatomic surfaces onto the plane are shown for each bond path. Dashed contours denote positive values.

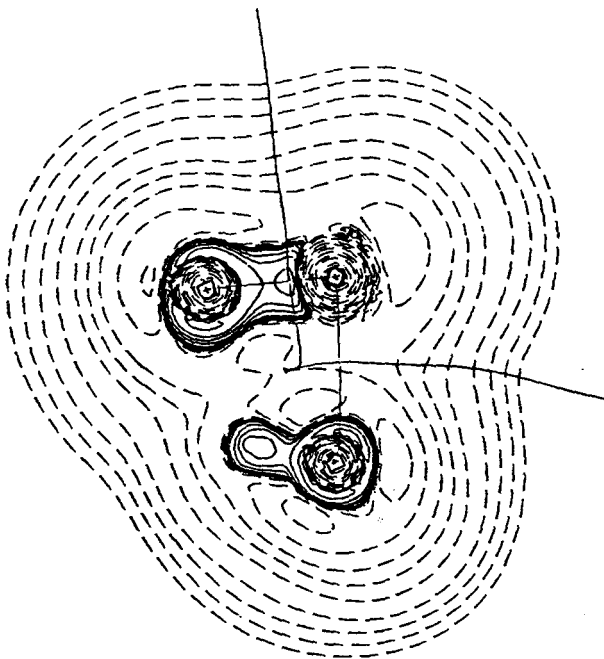
- a-c) configurations on the reaction path leading to the first transition state.
- d) the first transition state.
- e-f) configurations on the reaction path leading to the intermediate.
- g) the intermediate.
- h-i) configurations on the reaction path leading to the second transition state.
- j) the second transition state.
- k) configuration on the reaction path leading to the product.
- l) the hydrogen-bonded product.



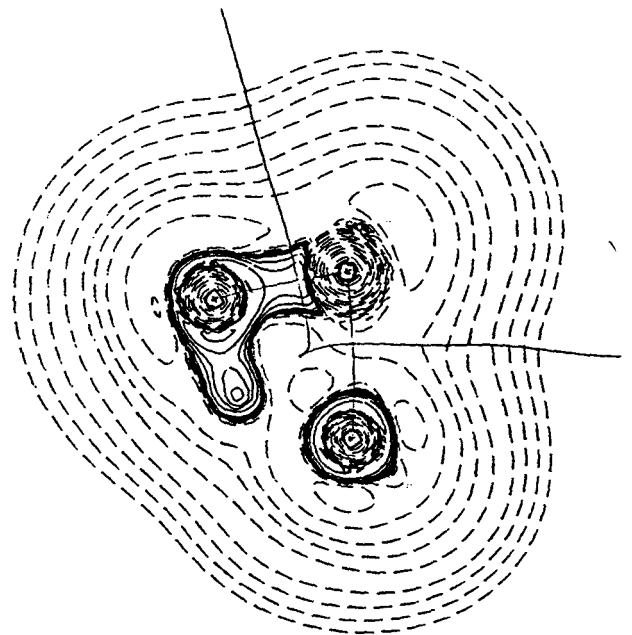
a



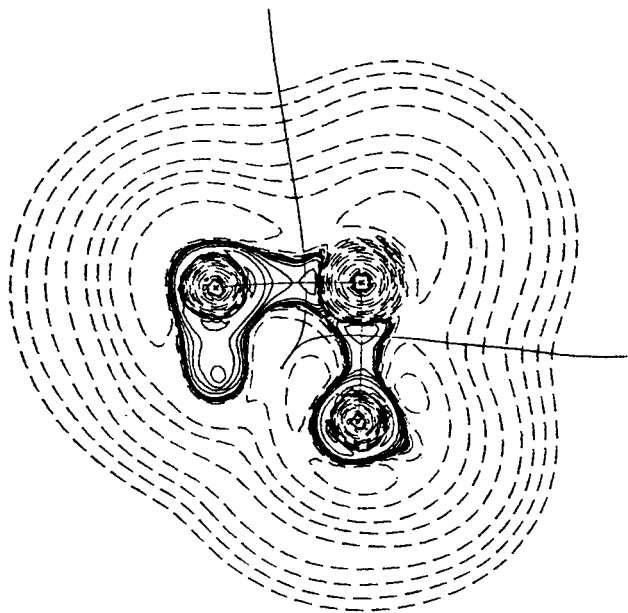
b



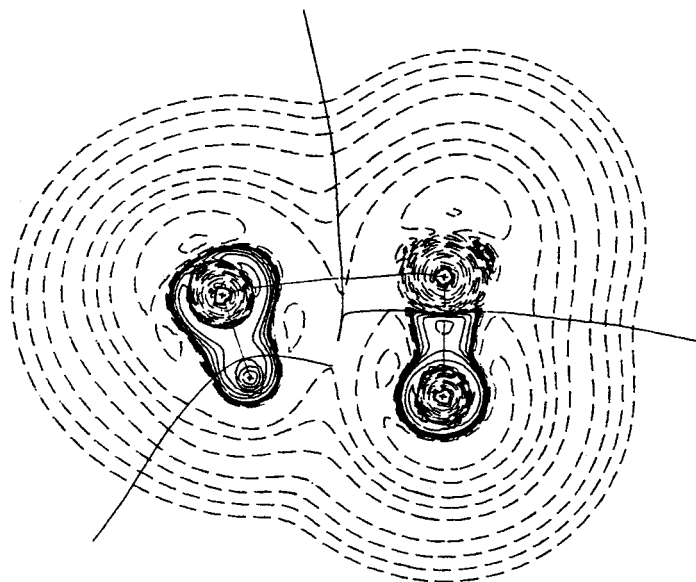
c



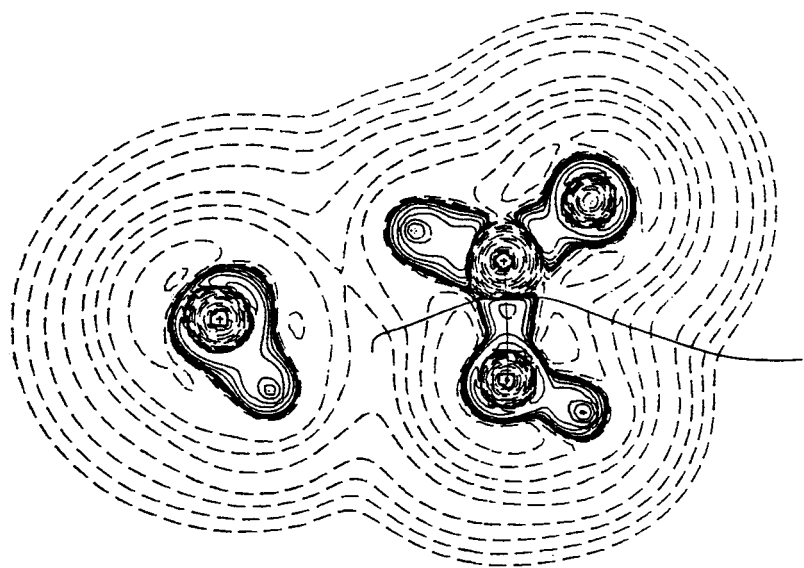
d



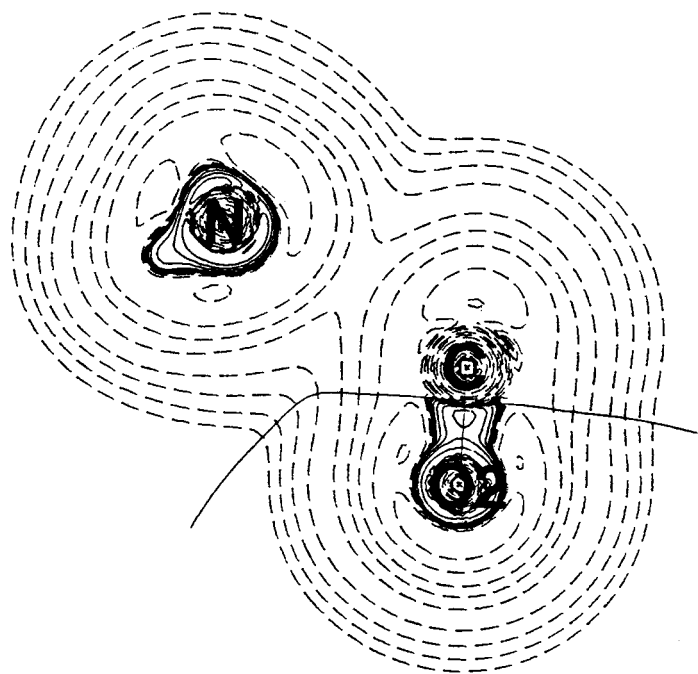
e



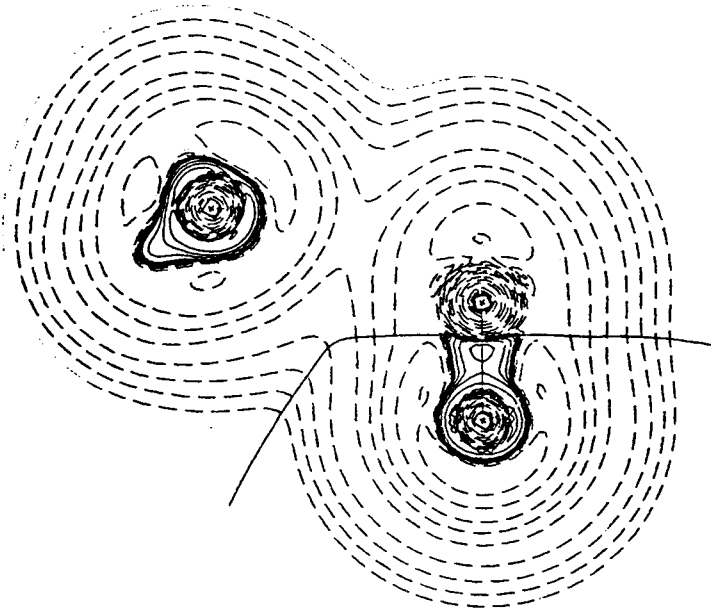
f



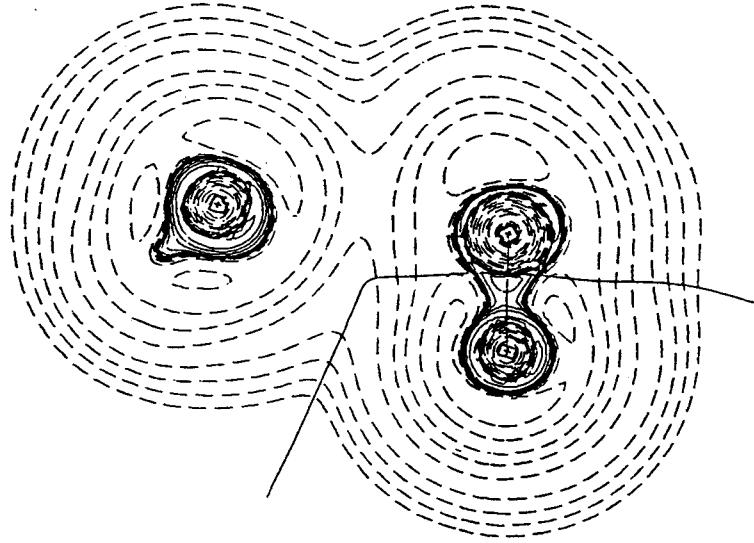
g



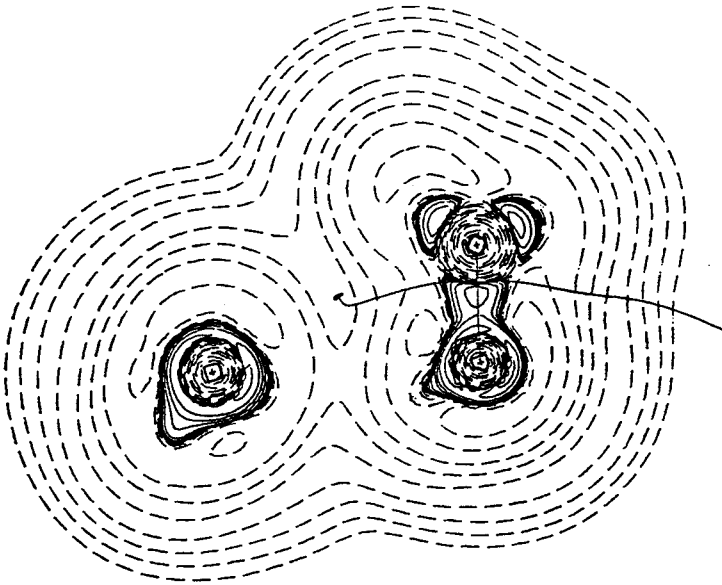
h



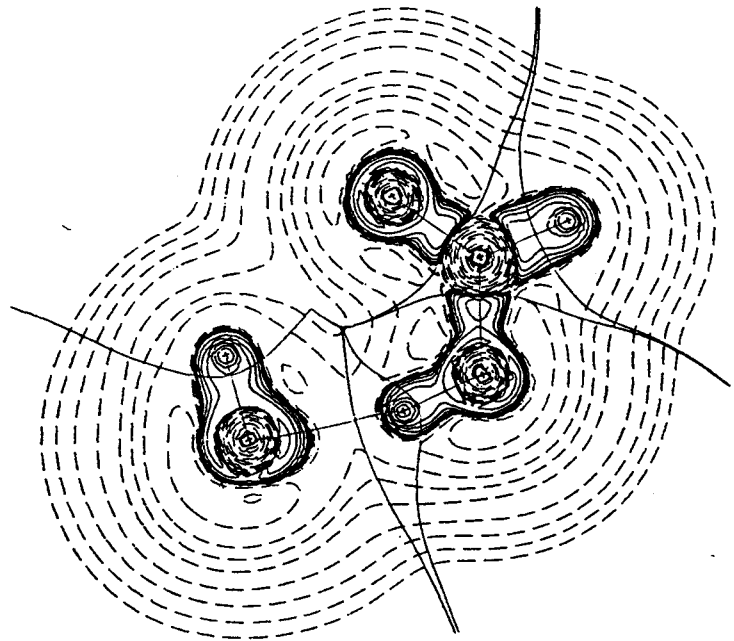
i



j



k



l

atom of the approaching water molecule is bent so far towards the nitrogen atom. The contour diagrams of $\rho(r)$, given in Figure IV.4, show that prior to this acid/base reaction there is virtually no accumulation of charge between the oxygen and carbon nuclei. This is in sharp contrast to the changes in the charge density of O-protonated formamide on approach of the water molecule as illustrated in Figures III.B.4 and III.B.5. In the acid catalyzed reaction the oxygen atom reacts with the carbon atom and charge is accumulated between the two nuclei early in the reaction. The formation of a new bond between these nuclei is evident from Figure III.B.5c, which shows that charge is locally concentrated in this region. It is only after the new bond path is formed that the transfer of the hydrogen atom takes place in the catalyzed reaction. On the other hand the sequence of these two steps is reversed in the neutral hydrolysis. This implies that without protonation of the keto oxygen atom the water molecule is not a strong enough nucleophile to react with the carbon atom whereas the NH_2 group is a strong enough base to react with the water molecule. In the reaction of formamide with OH^- not only is the hydroxide ion a much better nucleophile than the water molecule but it is also a much stronger

base than the NH_2 group. After the water molecule has protonated the NH_2 group, then what remains is N-protonated formamide with OH^- at the carbon atom, which together make a very reactive pair. It then comes as no surprise that the entire activation barrier comes from the protonation of the NH_2 group by water, which is after all only a very weak acid. Once this protonation has taken place the remainder of the reaction is energetically downhill as demonstrated by the large energy drop after the transition state. It is during this period at the transition state and immediately following that the actual nucleophilic addition reaction takes place. This fact is evident in Figure IV.5e which shows the reaction between the carbon and oxygen atoms. The values of ρ for the bond critical point between the C and O2 nuclei, given in Table IV.3, also support the conclusion that the bond between the carbon atom and the oxygen atom of the water molecule is formed late in this reaction. In the first transition state the value of ρ for this bond path is only 0.08 au, which is much less than the value of 0.20 au for the corresponding critical point in the transition state of the O-protonation mechanism. However, in the steps immediately following the transition state the

value of ρ at this critical point increases markedly and when the intermediate is reached the value of ρ at this critical point is 0.29 au, which is almost identical to the value of 0.30 au at the corresponding critical point in the intermediate formed in the O-protonation mechanism.

The values of $\nabla^2\rho$ at the (3,+1) critical point in the VSCC of the carbon atom are given in Table IV.4. Unlike the corresponding (3,+1) critical point in O-protonated formamide, which was attacked by the water molecule early in the reaction, in this reaction the (3,+1) critical point exists up to the transition state, ie. the hole in the VSCC of the carbon atom is filled in only after the transition state is reached. This fact further substantiates the claim that the C-O bond formation begins late in this reaction. The angle formed between this critical point and the C-N bond is very close to that formed between the approaching oxygen atom and the C-N bond. This is surprising in light of the fact that it is the hydrogen atom on the water molecule that reacts first so it would be expected that this acid/base reaction would divert the water molecule from the carbon atom. This suggests that even

Table IV.4

The properties of the (3,+1) critical point (cp) in $\nabla^2\rho$ at the carbon atom of formamide during the initial steps of reaction with water.

	formamide	a	b	c	transition state d
$\nabla^2\rho^a$	0.129	0.162	0.175	0.172	0.106
$r(C), \text{\AA}$	0.570	0.579	0.585	0.585	0.554
$r(O2), \text{\AA}$		1.883	1.621	1.527	1.406
$\angle C\text{-cp-O2}^b$		162.92	165.53	166.64	145.19
$\angle N\text{-C-cp}$	77.12	79.44	78.44	79.45	94.87
$\angle N\text{-C-O2}$		90.31	86.53	84.02	79.63

^a The units of $\nabla^2\rho$ are $e/a_0^5 = 24.100e/\text{\AA}^5$

^b All angles are in degrees.

though the acid/base reaction at the nitrogen atom takes place first there is still some interaction between the carbon atom and the oxygen atom of the water molecule during the early stage of the reaction. Table IV.5 gives the values of $\nabla^2\rho$ at the nonbonded maximum in the VSCC of the nitrogen atom to which the hydrogen atom will be transferred. The value of $\nabla^2\rho$ at this point decreases as the reaction proceeds and this can be attributed to the formation of the N-H bond. The angle formed between this (3,-3) critical point and the C-N bond is very close to the angle formed between this bond and the hydrogen atom being transferred, therefore the charge concentration is directed towards the hydrogen. This illustrates the importance of these local concentrations in $\nabla^2\rho$ in attracting protons in acid/base reactions. Table IV.6 gives the values of $\nabla^2\rho$ for the (3,-3) nonbonded charge concentration in the VSCC of the oxygen atom of the water molecule. A very noticeable feature is the increasing distance between this critical point and the oxygen nucleus. This is consistent with the observation that the bonded maxima in $\nabla^2\rho$ occur farther from the nucleus than nonbonded maxima when in the same atom. The fact that the magnitude of this maximum decreases sharply at the transition state indicates that at this point of the

Table IV.5

The properties of the nonbonded (3,-3) critical point (cp) in $\nabla^2\rho$ at the nitrogen atom of formamide during the initial stages of the hydrogen transfer from water.

	formamide	a	b	c	transition state d
$\nabla^2\rho^a$	-2.129	-2.490	-2.787	-2.895	-2.829
$r(\text{N}), \text{\AA}$	0.399	0.395	0.393	0.393	0.404
$r(\text{H1}), \text{\AA}$		2.117	1.710	1.441	0.732
$\angle \text{N-cp-H1}^b$		164.14	154.98	153.64	166.89
$\angle \text{C-N-cp}$	80.95	79.50	100.74	102.07	96.50
$\angle \text{C-N-H1}$		71.46	80.32	81.27	88.04

^a The units of $\nabla^2\rho$ are $e/a_0^5 = 24.100e/\text{\AA}^5$

^b All angles are in degrees.

Table IV.6

The properties of the nonbonded (3,-3) critical point (cp) in $\nabla^2\rho$ at the oxygen atom of water during the initial steps of the attack on formamide.

	water	a	b	c	transition state d
$\nabla^2\rho^a$	-6.584	-6.550	-6.349	-6.089	-5.137
$r(O_2), \text{Å}$	0.335	0.335	0.336	0.338	0.342
$r(C), \text{Å}$		2.165	1.919	1.822	1.817
$\angle C\text{-cp-O}_2^b$		143.26	141.53	143.04	96.77

^a The units of $\nabla^2\rho$ are $e/a_0^5 = 24.100e/\text{Å}^5$

^b All angles are in degrees.

reaction the nonbonded maximum on the oxygen atom is starting to react with the carbon atom.

The relative atomic populations and relative atomic energies are given in Table IV.7 and Table IV.8 respectively. The relative populations of the transition state show the large transfer of charge from the nitrogen atom and concurrent transfer of charge to the carbon atom. On reaching the intermediate, however, all of the excess charge that was placed on the carbon atom prior to the transition state has been removed. This feature, in which charge is transferred from the nitrogen atom is common with all of the mechanisms studied. It can be rationalized on the basis that the atomic population of the nitrogen atom in NH_3 is much less than that in formamide or O-protonated formamide. Therefore in any step in which the C-N bond is being weakened or broken to create NH_3 as a leaving group it is expected that the atomic population of the nitrogen atom will decrease.¹ With this observation it is

¹ The reason why this characteristic decrease in the atomic population of nitrogen is not apparent in the hydrolysis of N-protonated formamide will be discussed in the conclusion.

Table IV.7

Changes in the atomic populations for the reaction of formamide with water relative to their values in the isolated reactants.

reactants	Atom ^a	transition state	intermediate	transition state	product	isolated products
4.0522	C	0.1764	0.0212	-0.0598	-0.0714	-0.0423
8.4803	N	-0.1741	-0.2451	-0.2414	-0.2407	-0.3613
9.3704	O1	0.0441	0.0036	0.0096	0.0250	-0.0049
9.2511	O2	0.0536	0.0792	0.0742	0.1579	0.0760
0.3745	H1	-0.0528	0.1980	0.2256	0.1687	0.2525
0.3745	H2	0.0196	-0.0319	-0.0374	-0.0902	-0.0377
1.0296	H3	-0.0643	-0.1397	-0.0631	-0.0481	-0.0650
0.5248	H4	-0.0029	0.0659	0.0362	0.0579	0.1021
0.5424	H5	0.0065	0.0490	0.0563	0.0402	0.0845

^a for the numbering of atoms see fig. IV.1

Table IV.8

Changes in the atomic energies^a for the reaction of formamide with water relative to their values in the isolated reactants.

reactants	Atom ^b	transition state	intermediate	transition state	product	isolated products
-36.5794	C	-0.0524	0.0052	0.0643	0.0718	0.0443
-55.2578	N	0.0887	0.3706	0.3713	0.3284	0.4858
-75.5897	O1	-0.0593	-0.0638	-0.0645	-0.0492	-0.0860
-75.3474	O2	0.0563	-0.2245	-0.2474	-0.3143	-0.2624
-0.3376	H1	0.0586	-0.1091	-0.1244	-0.0891	-0.1369
-0.3376	H2	-0.0104	0.0210	0.0241	0.0712	0.0245
-0.6587	H3	0.0168	0.0565	0.0232	0.0122	0.0248
-0.4207	H4	0.0033	-0.0360	-0.0207	-0.0308	-0.0538
-0.4334	H5	-0.0008	-0.0236	-0.0278	-0.0179	-0.0411

^a in au.

^b for the numbering of atoms see fig. IV.1

interesting to note that although some charge is transferred from the nitrogen atom prior to the transition state this is not as much as expected based on the values for the O-protonation mechanism. In the steps after the transition state leading to the intermediate a considerable amount of charge is still transferred from the nitrogen atom. This implies that much of the actual bond breaking takes place after the transition state. The C-N bond lengths given in Table IV.1 support this hypothesis. The C-N bond only gradually lengthens during the reaction leading to the transition state, the total increase in the length of the C-N bond up to this point is only 0.1904 \AA . However, immediately following the transition state this bond lengthens dramatically so that by the time configuration e is reached the C-N bond is 2.5291 \AA longer than it was in the reactants and this is an increase of 1 \AA over that at the transition state. It is interesting to note that the C-N bond length at the transition state is almost exactly the same as that in N-protonated formamide. This observation supports the conclusion that the reaction of formamide and water prior to the first transition state is predominantly a nitrogen protonation reaction with the nucleophilic reaction commencing immediately at the transition state.

It was noted earlier that the geometry of the intermediate in this reaction resembles that of the separated ammonia and formic acid molecules. Not only does the geometry resemble that of the separated molecules but so do the atomic populations and atomic energies, although here the degree of similarity is not so close. A comparison of the relative atomic populations of the intermediate with those of the isolated products (compare the values in the second column of Table IV.7 with those in the last column) would show that some similarity exists. The same can be done for the relative atomic energies (compare the values in the second column of Table IV.8 with those in the last column). The electron population of the NH_3 group in the intermediate is 9.99 which is very close to the electron population of the isolated ammonia molecule. Likewise the electron population of the HCOOH group is 24.01 which is very close to that in the formic acid molecule. The energies of the NH_3 group and HCOOH groups are -56.2476 au and -188.7131 au respectively and both of these are close to the values of -56.1916 au and -188.7682 au for the corresponding isolated molecules.

In conclusion, the study of the neutral hydrolysis of formamide has provided valuable information on what must be done to facilitate the hydrolysis of an amide bond. The water molecule is neither a strong enough acid nor a strong enough nucleophile to bring about hydrolysis. Either a stronger acid, such as H_3O^+ or a stronger nucleophile such as OH^- must be used.

Chapter 5

Conclusion

In the preceding chapters a description of the possible pathways of amide hydrolysis was given using formamide as a model of an amide bond. Experimental studies on amide hydrolysis have yielded many important observations and it is the purpose of this chapter to explain and rationalize those observations and in so doing, arrive at some conclusions regarding the mechanism followed in amide hydrolysis.

The final product formed in the acid catalyzed reaction consists of the NH_4^+ ion hydrogen bonded to formic acid. In the product of the N-protonation mechanism a hydrogen of NH_4^+ is bonded to the hydroxyl oxygen of formic acid whereas in the O-protonation mechanism it is bonded to the keto oxygen atom. The latter product is more stable than the former by 13.1 kcal/mole. Therefore the product of the N-protonation mechanism can convert to the more stable product by a

transfer of a proton from the one oxygen atom to the other. In that case the final products of the two reactions will be the same and if the initial protonation step is taken as the beginning of the reaction then they also have the same reactants and ΔH_0° value. These two reaction paths connect the same two points on the potential energy hypersurface and the value of any state function will be the same for both mechanisms. The kinetics of these two reactions are expected to be radically different because the hydrolysis via the N-protonation mechanism is a barrierless process whereas the O-protonation mechanism is not. This is the explanation of the experimental observation that the rate of hydrolysis through the N-protonation pathway is on the order of 10^5 times that through the O-protonation pathway.

This leads directly to another question; Why is the N-protonation pathway barrierless? The answer to this question becomes even more important in light of the recent observation referred to in the introduction that amides in which the nitrogen atom is pyramidalized with attendant lengthening of the C-N bond are activated toward nucleophilic attack and exhibit an accelerat-

ed rate of hydrolysis (Brown et al., 1991). In comparing the relative atomic populations of the four reactions the most noticeable feature is the large decrease in the atomic population of the nitrogen atom during the transfer of the hydrogen atom from the water molecule (or OH^- ion in the case of the base enhanced reaction). This decrease is present in the first step of each reaction with the exception of the hydrolysis of N-protonated formamide, and in each case the relative change in the value of the electron population of nitrogen is around 0.2 au. Since the transfer of charge from the nitrogen to the carbon atom is accompanied by the weakening and eventual breakage of the C-N bond, this implies that the transfer of charge from the nitrogen atom to the carbon atom must have occurred some time earlier for the N-protonation mechanism, i.e. during the initial protonation step. The relative atomic populations of protonated formamide, given in Table V.1, show that this is indeed the case. During the protonation of formamide, 0.2150e of charge is transferred from the nitrogen atom if protonation takes place on the nitrogen atom. If the oxygen atom is protonated then there is very little change in the population of the nitrogen atom. The population of the

Table V.1

Changes in the atomic populations of formamide on protonation relative to their values in neutral formamide.

formamide	Atom ^a	N-protonated formamide	O-protonated formamide
4.0522	C	0.2768	0.1056
8.4803	N	-0.2150	0.0455
9.3704	O1	-0.1532	-0.0423
1.0296	H3	-0.1818	-0.1894
0.5248	H4	-0.0716	-0.0886
0.5424	H5	-0.0852	-0.1026

^a for the numbering of the atoms see fig. V.1

carbon atom increases to a much greater extent when the protonation is on nitrogen rather than oxygen. This implies that upon protonation at the nitrogen atom, the C-N bond is already considerably weakened and the hydrolysis is to a large extent facilitated even prior to the approach of the water molecule. If this is the case then it would be very informative to look at the changes that occur in the properties of the C-N bond when formamide is protonated. These properties are given in Table V.2. When formamide is protonated on the nitrogen atom the C-N bond lengthens whereas when the protonation takes place on the oxygen atom the C-N bond length actually decreases. In addition the value of ρ at the bond critical point decreases substantially on protonation of the nitrogen atom whereas the value of ρ at this critical point increases during the protonation of the oxygen atom. This suggests that the C-N bond is lengthened and weakened on protonation at the nitrogen atom.

Formamide protonated on the oxygen atom is 22.0 kcal/mole more stable than the nitrogen protonated isomer. The relative atomic energies of protonated formamide, given in Table V.3, show that the energies of both the carbon and nitrogen atoms of formamide are

Table V.2

The properties of the C-N bond critical point in $\rho(r)$ for formamide and protonated formamide.

	formamide	O-protonated formamide	N-protonated formamide
$R_e, \text{\AA}$	1.3467	1.2784	1.5284
$r_c, \text{\AA}$	0.4398	0.4213	0.5472
$r_N, \text{\AA}$	0.9068	0.8571	0.9812
$\rho(r)^a$	0.3334	0.3906	0.2291
$\nabla^2\rho^b$	-0.7721	-0.8035	-0.6721

^a The units of ρ are $e/a_0^3 = 6.7483e/\text{\AA}^3$

^b The units of $\nabla^2\rho$ are $e/a_0^5 = 24.100e/\text{\AA}^5$

Table V.3

Changes in the atomic energies^b of formamide on protonation relative to their values in neutral formamide.

formamide	Atom ^a	N-protonated formamide	O-protonated formamide
-36.5794	C	-0.1845	-0.0858
-55.2578	N	0.1129	-0.1379
-75.5897	O1	-0.0572	-0.0476
-0.6587	H3	0.0847	0.0854
-0.4207	H4	0.0446	0.0530
-0.4334	H5	0.0536	0.0609

^a for the numbering of the atoms see fig. V.1
^b in au.

substantially decreased on protonation of the oxygen atom. When the nitrogen atom is protonated the energy of the carbon atom is also decreased, however, this is to a large extent offset by a large increase in the energy of the nitrogen atom.

The explanations given above raise another question, and that is; If the pathway involving protonation at the nitrogen is much more favorable from a kinetic point of view, then why does the acid catalyzed hydrolysis not follow this route? Experimental studies have demonstrated that only a small percentage of the acid catalyzed hydrolysis of an amide actually follows the N-protonation pathway. The reason for this is that most of the protonated formamide molecules are in the O-protonated form and once they have been protonated on the oxygen there is little chance for them to isomerize to the N-protonated form before being attacked by a water molecule. The fact that the O-protonated isomer is more stable than the N-protonated isomer does not necessarily mean that formamide will protonate preferentially on the oxygen atom. The thermodynamic stability of the product cannot be used to explain the enhanced basicity of the oxygen atom over the nitrogen

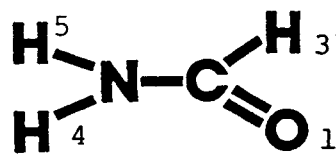
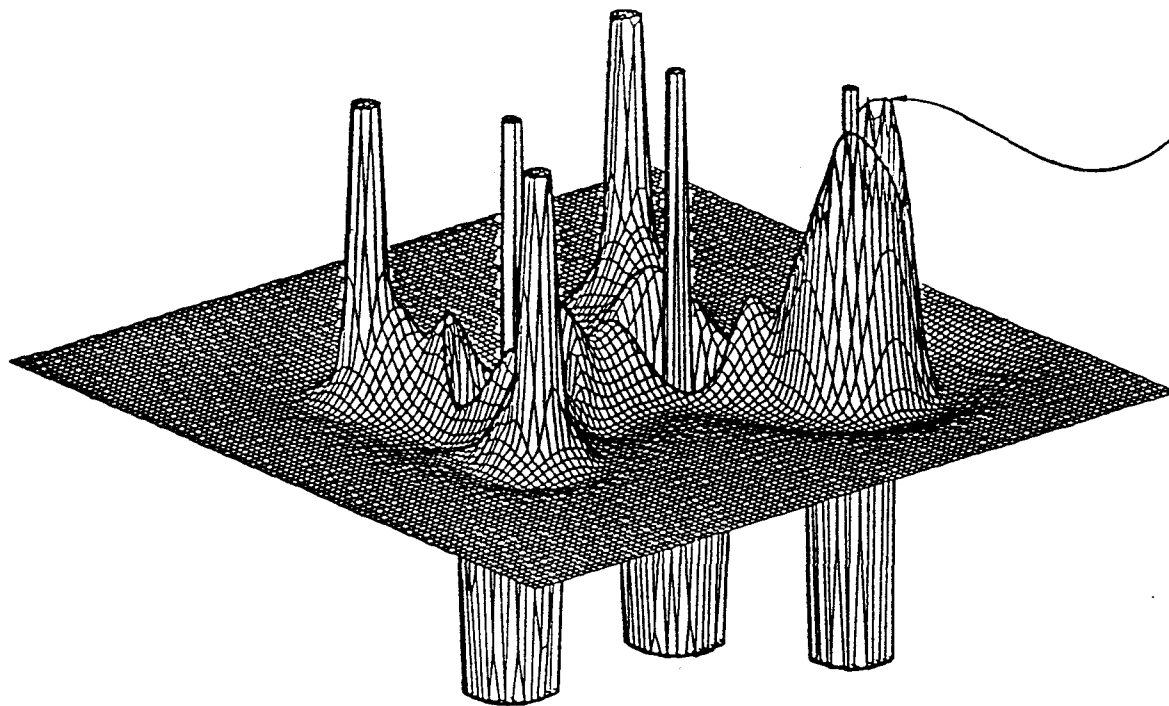
atom in formamide. The explanation can, however, be obtained from the Laplacian of the charge density of formamide, and in particular, by a comparison between the local charge concentrations of the oxygen atom with those of the nitrogen atom. The relief map of the Laplacian in formamide is shown in Figure V.1. The oxygen atom in the formamide molecule has two large nonbonded charge concentrations in the plane of the nuclei ($\nabla^2\rho = -6.329$ au and -6.373 au) while the nitrogen atom exhibits two such maxima of lesser magnitude ($\nabla^2\rho = -2.129$ au) above and below the plane of the molecule. On the basis of this information one correctly predicts that the formamide molecule will preferentially protonate at the oxygen atom, specifically at the position of the largest of the two charge concentrations and in the plane of the nuclei. When formamide protonates at this position the anti isomer of O-protonated formamide is formed (the proton and the NH_2 group are on opposite sides of the C-O bond) and it is this conformer that undergoes hydrolysis. In order for the syn isomer (the isomer in which the proton and the NH_2 group are on the same side of the C-O bond) to react it must isomerize to the anti isomer. The activation barrier for this conversion is 34.3 kcal/mole, which is more than the 32.2 kcal/mole barrier which

Figure V.1

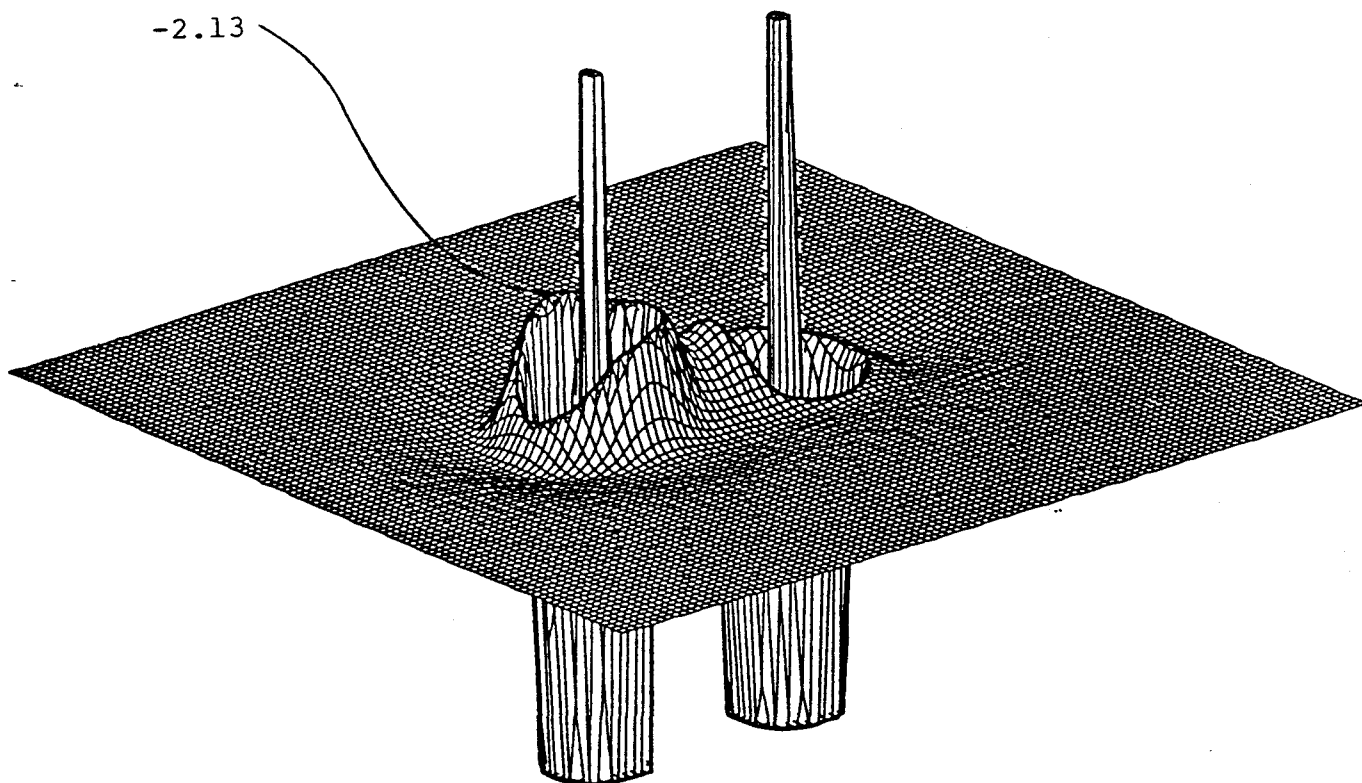
Relief maps of the Laplacian in formamide. The top figure illustrates the Laplacian in the plane containing the nuclear framework, while the lower figure shows the Laplacian in the π plane of the N-C bond. The value of $\nabla^2\rho$ at the largest of the two nonbonded maxima in the VSCC of the oxygen atom is shown in the top figure. The value of $\nabla^2\rho$ at one of the two equivalent nonbonded maxima in the VSCC of the nitrogen atom is shown in the lower figure.

153

-6.37



-2.13



must be surmounted for the deprotonation of the syn isomer to formamide and H_3O^+ . The anti-protonated isomer is 3.2 kcal/mole more stable than the syn-protonated isomer.

In general, hydroxide ions are much more effective in catalyzing amide hydrolysis than hydronium ions (Hine et al., 1981). This experimental observation was pointed out in the first chapter and at this point it can be explained on the basis of the results of this study. The reason for the greater effectiveness of OH^- is the fact that it is a much stronger nucleophile than water and attacks the carbon atom without a barrier. Since the acid catalyzed hydrolysis proceeds through an O-protonation mechanism there is a barrier to the attack of the water molecule. The energy required for the intermediate in the OH^- catalyzed reaction to decompose to the product is 21.8 kcal/mole which is much less than the 38.8 kcal/mole barrier for the water molecule to hydrolyze O-protonated formamide.

In the discussion on the uncatalyzed hydrolysis mechanism it was noted that the water molecule reacted first with the nitrogen atom in an acid/base reaction before reacting with the carbon atom. The explanation

for this was that the NH_2 group is a good base whereas the water molecule is a weak nucleophile so the acid/base reaction occurs first. In the hydrolysis of O-protonated formamide the nucleophilic reaction is first and an intramolecular acid/base reaction follows. Since these two reactions both have the same nucleophile, ie. H_2O , and it is unlikely that protonation at the keto oxygen will alter the basicity of the NH_2 group to any significant extent, the main difference in these two reactions must be in the reactivity of the carbon atom. In other words, protonation on the oxygen atom must greatly enhance the reactivity of the carbon atom towards nucleophilic attack. From the relative atomic populations given in Table V.1 it can be seen that the charge on the carbon atom actually becomes less positive on protonation of the oxygen atom. The atomic populations are therefore not of much help in explaining this enhanced reactivity and it is necessary to look at the Laplacian of ρ for an explanation. The values of $\nabla^2\rho$ at the (3,+1) critical point in the VSCC of the carbon atom above and below the molecular plane are given in Table V.4. The value of $\nabla^2\rho$ at this point increases from 0.129 au to 0.161 au on protonation of the oxygen atom. This increase in the magnitude of the

Table V.4

The properties of the (3,+1) critical points in $\nabla^2\rho$ at the carbon atom of formamide and protonated formamide.

	formamide	N-protonated formamide	O-protonated formamide
$\nabla^2\rho^a$	0.129	0.093	0.161
$r(C), \text{\AA}$	0.570	0.551	0.655
$\nabla^2\rho$	0.129	0.094	0.161
$r(C), \text{\AA}$	0.570	0.551	0.655

^a The units of $\nabla^2\rho$ are $e/a_0^5 = 24.100e/\text{\AA}^5$

local charge depletion is accompanied by an increase in the size of the hole in the VSCC and hence an increased reactivity towards nucleophilic attack. ¹

The correlation of the results from these calculations on the potential energy hypersurface with experimental kinetic results is not straightforward. There are several reasons for this, the most important one is that the kinetic data refers to the free energies of activation in solution. The solvent can alter the free energy along the reaction coordinate. In addition a statistical analysis over all of the trajectories would be necessary. When considering the calculated energy differences (all of which neglect the changes in zero point vibrational energy) it is important to remember that they are the heats of reaction at 0K, ΔH_0° . The equilibrium at 25°C will depend on ΔG_{298}° ,

¹ This is not always the case; some (3,+1) critical points in the VSCC of a carbonyl carbon have large values of $\nabla^2\rho$ but relatively narrow holes in the VSCC. Since the nucleophile must react through the hole in the VSCC, the size of the hole is a very important property. Unfortunately the size of the hole in the VSCC is difficult to quantify, however when comparing the same (3,+1) critical points on a series of related molecules the generalization can be made that the size of the hole is proportional to the value of $\nabla^2\rho$ at the critical point.

which has large contributions from the enthalpies and entropies of solution. Since the products are ions they would probably be solvated by the solvent and therefore the hydrogen-bonded products calculated for each reaction pathway might not exist. The separation of the associated product molecules might not raise the energy of the system however, because the energy of the separated ions would be lowered considerably by solvation. Differential effects of solvation along the reaction path will be very important. The different dimensions of the charged species suggests that the hydration energy of OH^- will be greater than that of the formate anion and this might lead to the formation of an energy barrier for the attack of OH^- on formamide. Although the energy profiles of the acid catalyzed and uncatalyzed reactions may be altered considerably by the presence of the solvent, these changes will probably affect each mechanism to a similar extent and thus will not alter the relative ordering of the energies of activation for these three mechanisms. This assumption can be justified by the fact that the computed activation barriers agree qualitatively very well with those determined experimentally.

In spite of the difficulties in correlating gas-phase calculations to the results measured in solution, the calculations are very valuable in increasing our understanding of the factors which enhance the reactivity of an amide bond towards nucleophilic attack. The gas-phase results may in fact be more relevant than those obtained from solution for explaining the enzymatic hydrolysis of an amide bond. Since the active site is often enclosed in the hydrophobic environment within the enzyme, water molecules might not be present, except for one positioned optimally for the hydrolysis. Enzymes are very efficient at catalyzing the hydrolysis of amide bonds and the rates of reaction for the enzymatic hydrolysis are much faster than the rate of the acid catalyzed hydrolysis. The acid catalyzed reaction follows the O-protonation pathway because it is more energetically favorable for an amide to protonate on oxygen. An enzyme may, however, selectively protonate the amide bond on the nitrogen atom and thereby gain the 10^5 rate increase that the N-protonation pathway provides.

Further work on this reaction would involve studying the effects of hydrogen bonding by the solvent. These effects might alter the heights of the

energy barriers and for this reason are very important. Such a study would not be very time consuming because it would only require consideration of the two major hydrogen bonding interactions, that between the solvent molecule and either the nitrogen or the keto oxygen atom.

The study of the effects of structural distortion on the reactivity of the amide unit towards nucleophilic attack is currently a very active field of study. It has been found that amide distortions that involve either the rotation about the N-C bond or N-pyramidalization greatly accelerate the attack of nucleophiles on the C=O unit of amides (Brown et al., 1991). Studies have also shown that the value of $\nabla^2\rho$ at the (3,+1) critical point in the VSCC of the carbon atom increases on pyramidalization of the nitrogen (Laidig and Bader, 1991). It would be very interesting to see if such distortions of the amide unit also lower the calculated energy barriers. For example; the reaction profiles for the acid catalyzed O-protonation and neutral hydrolysis reactions Figure III.B.3 and Figure IV.3 show that the nucleophilic attack of the water molecule on the C=O unit involves the passage over an energy barrier of 38.6 kcal/mole. The question

is; would a distortion of formamide (or O-protonated formamide) lower this energy barrier? It would not be difficult to find out. Calculations could be made in which the water molecule is gradually moved closer to the formamide (or O-protonated formamide) molecule in which either the N-C bond has been twisted or the nitrogen atom pyramidalized. At some point a reaction will occur and the barrier for this reaction could be compared with that obtained with planar formamide (or planar O-protonated formamide). It was discussed earlier that the NH_3 group makes a large contribution to the energy barriers (see Table III.B.5 and Table IV.8), and it would be interesting to see if these contributions are reduced on distortion. If this is the case then a study could be done to find the optimum distortions for lowering the energy of these contributions while simultaneously maximizing the value of $\nabla^2\rho$ at the (3,+1) critical point in the VSCC of the carbon atom. This would lead to the determination of the geometry of formamide (or O-protonated formamide) which is most labile towards hydrolysis. Such studies would be very valuable in giving insight into the manner through which enzymes catalyze the hydrolysis of amide bonds.

The mechanisms described in this study could be applied to other amides by substituting the hydrogen atoms with heavier groups. This would surely alter some aspects of the minimum energy path, especially if the hydrogen atoms were substituted by less reactive groups. For example, the final energy minimum corresponding to an association of the products, would be less deep if the substitution did not allow for the formation of hydrogen bonds. In this case the interactions between the product molecules would be reduced to polarization effects. If the groups are very bulky then steric effects may destabilize the transition state structures to the extent that the forward direction is inhibited and the system reverts back to the reactants. Substitution of the hydrogen atom bonded to the carbon atom may reduce the reactivity of the nucleophilic site thereby impeding the advance of the nucleophile. Such hinderance could either force the reaction to follow some other mechanism or possibly curtail the reaction altogether. At present such a study would not be feasible because with the inclusion of bulky groups the increased number of degrees of freedom on the potential energy hypersurface would make the complexity of such calculations prohibitive.

References

- Bader, R.F.W. (1990) "Atoms in Molecules - A Quantum Theory"
University of Oxford Press, Oxford.
- Bader, R.F.W. (1985) Acc. Chem. Res. **18**, 9
- Bader, R.F.W. (1986) Can. J. Chem. **64**, 1036
- Bader, R.F.W.; Chang, C. (1989) J. Phys. Chem. **93**, 2946
- Bader, R.F.W. (1981) Rep. Prog. Phys. **44**, 893
- Bender, M.L. (1960) Chem. Rev. **60**, 53
- Bender, M.L.; Ginger, R.D. (1954) J. Am. Chem. Soc. **77**, 348
- Brookhart, M.; Levy, G.C.; Winstein, S. (1967) J. Am. Chem. Soc.
89, 1735
- Brown, R.S.; Bennet, A.J.; Wang, Q.; Santarsiero, B. (1991) J. Am.
Chem. Soc. **113**, 5757
- Brown, R.S.; Bennet, A.J.; Wang, Q.P.; Slebocka-Tilk, H.; Somayaji, V.;
Santarsiero, B.D. (1990) J. Am. Chem. Soc. **112**, 6383
- Brown, R.S.; Bennet, A.J.; Wang, Q. (1990) Can. J. Chem. **68**, 1732
- Brown, R.S.; Somayaji, V.; (1986) J. Org. Chem. **51**, 2676
- Csizmadia, I.G.; Hopkinson, A.C.; McClelland, R.A.; Yates, K.
(1969) Theoret. Chim. Acta **13**, 65
- Deno, N.C.; Pittman, C.U.; Wisotsky, M.J. (1964) J. Am. Chem.
Soc. **86**, 4370
- Duffy, J.A.; Leisten, J.A. (1960) J. Chem. Soc. **853**

- Edward, J.T.; Meacock, S.C. (1957) J. Chem. Soc. 2001
- Fersht, A.R. (1971) J. Am. Chem. Soc. 93, 3504
- Fraenkel, G.; Niemann, C. (1958) Proc. Natl. Acad. Sci. 44, 688
- Fukui, K. (1981) Acc. Chem. Res. 14, 363
- Gillespie, R.J.; Birchall, T. (1963) Can. J. Chem. 41, 149
- Gonzalez, C.; Schlegel, B.H. (1989) J. Chem. Phys. 90(4), 2154
- Guthrie, J.P. (1974) J. Am. Chem. Soc. 96, 3608
- Hehre, W.J.; Radom, L.; Schleyer, P.v.R.; Pople, J.A.; (1986)
"Ab initio Molecular Orbital Theory", Wiley, New York.
- Hine, J. (1962) "Physical Organic Chemistry", 2nd ed. McGraw-Hill, N.Y.
- Hine, J.; King, R.S.; Midden, W.R.; Sinha, A. (1981) J. Am. Chem. Soc. 86, 3186
- Hopkinson, A.C.; Csizmadia, I.G. (1973) Theoret. Chim. Acta 31, 83
- Ingold, C. (1953) "Structure and Mechanism in Organic Chemistry", G. Bell and Sons, London, 1953
- Kopple, K.D. (1966) "Peptides and Amino acids", W.A. Benjamin inc., N.Y.
- Kriebel, V.K.; Holst, K.A. (1938) J. Am. Chem. Soc. 60, 2976
- Laidig, K.E.; Bader, R.F.W. (1991) J. Am. Chem. Soc. 113, 6312
- Lehn, J.M.; Wipff, G. (1974) J. Am. Chem. Soc. 96, 4048
- Lehn, J.M.; Wipff, G. (1978) Helv. Chim. Acta 61, 1274

- Lehn, J.M.; Wipff, G. (1980) J. Am. Chem. Soc. **80**, 1347
- March, J. (1985) "Advanced Organic Chemistry", 3rd ed.
Wiley-Interscience, N.Y.
- Morrison, R.T.; Boyd, R.N. (1959) "Organic Chemistry", Allyn
and Bacon, Boston.
- Reid, E.E. (1899) J. Am. Chem. Soc. **21**, 281
- Schlegel, H.B. (1987) Adv. Chem. Phys. **67**, 249
- Schlegel, H.B. (1982) J. Comp. Chem. **3**, 214
- Schowen, R.L.; Kershner, L.D. (1971) J. Am. Chem. Soc. **93**, 2014
- Smith, C.; Yates, K. (1972) Can. J. Chem. **50**, 771
- Spinner, E. (1960) J. Phys. Chem. **64**, 275
- Stewart, R.; Yates, K. (1960) J. Am. Chem. Soc. **82**, 4059
- Streitwieser, A. Jr.; Heathcock, C.H. (1985) "Introduction to
Organic Chemistry" 3rd ed.; MacMillan, N.Y.
- Talbot, R.J.E. (1972) in "Comprehensive chemical kinetics",
Bamford, C.H.; Tipper, C.F., Eds; Elsevier, N.Y. vol. 10
p. 257
- Tomasi, J.; Scrocco, E.; Alagona, G. (1974) J. Am. Chem. Soc.
97, 6976
- Williams, A. (1976) J. Am. Chem. Soc. **98**, 5645